

AD-A188 369

AIR CUSHION EQUIPMENT TRANSPORTER (ACET) TESTING VOLUME  
2(U) BELL AEROSPACE CANADA TEXTRON GRAND BEND (ONTARIO)  
T D EARL ET AL. OCT 86 7624-928882-VOL-2

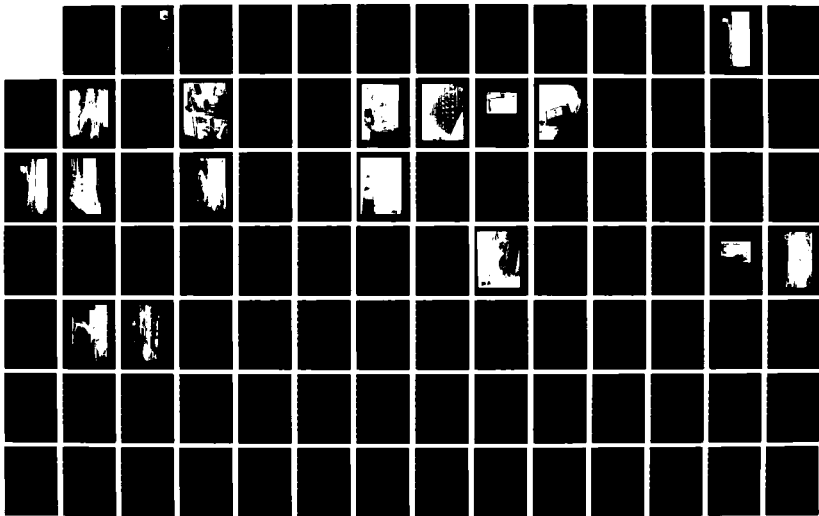
1/2

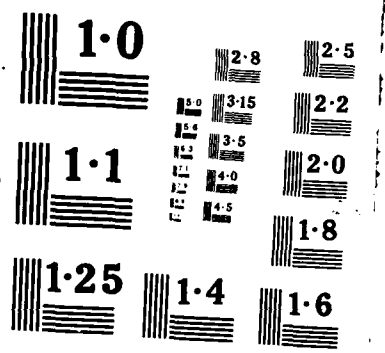
UNCLASSIFIED

AFMIL-TR-86-3888-VOL-2

F/G 13/6

NL





**AD-A188 369**

**AFWAL-TR-86-3088  
VOLUME II**



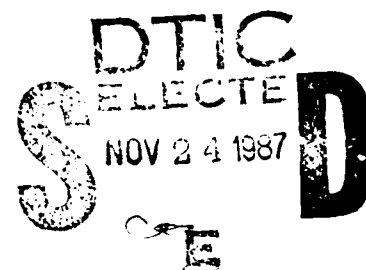
**AIR CUSHION EQUIPMENT TRANSPORTER (ACET)  
TESTING**

T.D. EARL  
R.W. HELM  
G.C.C. SMITH

BELL AEROSPACE CANADA TEXTRON  
DIVISION OF TEXTRON CANADA LTD  
P.O. BOX 160  
GRAND BEND ONTARIO NOM-1 TO

OCTOBER 1986

FINAL REPORT FOR PERIOD AUGUST 1982 - JUNE 1986



**APPROVED FOR PUBLIC RELEASE; DISTRIBUTION UNLIMITED**

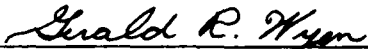
**FLIGHT DYNAMICS LABORATORY  
AIR FORCE AERONAUTICAL LABORATORIES  
AIR FORCE SYSTEMS COMMAND  
WRIGHT-PATTERSON AIR FORCE BASE, OHIO 45433-6553**

NOTICE

When Government drawings, specifications, or other data are used for any purpose other than in connection with a definitely related Government procurement operation, the United States Government thereby incurs no responsibility nor any obligation whatsoever; and the fact that the government may have formulated, furnished, or in any way supplied the said drawings, specifications, or other data, is not to be regarded by implication or otherwise as in any manner licensing the holder or any other person or corporation, or conveying any rights or permission to manufacture use, or sell any patented invention that may in any way be related thereto.

This report has been reviewed by the Office of Public Affairs (ASD/PA) and is releasable to the National Technical Information Service (NTIS). At NTIS, it will be available to the general public, including foreign nations.

This technical report has been reviewed and is approved for publication.



GERALD R. WYEN, Project Engineer  
Special Projects Group  
Mechanical Branch



AIVARS V. PETERSONS  
Chief, Mechanical Branch  
Vehicle Equipment Division

FOR THE COMMANDER



**RICHARD E. COLCLOUGH, JR.**  
Chief  
Vehicle Equipment Division

If your address has changed, if you wish to be removed from our mailing list, or if the addressee is no longer employed by your organization please notify AFWAL/FIEMB W-PAFB, OH 45433 to help us maintain a current mailing list.

Copies of this report should not be returned unless return is required by security considerations, contractual obligations, or notice on a specific document.

UNCLASSIFIED

SECURITY CLASSIFICATION OF THIS PAGE

## REPORT DOCUMENTATION PAGE

1a. REPORT SECURITY CLASSIFICATION <b>UNCLASSIFIED</b>			1b. RESTRICTIVE MARKINGS			
2a. SECURITY CLASSIFICATION AUTHORITY			3. DISTRIBUTION/AVAILABILITY OF REPORT <b>APPROVED FOR PUBLIC RELEASE DISTRIBUTION IS UNLIMITED</b>			
2b. DECLASSIFICATION/DOWNGRADING SCHEDULE						
4. PERFORMING ORGANIZATION REPORT NUMBER(S) 7624-928002-151-9.			5. MONITORING ORGANIZATION REPORT NUMBER(S) AFWAL-TR-86-3088, VOLUME II			
6a. NAME OF PERFORMING ORGANIZATION BELL AEROSPACE CANADA TEXTRON		6b. OFFICE SYMBOL (If applicable)	7a. NAME OF MONITORING ORGANIZATION FLIGHT DYNAMICS LABORATORY AIR FORCE WRIGHT AERONAUTICAL LABORATORY			
6c. ADDRESS (City, State and ZIP Code) P.O. BOX 160 GRAND BEND ONTARIO NOM 150			7b. ADDRESS (City, State and ZIP Code) (AFWAL/FIEMB) AIR FORCE SYSTEMS COMMAND 45433- WRIGHT-PATTERSON AIR FORCE BASE OH 6553			
8a. NAME OF FUNDING/SPONSORING ORGANIZATION		8b. OFFICE SYMBOL (If applicable)	9. PROCUREMENT INSTRUMENT IDENTIFICATION NUMBER F33615-81-C-3420			
8c. ADDRESS (City, State and ZIP Code)			10. SOURCE OF FUNDING NOS.			
			PROGRAM ELEMENT NO.	PROJECT NO.	TASK NO.	WORK UNIT NO.
			62201F	2402	01	34
11. TITLE (Include Security Classification)						
12. PERSONAL AUTHOR(S) T.D. EARL, R.W. HELM, G.C.C. SMITH						
13a. TYPE OF REPORT FINAL		13b. TIME COVERED FROM AUG 82 TO Jun 86		14. DATE OF REPORT (Yr., Mo., Day) October 1986		15. PAGE COUNT 122
16. SUPPLEMENTARY NOTATION						
17. COSATI CODES			18. SUBJECT TERMS (Continue on reverse if necessary and identify by block number)			
FIELD	GROUP	SUB. GR.	1. Aircraft transporter, equipment transporter, air cushion vehicle, survivability			
01	03					
13	06					
19. ABSTRACT (Continue on reverse if necessary and identify by block number)						
<p>The Air Cushion Equipment Transporter (ACET) is designed as an air base survivability item, to transport vital heavy equipment (especially aircraft) across battle damaged terrain. This report presents the results of the first ACET program which consisted of the design, construction, and testing of a prototype vehicle.</p> <p>Based upon the design concept evolved for the AATS program, the ACET is essentially a lower performance derivative of the vehicle proposed for that program. Its construction follows closely the methods used in producing the LACV-30 and its cushion lift air system employs, almost exclusively, the hardware previously installed on the XC-8A aircraft used in the ACLS program.</p> <p>This report summarizes the design and construction of the prototype vehicle and presents the results of the test program with the ACET equipped with a full fingered skirt, carrying an F101B aircraft, to simulate realistic payloads.</p>						
20. DISTRIBUTION/AVAILABILITY OF ABSTRACT UNCLASSIFIED/UNLIMITED <input checked="" type="checkbox"/> SAME AS RPT <input type="checkbox"/> DTIC USERS <input type="checkbox"/>			21. ABSTRACT SECURITY CLASSIFICATION UNCLASSIFIED			
22a. NAME OF RESPONSIBLE INDIVIDUAL GERALD R. WYEN			22b. TELEPHONE NUMBER (Include Area Code) (513)257-7804		22c. OFFICE SYMBOL AFWAL/FIEMB	

DD FORM 1473, 83 APR

EDITION OF 1 JAN 73 IS OBSOLETE

UNCLASSIFIED

SECURITY CLASSIFICATION OF THIS PAGE

A188 369

## TABLE OF CONTENTS

SECTION		PAGE
I	INTRODUCTION AND SUMMARY. . . . .	1
II	DESCRIPTION . . . . .	4
	1. Configuration . . . . .	4
	2. Structure. . . . .	4
	3. Cushion Powering . . . . .	9
	4. Skirt System . . . . .	9
	5. Auxiliary System . . . . .	15
III	DESIGN ANALYSIS . . . . .	22
	1. Dynamic Stability. . . . .	22
	2. Control in Wind and on Sideslope . . . . .	22
	3. Mounting and Dismounting . . . . .	25
	4. Cushion Powering . . . . .	27
IV	CONSTRUCTION PHASE. . . . .	39
V	DEVELOPMENT PROBLEMS. . . . .	42
	1. Minor Problems . . . . .	42
	2. Major Problems . . . . .	43
VI	ACET AND F-101 AIRCRAFT WEIGHT AND C.G. SUMMARY. . . . .	54
	1. ACET . . . . .	54
	2. F-101-B Aircraft . . . . .	54
VII	STATIC HEAVE 7 STABILITY SHAKE-DOWN TESTS . . . . .	58
VIII	TERRAIN TESTS . . . . .	71
	1. General. . . . .	71
	2. Test Description . . . . .	71
IX	CONCLUSIONS . . . . .	86
X	RECOMMENDATIONS . . . . .	87
	APPENDIX A - ACET HEAVE STABILITY ANALYSIS - BOEING REPORT L-7170-84-SMW-007. . . . .	95
	REFERENCES. . . . .	122

**LIST OF FIGURES**

1.	ACET with F-101, towed by UMIMOG over Wheat Field . . . . .	2
2.	F-15's Taking Off Using the AATS . . . . .	5
3.	ACET General Arrangement . . . . .	6
4.	Automatic Welding of Hollowcore Planks . . . . .	7
5.	Flotation Box Structure/Splice Assembly - Typical . . . . .	8
6.	ASP-10 Fan-Engine Installed on ACET . . . . .	10
7.	Rear Module in Construction (Inverted) Showing Air Feed Holes . . . . .	11
8.	Electrical Compartment . . . . .	12
9.	Remote Control Ready for Tow Vehicle . . . . .	13
10.	Finger Geometry . . . . .	14
11.	Landing Pad Locations . . . . .	16
12.	F-101B Mounting the ACET . . . . .	18
13.	Close-Up of ACET Showing Skirt Lifters . . . . .	19
14.	F-101B on Cushionborne ACET Showing Tow Hitch, etc. . . . .	21
15.	Predicted ACET Stability Boundaries . . . . .	23
16.	Skirted Plenum Configuration Showing Pleats . . . . .	24
17.	Forces and Reactions in 30 Knot Crosswind . . . . .	26
18.	Plane of Symmetry Forces Mounting 7 <sup>o</sup> Ramp . . . . .	28
19.	ASP-10 Fan Characteristics . . . . .	29
20.	Duct Pressure & Heave Survey . . . . .	31
21(A),(B)	ACET Air Gaps at Skirt Stations (Plenum Skirts) . . . . .	32, 33
22.	Variation of Air Gap with Fan RPM . . . . .	34
23.	Variation of Cushion Pressure with Fan RPM . . . . .	35

24.	Volume Flow vs Fan ( $N_f$ ) and Compressor ( $N_g$ ) % RPM . . . . .	37
25.	ST-6 Engine Flow Data $N - N$ . . . . . $f \quad g$	37
26.	ACET Internal Duct Pressure Survey . . . . .	38
27.	ACET Rear Module on Assembly Jig . . . . .	40
28.	Perspective of Engine Mounting . . . . .	41
29.	Nose of ACET Showing Inlet Fence and Exhaust . . . . .	44
30.	Typical Grand Bend Runway Surface with ACET and F-101B . . . . .	45
31.	F-101B Mounted on ACET Showing Load Spreaders . . . . .	47
32.	Damage Caused by F-101B Wheel . . . . .	48
33.	Recommended Skirt Lift Cable Run . . . . .	50
34.	Aircraft Line-up Technique . . . . .	52
35.	F-101B Airplane . . . . .	56
36.	Combined C.G. Variation with Aircraft Position . . . . .	57
37.	Cushion Gap - Variation with Power - ACET; Weight 13,827 lb. at C.G. 313 in. . . . .	59
38.	Heave Height - Variation with Power - ACET; Weight 13,827 lb. at C.G. 313 in. . . . .	60
39.	Heave Height (Rear Cell Outboard) - Power - Roll Stiffness Tests . . . . .	62
40.	Air Gap (Rear Cell Outboard) - Power - Roll Stiffness Test . . . . .	63
41.	Roll Stiffness and Derivative . . . . .	64
42.	Rear Wheel Ground Reaction . . . . .	66
43.	Heave/Pitch Attitude of Aircraft/ACET as Function of Main Wheel Position and Power . . . . .	68
44.	Moment/Pitch - Various Aircraft Positions on ACET. . . . .	69
45.	Lift/Weight and C.G./C.P. Correlation . . . . .	70
46(A), (B)&(C)	Heave/Pitch Attitude of Aircraft/ACET as Function of Power . . . . .	75
47.	Fan Flow and Cushion Pressure - Power - Various Gross Weights . . . . .	78

48.	Down-Uphill Circuit Characteristics . . . . .	80
49.	Down/Up Circuits - (44,297 lb. Gross at 403.3 in.) Tow Force Histories . . . . .	81
50.	Plan of Typical Hardstand/Hill/Field/Crater Area of General Terrain Testing . . . . .	83
51.	69,297 lb. Gross Weight Circuit - 6-18-85 . . . . .	84
52.	DDA 8V92TA Diesel and Centrifugal Fans Installation . . . . .	88
53.	Methods of Providing Sloping Deck . . . . .	89
54.	Proposed Method of Vehicle Jacking . . . . .	91

LIST OF TABLES

		PAGE
1	Cross Wind Parameters . . . . .	25
2	Comparison of Air Cushion Conditions . . . . .	36
3	Internal Pressure Loss and Flow . . . . .	36
4	Terrain Tests - Chronological . . . . .	72
5	Summary of Test Parameters - Procedure and Practice . . . . .	73



Accession For	
NTIS GRA&I	<input checked="" type="checkbox"/>
DTIC TAB	<input type="checkbox"/>
Unannounced	<input type="checkbox"/>
Justification	
By	
Distribution/	
Availability Codes	
Dist	Avail and/or Special
<b>A-1</b>	

## LIST OF ABBREVIATIONS AND SYMBOLS

AATS	Alternate Aircraft Take-off System
ACET	Air Cushion Equipment Transporter
ACLS	Air Cushion Landing System
BACT	Bell Aerospace Canada Textron
c	Reference Length Inches, or Cushion Length Feet
C	Discharge Coefficient
D	
C.G./c.g.	Center of Gravity
cm	Centimeters
C	Yawing Moment Coefficient
n	
C.P.	Rolling or Pitching Moment Coefficient
c.p.	Center of Pressure
C.P. <sub>θ</sub>	Pitching Moment Derivative
C.P. <sub>φ</sub>	Rolling Moment Derivative
C	Side Force Coefficient
y	
EASY	Boeing Military Airplane Company Computer Program
FOD	Foreign Object Damage
ft/FT	Feet
g	Gravitational Acceleration
h	Jet Height
j	
H.P.	Horsepower
Hz	Hertz - Cycles/second
LACV-30	Lighter Air Cushion Vehicle - 30 Ton Payload
lb.	Pounds
int.	Intermediate
LBL	Lateral Buttock Line
M, N	Subscripts Main/Nose

max.	Maximum
min.	Minimum
N	Free Turbine - % Max. RPM
N <sub>f</sub>	Gas Generator - % Max. RPM
N <sub>g</sub>	
P	Cushion Pressure - psf
P <sub>c</sub>	
psi	Pounds per Sq. Inch
psig	Pounds per Sq. Inch Gauge
q	Dynamic Presusre $1/2\rho v^2$ - lb/sq ft
Q	Airflow - cu ft/sec
RMS/rms	Root Mean Square
rpm	Revolutions per Minute
S	Area - sq ft
Sta	Longitudinal Station
Sq.Ft.	Square Feet
USAF	United States Air Force
vdc	Volts Direct Current
V	Jet Velocity - ft/sec
V <sub>j</sub>	
XC-8A	deHavilland Canada CC-115 Buffalo Aircraft
$\beta$	Beta, Yaw Angle
$\Delta p/$	Pressure Loss Coefficient
$\theta^g$	Pitch Angle
$\rho$	Air Density
$\phi$	Roll Angle

## SECTION I

### INTRODUCTION AND SUMMARY

The Air Cushion Equipment Transporter (ACET) is designed as an air base survivability item, to transport vital heavy equipment (especially aircraft) off-runway and across battle damaged areas. It is particularly envisaged as providing for prompt delivery of an attack aircraft from its shelter to a postulated undamaged runway segment for operation, after a devastating attack has prevented this access any other way.

This report presents results of the first ACET program. This program was jointly sponsored by the USAF Flight Dynamics Laboratory and the Canadian Department of Industry and Trade. It consisted of the design, construction and testing of an ACET prototype. During the tests the ACET payload was an F-101 provided by the USAF. Off-runway and rough terrain traverses were easily accomplished at up to 60,000 lb. payload. Figure 1 is a photograph of the ACET carrying the F-101 and being towed by a "Unimog" four wheel drive light farm vehicle. In its current form the ACET is not self-propelled, being designed to be towed, but two engine-driven fans are installed at the front to power the air cushion. The aircraft is winched aboard and chocked. Operation up to 15 or 20 mph over rough terrain in brisk winds is a smooth ride for the aircraft but speed may be limited by the rough ride tolerance of the crew in the tow vehicle. Operation in cross winds or on side slopes is enabled by the use of lightly loaded trailing wheels at the rear. On reaching its destination the aircraft can be rapidly dismounted by furling the rear skirt to create a nose-up ACET attitude, releasing the aircraft to roll off and then towing the ACET out of the way from beneath it.

Limiting rough surfaces were not encountered in the current program except for a restriction on operation over old crazed blacktop. On this surface, if the cushion air can penetrate the cracks it will lift the blacktop pieces from the surface on which it was laid, with resulting damage. On the other hand the loaded 73,000 lb. vehicle left little trace of its passage across thick tufted long grass, wheatfield, or the simulated shallow crater prepared for the exercise, and was traversed smoothly up a sharp incline. In all of these operations the drag was small and the combination was readily towed, even across wet clay. Maneuverability was excellent, and the combination handles like a tractor trailer and can be turned in its own length.

Air cushion dynamic stability problems were encountered in the program requiring significant configuration development. Fully satisfactory operation was achieved with full depth finger skirts incorporating stabilizing bleed holes.

These problems and associated funding difficulties led to program stretch out, but planned tests for the initial phase have



Figure 1. ACFT With F-101, Towed by Umimog Over Wheat Field

now been completed and the prototype (which is modular for transport purposes) has been transferred to a new location for a follow-on test phase to be conducted by the USAF, Flight Dynamics Laboratory FIEMB branch of the Vehicle Equipment Division.

Results of the initial test phase are analyzed and discussed in Sections 6 and 7 of this report.

## SECTION II

### DESCRIPTION

#### 1. CONFIGURATION

The original design is fully described in the interim technical report (Ref. 1), which also presents analyses of structure, powering, airflow performance, stability, etc., together with a list of drawings prepared.

In summary, the design is based on the configuration developed for the Alternate Aircraft Take-off System (AATS) but it is a low cost derivative, having greater weight and limited to 25 knots speed under tow. The AATS was designed as a take-off sled for off-runway operation. It supports a fighter aircraft throughout its take-off run, typically to 175 knots, and is arrested and retrieved (Figure 2).

The ACET configuration is shown in the general arrangement three view of Figure 3.

The basis for the design is the use of three independent cells for air cushion support. Each main cell supports one of the airplane's main wheels and the nose cell supports the nose wheel, although this nose cell is some 40in further forward than the nose wheel because of the forward overhang of the craft's engines. The three independently pressurized cells provide a stiff air cushion platform which does not wallow in pitch and roll and can accept offset loads with little change in attitude.

The cushion skirts are a series of abutting full depth flexible fingers made of a special reinforced elastomeric fabric. They are mounted beneath the raft structure.

#### 2. STRUCTURE

The transporter is made from aluminum "hollowcore" extruded planking, machine edge-welded to form large panels which are used for the top and bottom decking of the 15in deep structure and for internal bulkheads. The latter are made by cutting additional large panels crosswise with a circular saw. Figure 4 is a photograph of the plank welding operation.

The structure is modular with the module sizes limited for air transportation in a C-130. The GA drawing, Figure 3, shows the three modules: the forward is the power module and is the leg of the tee-shaped planform. The center and aft modules are supported by the main cells and are assembled normal to the power module. The joints are made with splice plates top and bottom and also vertically for shear transfer. The joint design is similar to that used on the Army LACV-30, a Bell air cushion lighterage vehicle. Figure 5 is a perspective of a typical joint.



Figure 2. F-15's Taking Off Using the AATS

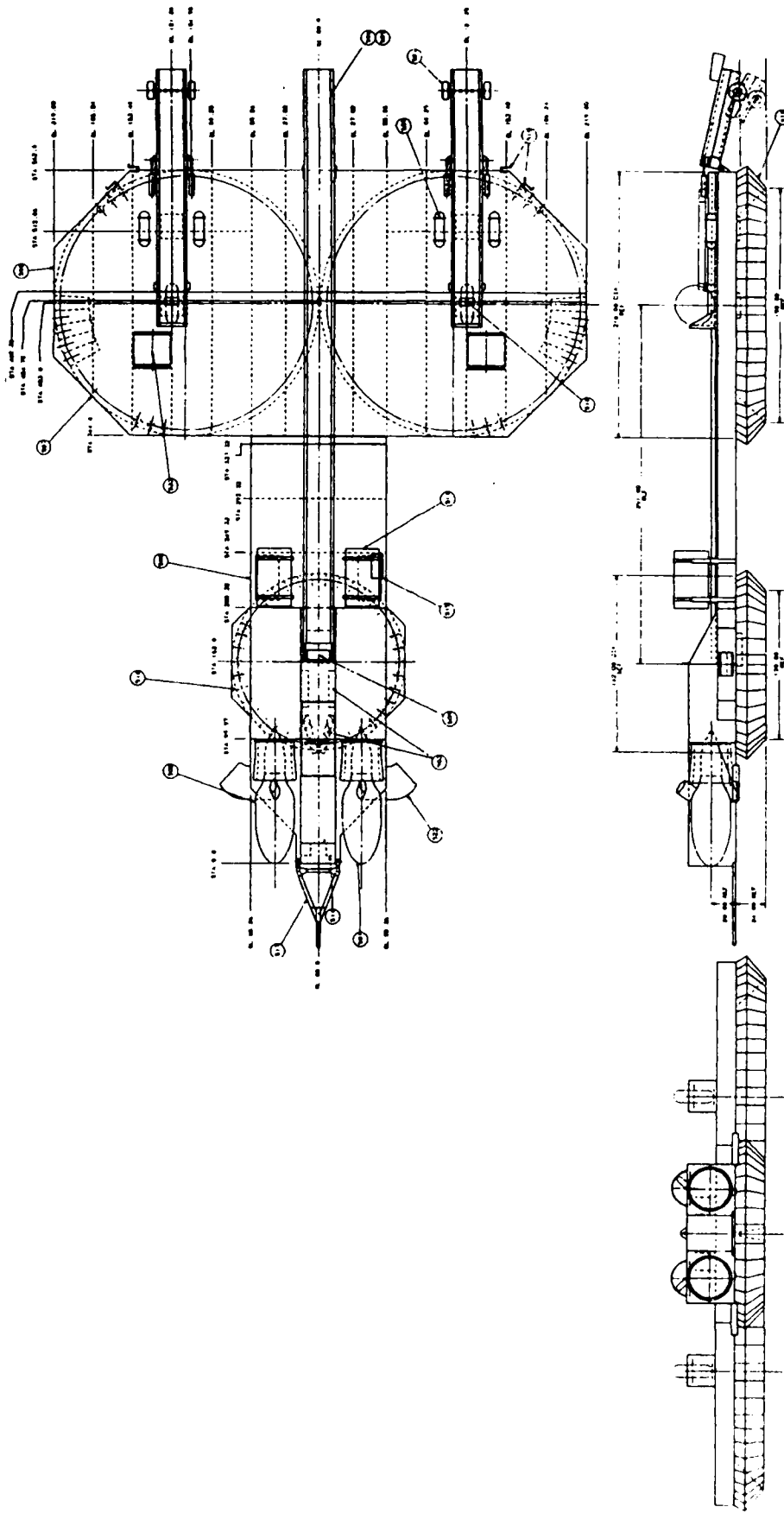
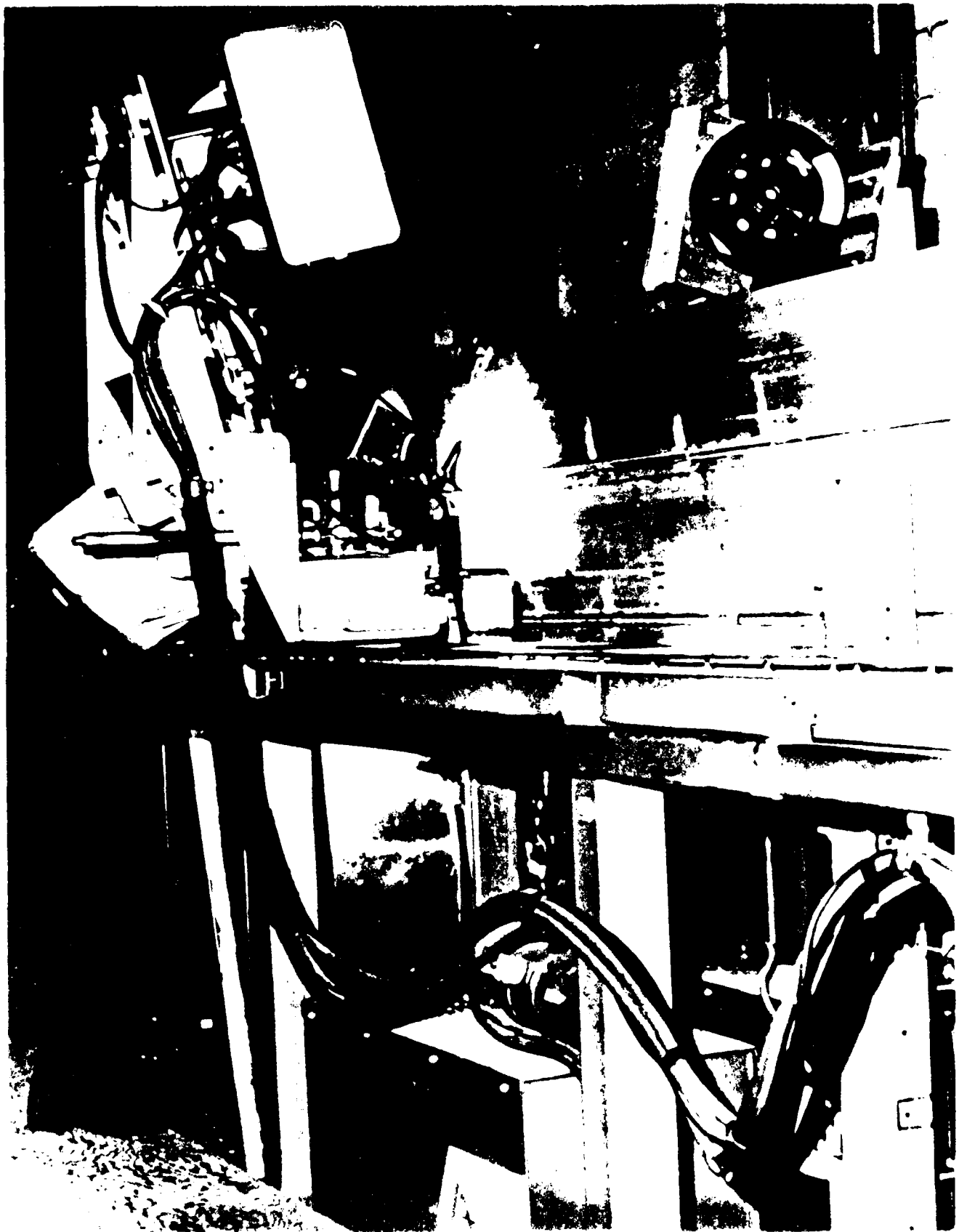


Figure 3. ACET General Arrangement



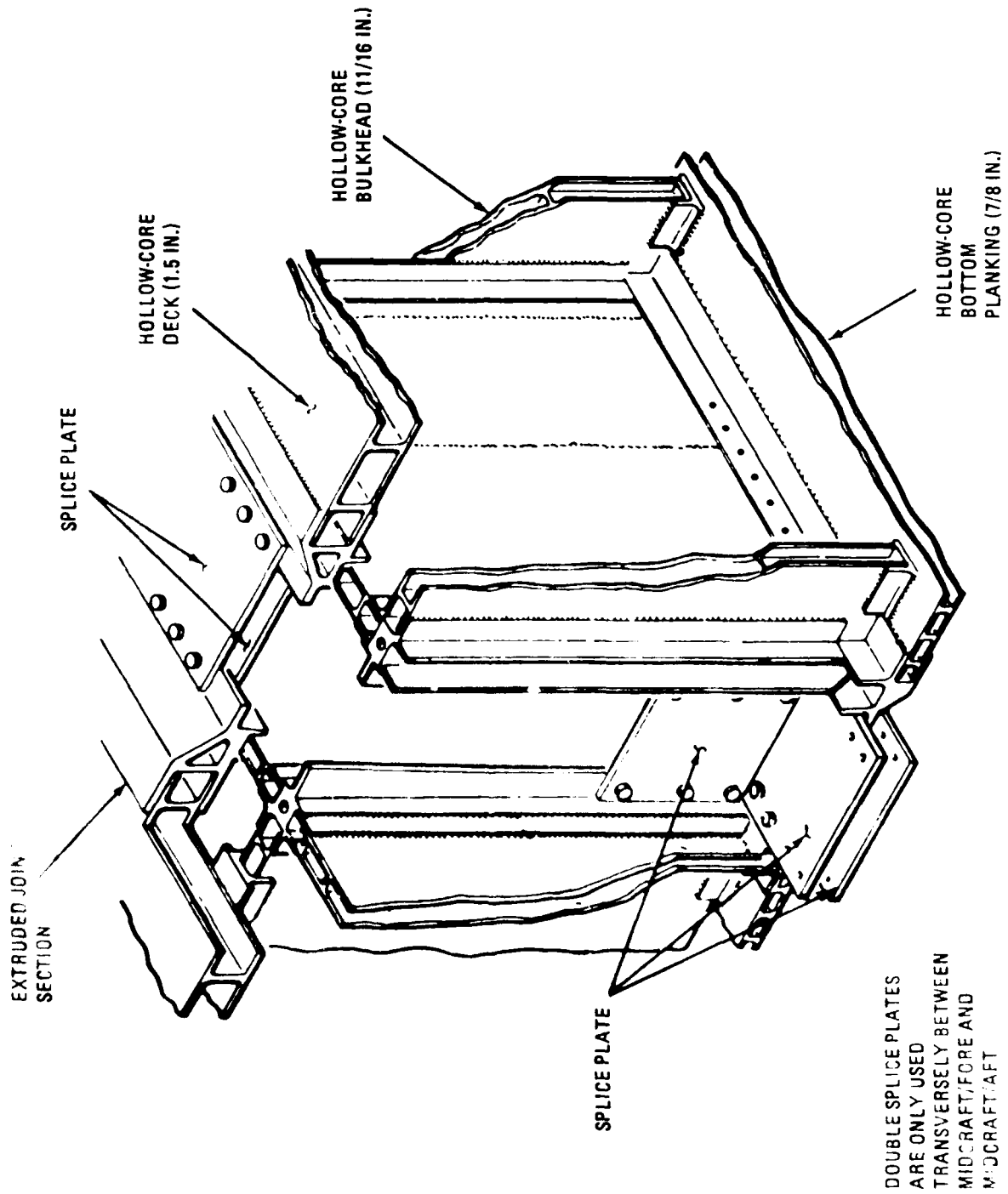


Figure 5. Flotation Box Structure/Splice Assembly -- Typical

Top and bottom plating consists of single integral panels made by welding 37 ft. long metal planks, edge to edge, nine planks center module, ten planks aft module. For the internal shear panels a truss structure can be alternated with a panel section in the same web. For example, the front bulkhead of the center module is a part truss, part hollowcore panel beam. Its top and bottom extrusions are chosen to fit the hollowcore and continue from end to end. For the change to trusses (for minimum airflow restriction) a tee-section is welded into these extrusions and the trusses are attached to its leg. All trusses are 1-1/2" square tube notched at each end to fit the leg, with two spacer blocks to take the bolt compression load.

### 3. CUSHION-POWERING

ACET cushion power and airflow are provided by two of the special ASP-10 fan engines developed for the XC-8A air cushion landing gear program. The principal reason for this choice was their availability. The flow capacity of the two fans is satisfactory, and although the power and pressure capacities exceed requirements, throttling the engine permits performance to be established over a wide range of power input. Figure 6 shows one of these installed on the ACET. The fan blades can just be discerned behind the inlet screen.

The engines are mounted on each side of a box beam extending forward from the main raft structure (Figure 3 and 6). The "F-10" fans providing the air flow are co-axial with the PT-6 core engines and are two-stage units of the axial flow type. The combination is designated ASP-10. The fan air enters an annular intake behind the engine pod and exhausts into 30 in. deep structural ducts, which taper to the deck level. A small part of the flow doubles back through the filters to feed the gas turbines, and about a quarter of the flow is immediately fed to the front cell. The major part flows aft to feed the main cells using the raft structure as a duct. For this reason the transverse bulkheads in the forward module are truss structures. In the rear modules, large diameter lightening holes in the bulkhead frames allow the air to reach the periphery internally (Figure 7). Each of the three cells is fed peripherally through a number of circular holes in the lower deck. The finger walls lie between these holes so that the airstreams feed each finger cavity individually.

The engine automatic control boxes and start batteries are housed in an electrical compartment at the front of the box beam (Figure 8). Remote control from a portable panel in the tow vehicle is provided via an umbilical (Figure 9). Fuel is carried in two deck mounted tanks.

### 4. SKIRT SYSTEM

The developed skirts are full depth fingers made from Bell/Avon 40 oz. hovercraft type reinforced fabric. Figure 10 shows the geometry of a single finger. All the finger sides radiate



Figure 6. ASP-10 Fan-Engine Installed on ACET

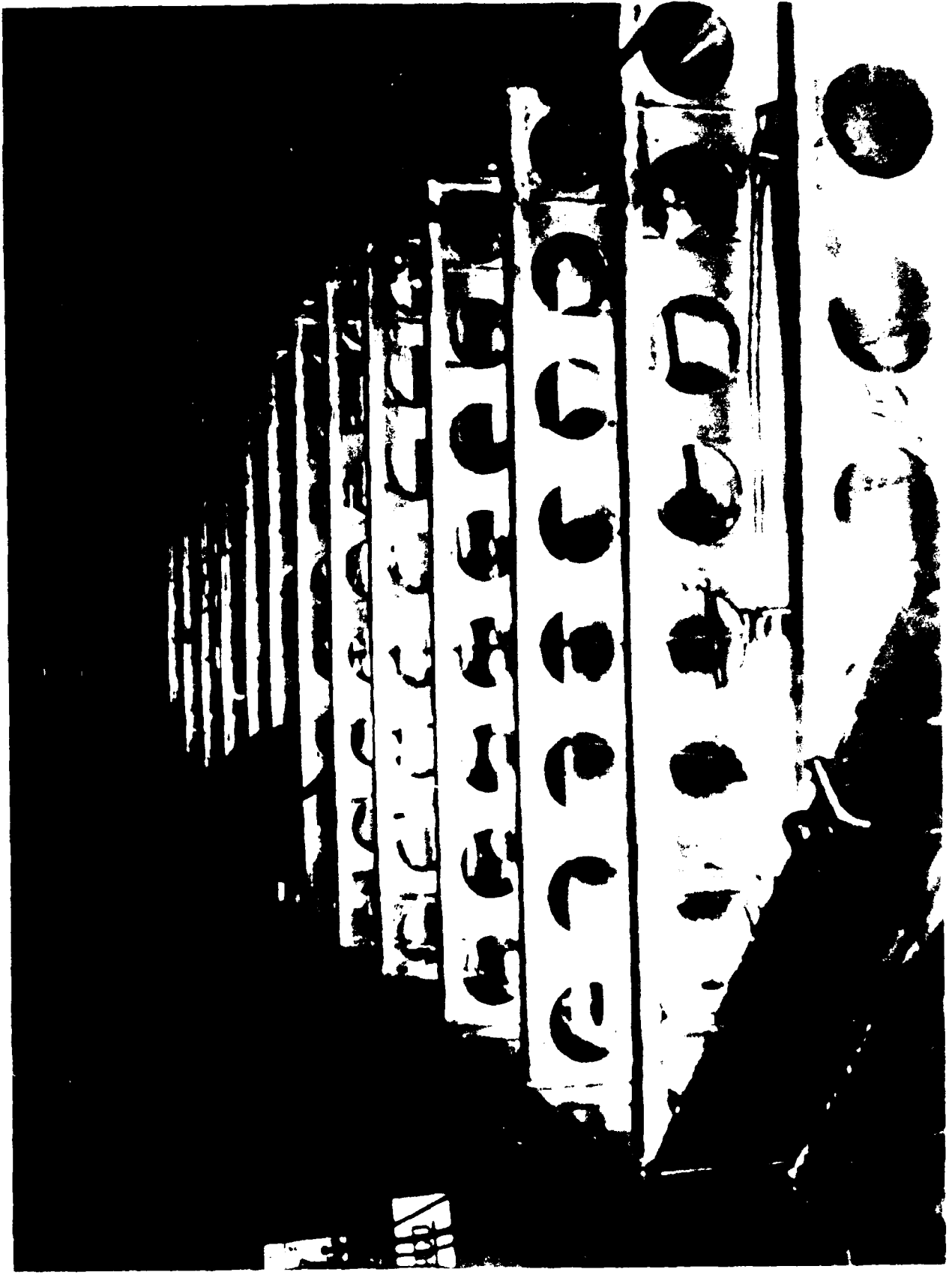


Figure 7 Rear Module in Construction (Inverted) Showing Air Feed Trays

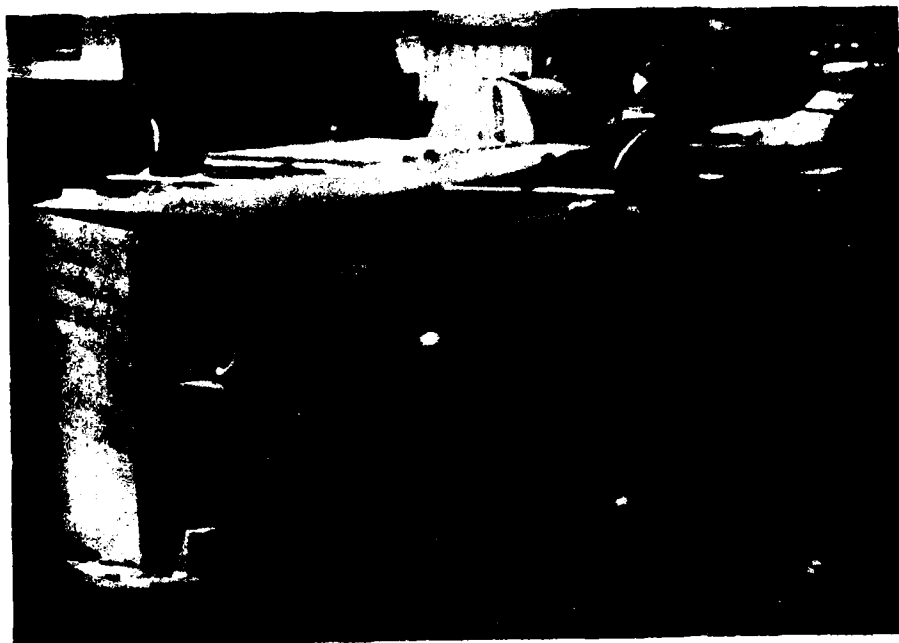


Figure 8. Electrical Compartment



Figure 9 - Remote Control Ready for Low Vel

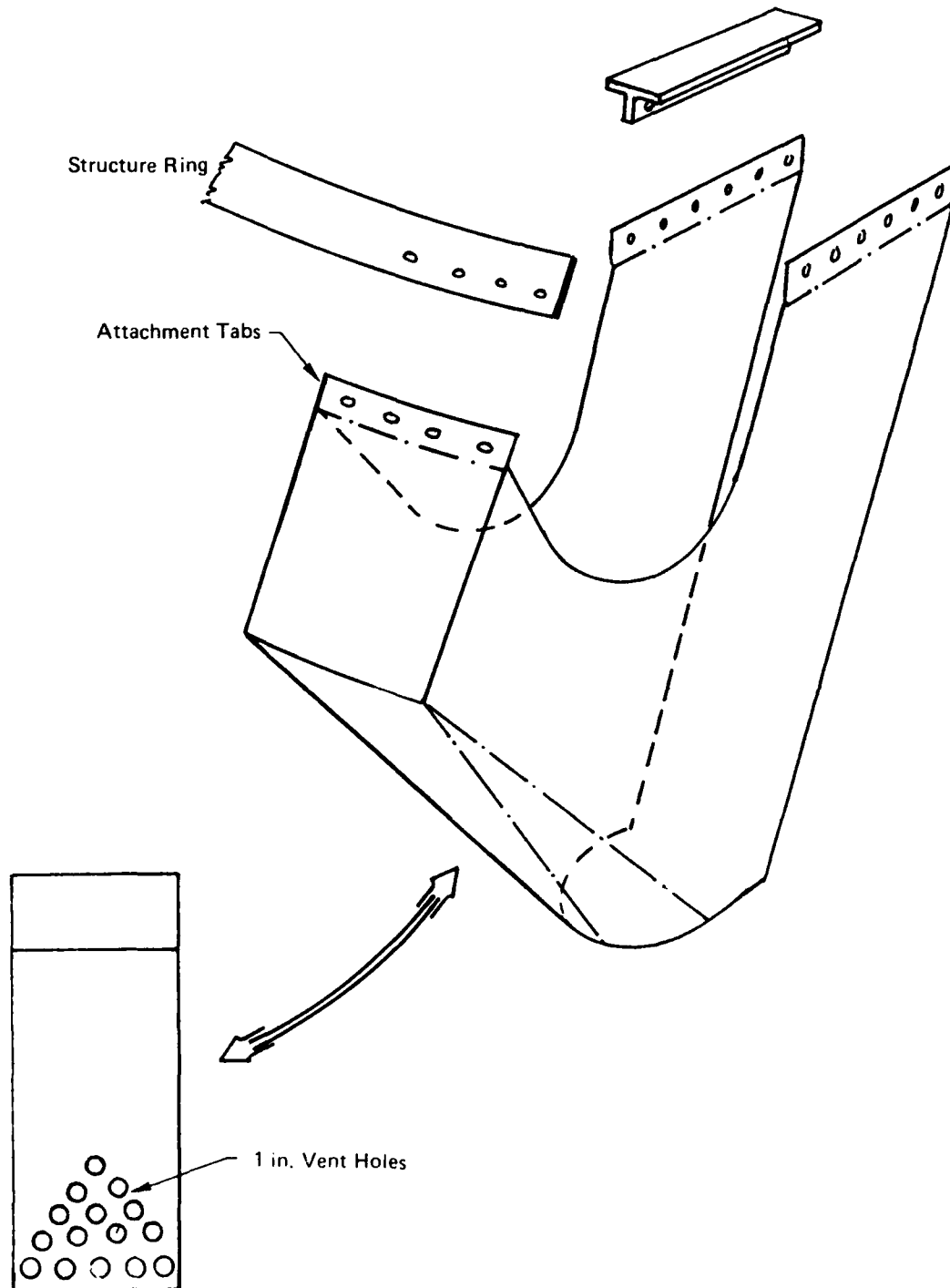


Figure 10. Finger Geometry

from the cell center. A large cut-out is provided in the finger sides abutting the bottom of the structure to reduce weight and to allow a modicum of circumferential flow redistribution should pressure gradients exist.

The fingers' outside faces are slanted inwardly over the lower two thirds to provide stability and there is a pattern of vent holes at the bottom of each fourth finger as shown on Figure 10. This venting was found to be necessary to control a dynamic instability in heave.

The fingers are attached to the structure at the outer face by means of attachment tabs (an extension of the finger outer face) which are riveted to a circumferential aluminum ring on the structure, and at their inner ends by short lengths of 1/8" aluminum tee-section riveted to the bottom panel. Each finger wall shares this tee-section with the adjacent one and they are riveted to the leg of the tee through washer strips. If a finger needs to be replaced the rivets are drilled out and replaced.

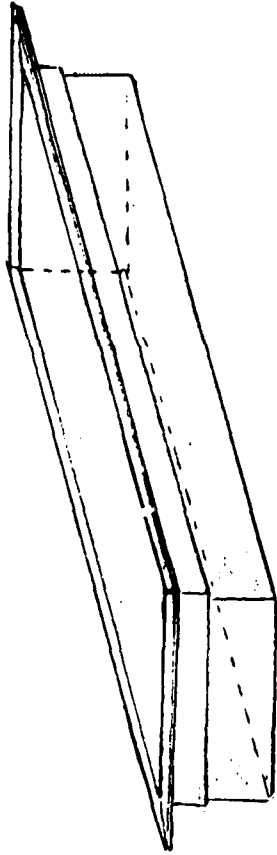
The concept of skirted plenum cells is based on a considerable air cushion vehicle background including the Bell Carabao tri-cell plenum - a similar configuration to the ACET and the modern large multi-cell plenum built by Sedam in France for cross channel ferry duty. These machines used simple skirted plenums. Similar simple skirted plenums were originally designed for and used on the ACET. Several problems were encountered with these including skirt stretch due to the large circumferential tension (large diameter to height ratio), but they were replaced by the individual fingers principally because of premature cell collapse and high drag when operating over churned up asphalt and snow. The sweeping action of the skirt was supposed to be compensated by release pleats contained by elastic straps but performance was marginal. It was considered that the rough surface negotiation of individual fingers would be much better, though at some increase in complexity, weight and cost.

The finger configuration as described was therefore installed for the remainder of the test program. See also Section 5.2.a.

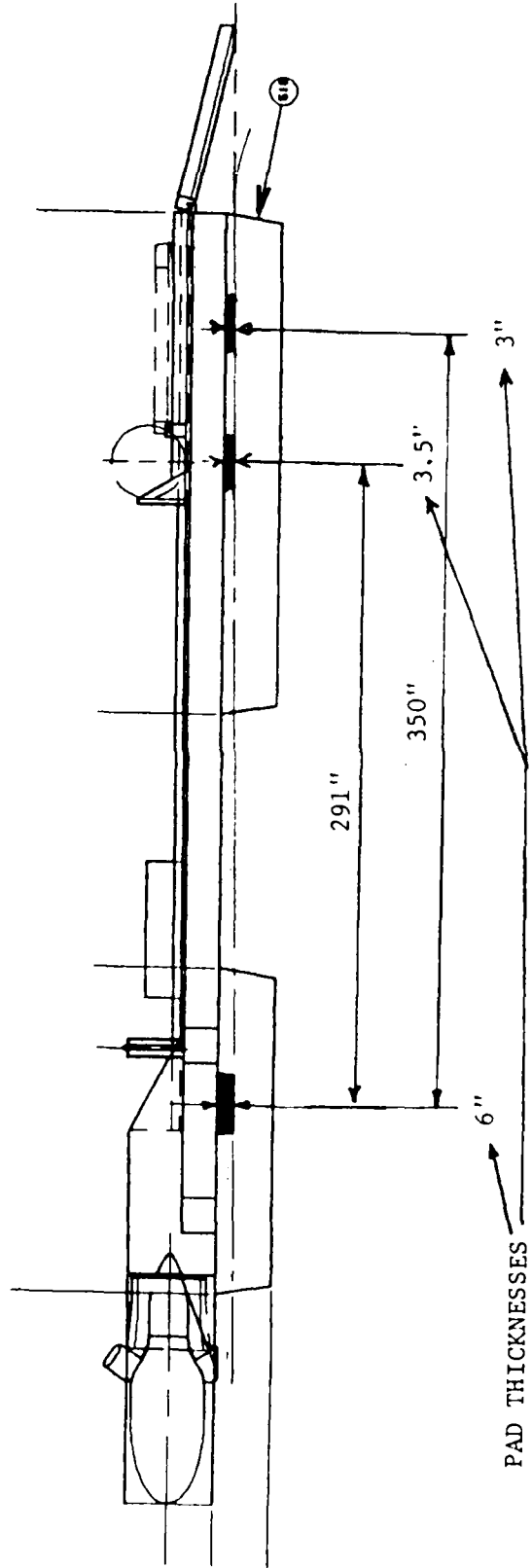
## 5. AUXILIARY SYSTEMS

### a. Parking

At rest on the ground the ACET is supported on three sets of landing pads - one beneath the front cell, two pairs centrally beneath each of the main cells and two more beneath each main cell halfway from the center to the rear edge of each. The pads are slightly different thicknesses so that on a flat surface the craft attitude is 1/2° nose up (Figure 11).



PERSPECTIVE OF THE MAIN  
AND REAR PADS INSTALLED IN FRAME



PAD THICKNESSES

Figure 11. Landing Pad Locations

#### b. Wheel Tracks and Ramps

Wheel tracks are fitted on the deck for both main and nose wheels. All are of similar construction. The nose wheel track is a structural spine adding to the raft strength and stiffness. Ramps adjoin the tracks at deck level (approx. 17in. above ground) at the rear. The main wheel ramps are folding units in two sections, which are almost identical to each other and of the same design as the tracks. The difference is that the forward section incorporates a wheel pair and the aft a support block and a folding rear flap. When ready for mounting the support block keeps the wheels just off the ground and the ramp angle is about  $7^{\circ}$ . The nose ramp is a removable unit which is carried on deck on the center track and consists of a single section similar to the main ramps. When deployed it has a  $16^{\circ}$  angle to the ground. The ramps can be seen in Figure 12 with the aircraft mounting.

#### c. Winching

For mounting the aircraft the ACET is backed into position ahead of it, the ramps deployed, and the winch cable attached to the nose wheel. The winch is a 2 HP electrical unit with a special manual brake to assist with dismount.

#### d. Heave Dampers

A passive heave damping system is fitted. This takes the form of shut spring-loaded doors which open to vent a portion of the cushion flow when pressure rises above a predetermined level. This level nominally consists of the pressure resulting from a gross weight of 45,000 lb. (vehicle and payload). The main cell vents are two 28insquare openings (one each cell) through the deck to the cushion space, sealed to prevent direct air escape from the duct (Figure 3). Each vent is closed by a door, piano-hinged at the rear, with tension springs internally at the front. Maximum bleed corresponds to a 3in. opening at the front. Each door is fitted with two single acting dampers (one each acting in opposite directions). The spring load and the damping forces are both adjustable externally.

A similar arrangement is incorporated in the front cell, using two blow-off doors (one each side), in the small removable port and starboard structural wings used to support this cell.

#### e. Skirt Lift

The skirt lift system is applied to ensure deflation of the rear skirts for dismount. It consists of four ratcheted hand winches (small-boat lander type) pulling up the twelve furthest aft fingers each side by means of multiple lightweight cables running through fiber fairleads (see Figure 13).



Figure 12. F-101B Mounting the ACET

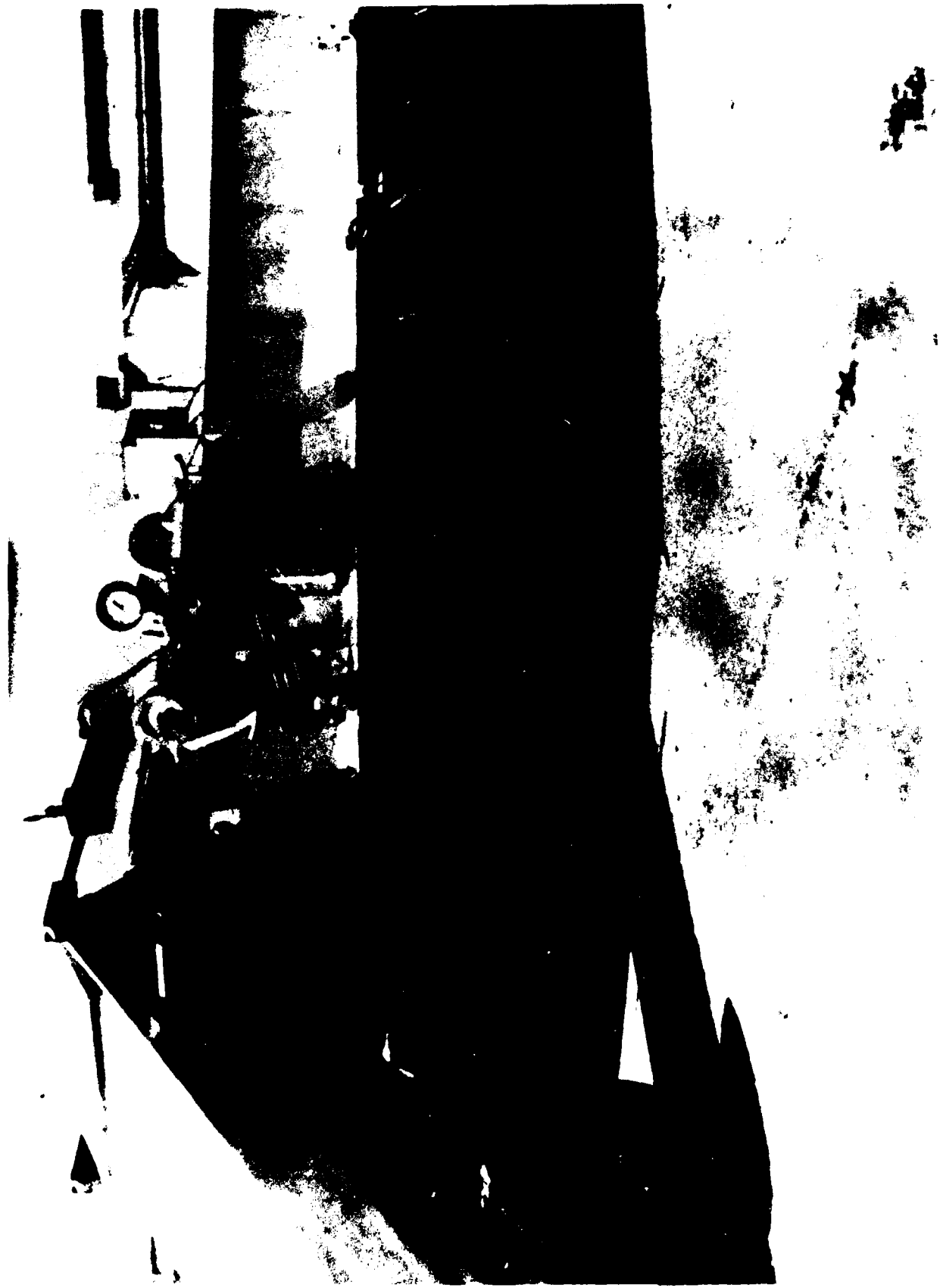


Figure 13. Close-up of ACET Showing Skirt Lifters

f. Towing System

The ACET is designed to be towed by a standard vehicle of inventory type. An A-frame tow-bar is attached to the front of the box beam with a lateral hinge to accommodate the rise and fall of the ACET (going on/off cushion) and also to allow towing by different vehicles. The apex of the frame carries an automotive type hitch (Figure 14). The attachment of the tow vehicle allows for an acute angle between its longitudinal axis and the longitudinal axis of the ACET so that tight turns can be made, space requirement being determined by the steering lock of the tug.

Since the air cushion does not provide sideforce, anti-drift partial load trailing wheels are provided to counteract the jack-knifing tendency in cross-wind or side-slope operation. The wheels are mounted beneath the forward section of the main wheel ramps, which are pivoted about a lateral axis near the deck level. Side arms on the ramps are connected to two pneumatic jacks each side. For the system to be activated, pneumatic pressure is introduced into the cylinders from a pair of bottles each side. These act as accumulators and are charged to a nominal 200 psi for operation. The loading cylinders and method can also be seen in Figure 13.



Figure 14. F-101B on Cushionborne ACFT Showing Tow Hitch etc

## SECTION III

### DESIGN ANALYSIS

#### 1. DYNAMIC STABILITY

The three plenum cell configuration provides a very steady air cushion platform, but there is considerable potential for dynamic instability in the heave axis, which may couple with pitch or roll, usually pitch, and may result in a sustained limit cycle oscillation or a divergence.

Because of this potential, dynamic stability was analyzed extensively in the design stage. These analyses used both simple linear techniques and also complex non-linear coupled simulations. For the latter, the "EASY" code developed by the Boeing Co. was used and Boeing assisted Bell by conducting the analyses. It was predicted that dynamic instability would occur as weight was increased unless a cushion vent, sensitive to cushion pressure, was introduced. A vent area of 1.22 sq. ft. and a sensitivity of 0.016 sq. ft./lb./sq. ft. (vent area divided by cushion pressure increment) were selected. This was calculated to provide the stability boundaries shown in Figure 15. In the original design with plain plenum skirts an attempt was made to incorporate this function into the release pleats (needed on the simple curtain skirts to shed obstacles without incurring skirt damage). For this purpose, the vents were incorporated in the pleats which would be progressively exposed as the pleat expanded. The pleat restraint straps were calibrated so that expansion of the pleat would not occur until needed. Initial operations were satisfactory up to 42,000 lb. and significant taxi tests including cornering, operation in 30 knot wind and traverse of the simulated crater were accomplished. Figure 16 is a photograph of one pleat and straps. There were two in each cell.

At higher weight, the skirt distortion that resulted from pleat expansion in the steady state resulted in unsatisfactory operation and heave instabilities were encountered. The skirt stretch that occurred aggravated the distortion and instabilities occurred at lower weight also in unpredictable random fashion. It was therefore decided to introduce the required venting by incorporating the spring loaded and damped door, with noles through the deck described in the previous section. A further analysis was conducted which included the dynamics of the proposed vent door elements. This analysis was performed by Boeing and is included as Appendix A. Stable behavior was predicted with the vent system operative but not otherwise.

#### 2. CONTROL IN WIND AND ON SIDESLOPE

The ability to hold track was analyzed. A maximum crosswind of 30 knots was considered and aerodynamic sideloads esti-

ACET DESIGN WITH 0.02 FT<sup>2</sup>/PSF CUSHION VENT SENSITIVITY

HEAVE STABILITY INDEX

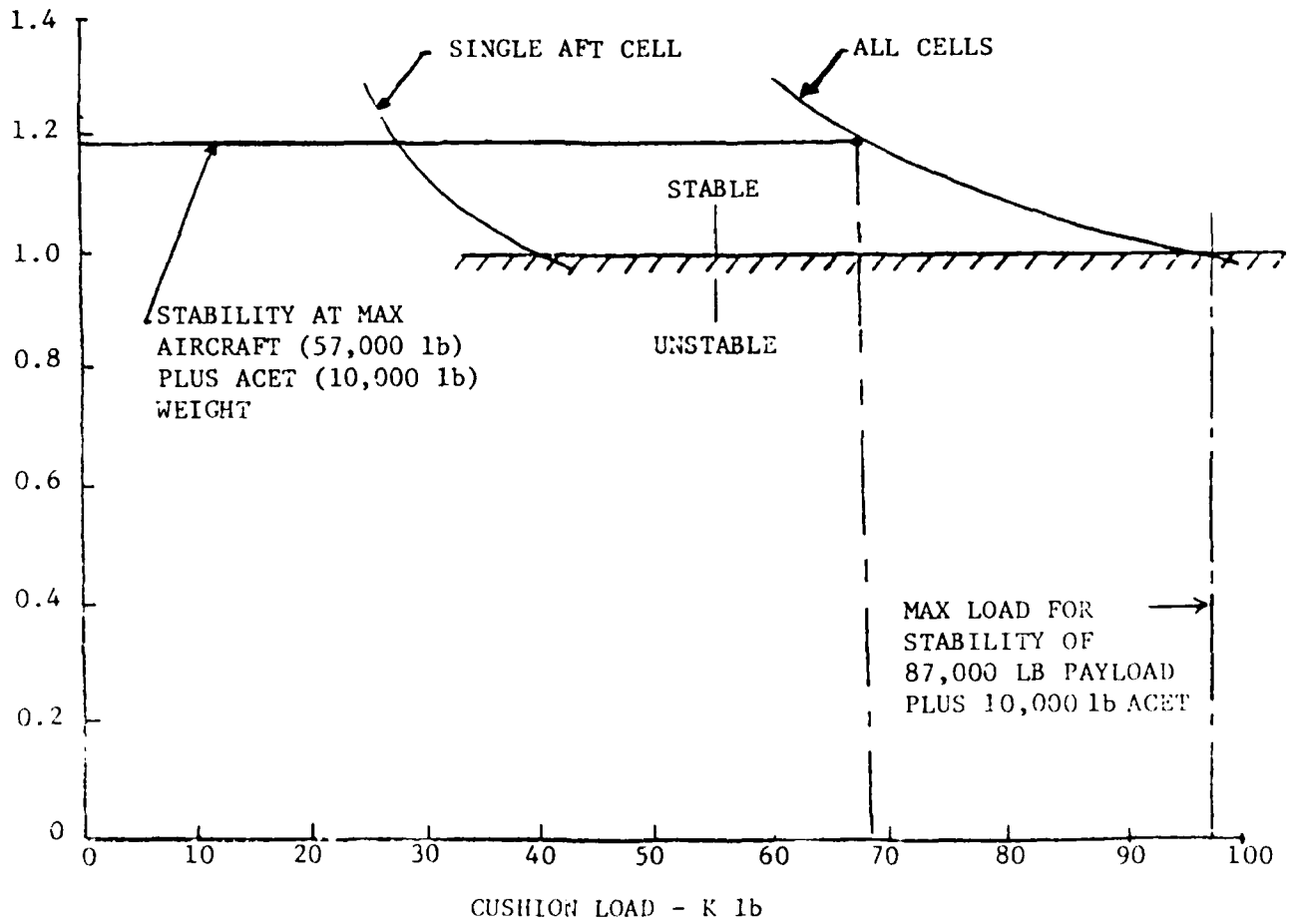


Figure 15. Predicted ACET Stability Boundaries

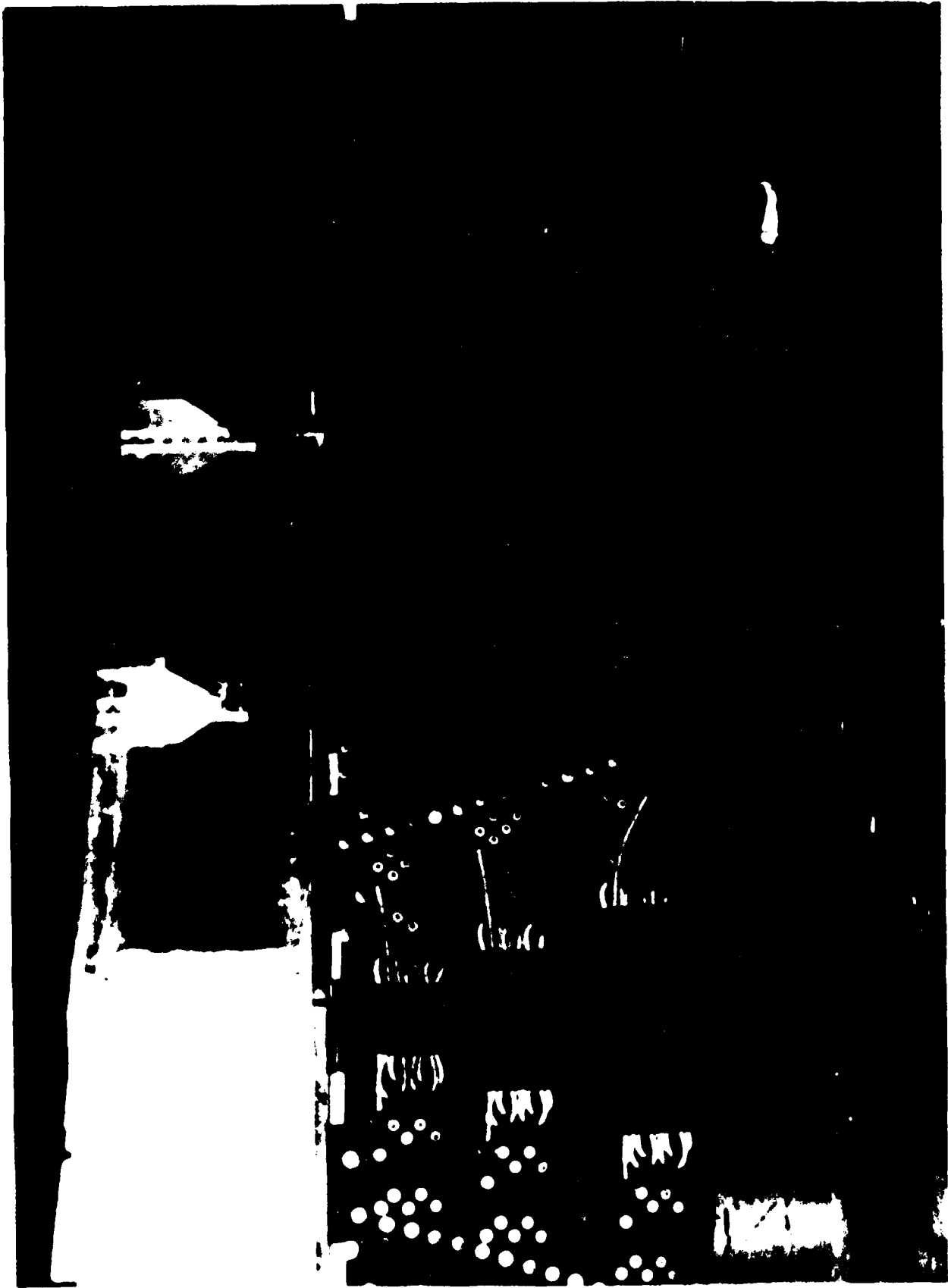


Figure 16. Skirted Plenum Configuration Showing Pleats

mated at 10 and 25 knots forward speed. Trailing wheel and tow hitch reactions were derived. A nominal 1750 lb. download was selected requiring a friction coefficient of up to 0.75.

The cross-wind calculations were based on AATS wind tunnel data which are applicable to an F-4 aircraft but sufficiently representative for this purpose. In any case, the wind tunnel data is available only to  $\beta = 15^\circ$  for the launcher and  $30^\circ$  for the aircraft. Rational extrapolations were used based on similar wind tunnel data on XC-8A in which tests were conducted from  $\beta = 0^\circ$  to  $\beta = 90^\circ$ . Forces and reactions at 25 knots in 30 knot crosswind are shown in Figure 17, calculated from values in the following Table 1.

The maximum wheel side load also limits the tolerable side slope angle. In the typical case, one third of the side load is reacted by the wheels of the tug. Thus, the maximum sideload becomes 2204 lb. which is approximately 3% sideslope.

TABLE 1  
CROSS WIND PARAMETERS

	Aircraft		Launcher	
	40	90	40	90
$\beta$	40	90	40	90
$C_y$	0.58	0.60	-0.01	0.08
$C_n$	-0.35	-0.55	-0.03	-0.04
$S$ , sq ft	530		580	
$c$ , ins	192.5		264	
$c C_n / C_y$ , ins	-116	-176.5	+792	-132
$C S_y$ , sq ft	307	318	5.8	42.4
Resultant $q$ , lb/sq ft	5.17	3.0	5.17	3.0
Relative Wind Sideforce, lb	1587	954	30	127
Tow Hitch Reaction, lb	307	115		
Wheel Reaction, lb	1310	966		

### 3. MOUNTING AND DISMOUNTING

The winch and skirt lift system are the important elements for mounting and dismounting. The winch is only 2 HP which is not considered sufficient for a production system but was selected because no alternative in the 5-10 HP range, electrically

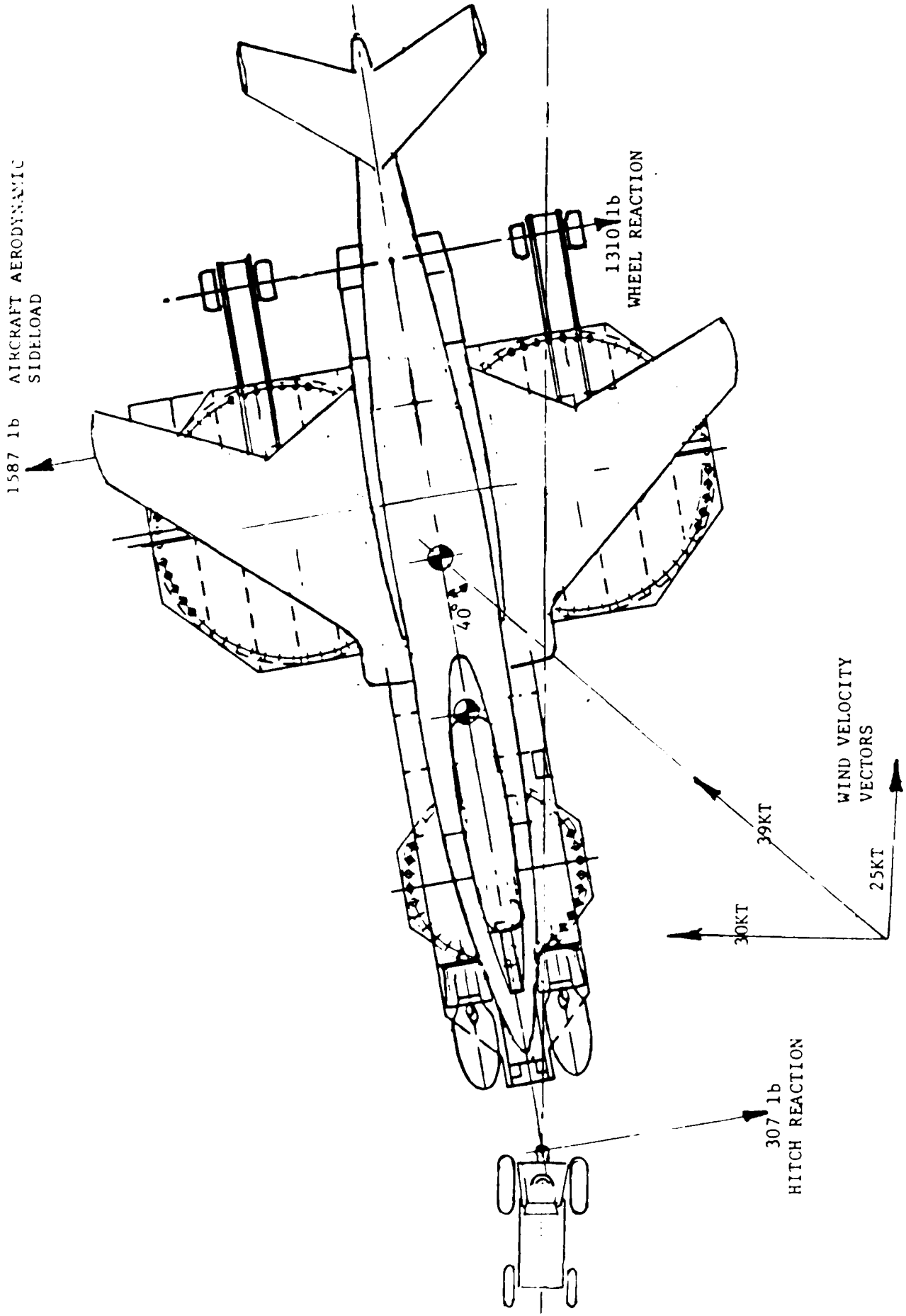


Figure 17. Forces and Reactions in 30 Knot Crosswind

driven from a 24 vdc system, could be found and the complexity of alternatives such as hydraulic drives was not justified (there is no hydraulic pump or system on the ACET). The choice of the low power winch results in slow loading and use of a pulley block to halve the line load. The latter results in an extended length of cable.

Initial calculations in Ref. 1 showed that the aircraft could be towed up a 16° ramp at full gross weight. The main ramps were designed and initially used to mount the aircraft up a single section at 16°. A number of problems and undesirable features were experienced however and these ramps were eventually modified to reduce the angle to 7°. Plane of symmetry forces are shown in Figure 18. The maximum tow load occurs with the main wheels just starting up their ramps, when the airplane attitude results in maximum main wheel vertical reaction. In this case the ramp reaction is  $50,716 \sin 7$  and the rolling friction is  $57,000 \times .02$ . Thus, the total load is

$$6100 + 1140 = 7320$$

for a total cable load of 3660 lb. Cable breaking strength (3/8 in aircraft cable) is 14,000 lb. giving a safety factor of nearly 4.0 which is acceptable. Furthermore, the load can be accepted by the aircraft when pulling directly on the nose gear which has a maximum forward load limitation of 10,000 lb.

For dismounting, if the rolling friction coefficient is 0.02 as was assumed above and is appropriate for high pressure tires then a 2% slope will have the aircraft poised for roll-off or starting to roll. The available attitude with the rear skids grounded and the front skirts inflated is 2-1/2° or 4.3%. Roll off can thus be expected if the skirt lift is effective enough to ground the rear pads. Note that the wheel load is still supported by cushion pressure in the rear cells, thus it does not matter if the center pads are not touching the ground. Further problems were experienced with this however (see Section V.2.b.)

#### 4. CUSHION POWERING

Powering analysis is given in Ref. 1. The ASP-10 engines were selected for the ACET because they were available and suitable. The performance requirements are:

1. Sufficient pressure to permit a margin above nominal cushion requirement to allow for duct loss and vertical acceleration loading at maximum gross weight.
2. Sufficient flow to provide the required terrain/obstacle performance at the same time ensuring satisfactory skirt life.

The F-10 fan map is shown in Figure 19 and superimposed on it is the calculated ACET operating line under throttle control at maximum gross weight. The fan pressure capacity at maximum

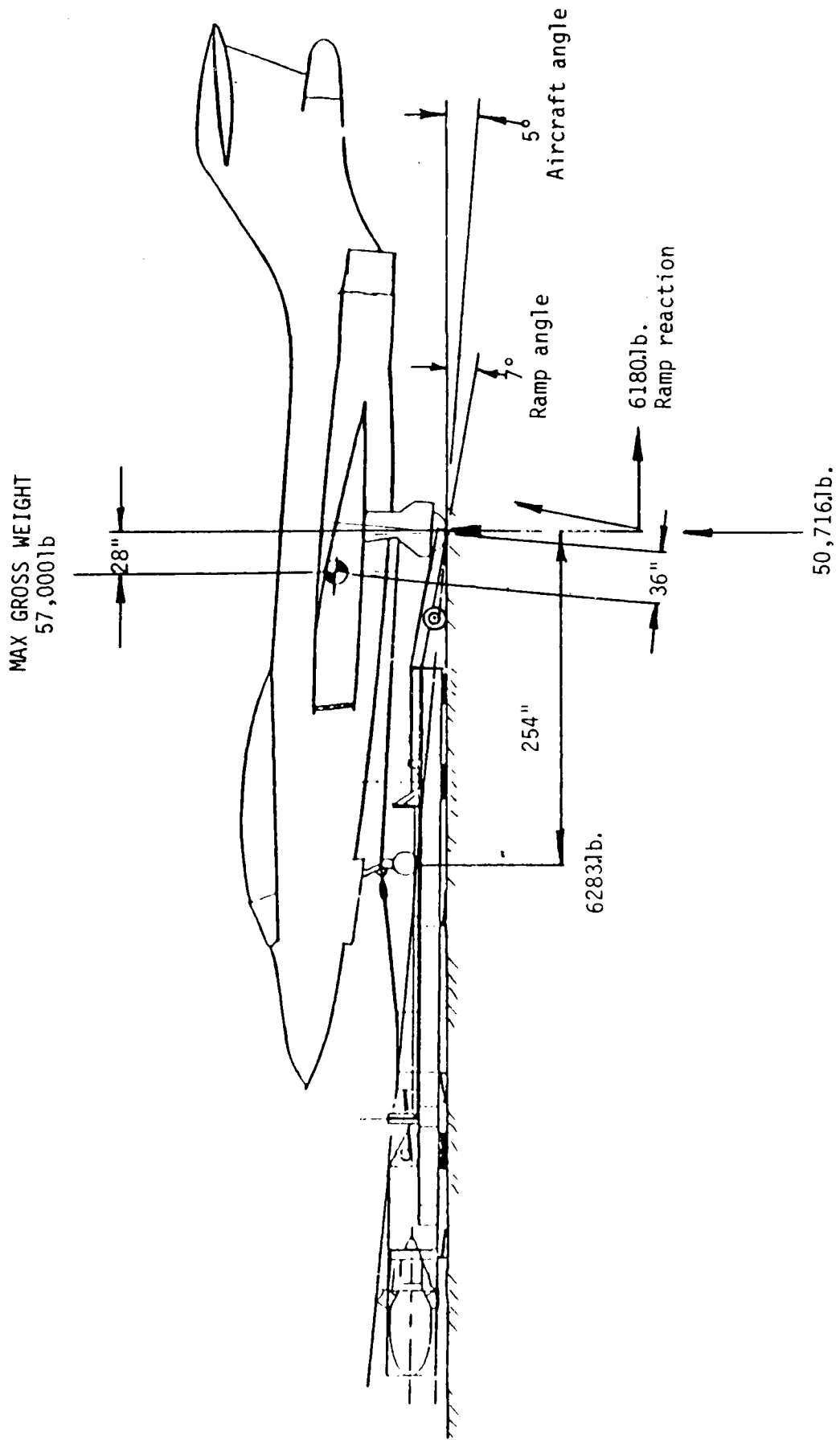


Figure 18. Plane of Symmetry Forces Mounting 7° Ramp

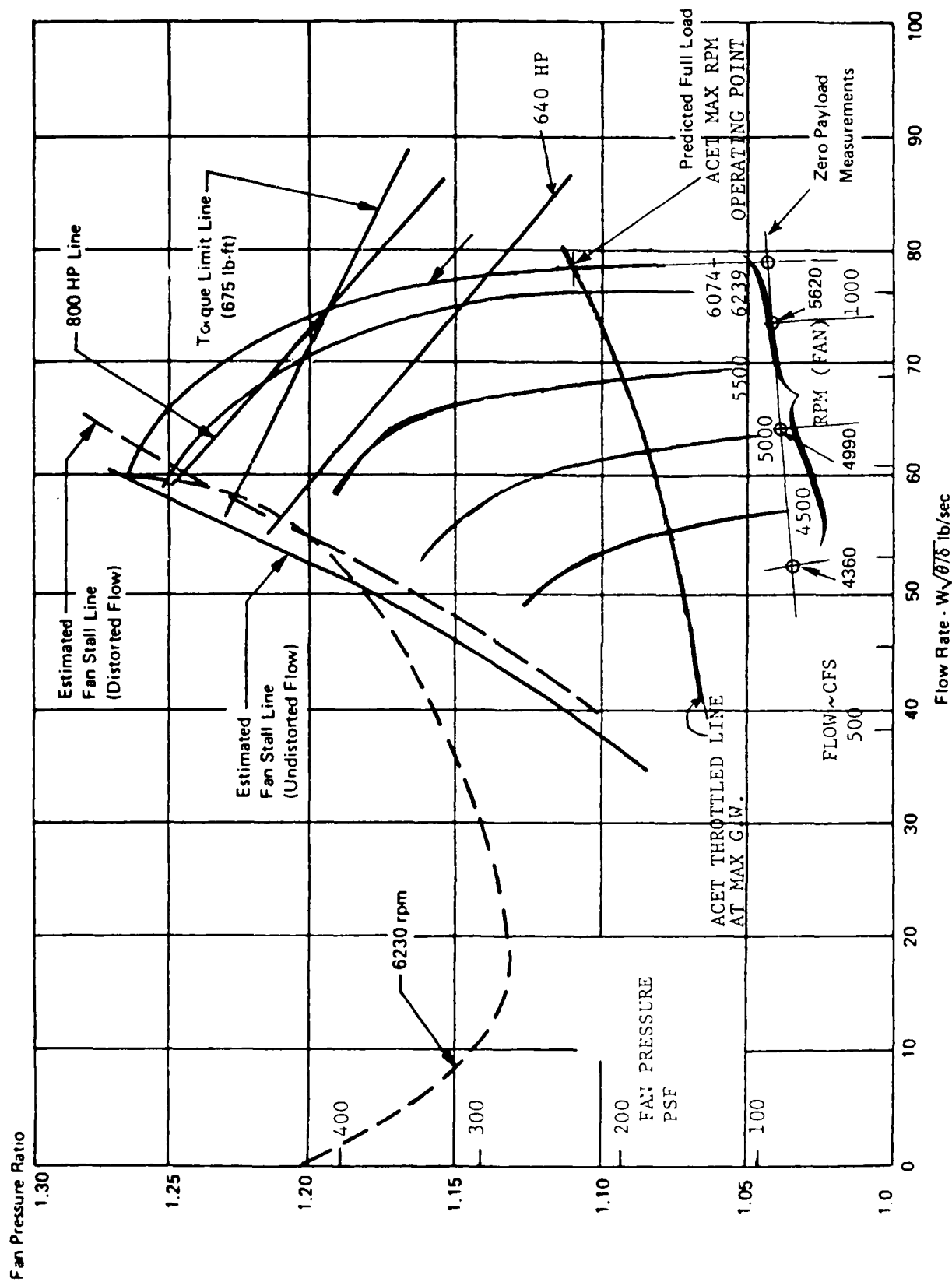


Figure 19. ASP-10 Fan Characteristics

rpm greatly exceeds what is required to provide sufficient pressure to support the full weight based on an analysis of duct loss. Well over 2 g can be accepted without fan stall. But the available flow from one fan at maximum rpm is calculated to be insufficient to maintain low drag (hence low skirt wear) on all surfaces of interest. For this reason two engines were used, for a total maximum flow of 158 lb/sec.

To perform the calculation the internal pressure losses are needed. In the design phase, these were estimated incrementally and are summarized on page 48 of Ref. 1 as follows:

	Losses lb/sq.ft.	
	Nose Cell	Main Cells
Fan diffuser loss	32	32
Nose distribution	22	--
Main duct drag	--	33
Gross distributions	<u>--</u>	<u>51</u>
TOTALS	54	116

The losses were calculated for a total airflow of 1830 cu.ft./sec. at a density of 0.082 lb/cu.ft. For the fixed duct geometry, loss is proportional to the square of airflow since the pressure loss coefficient  $\Delta p/g$  is constant.

In the early test phase of the ACET, measurements of internal duct pressure were taken at a series of stations, identified as a to x on the chart Figure 20, which gives this data and also the cushion pressures and daylight clearances or air gaps for 100% rpm. Similar data was taken for 70, 80 and 90% fan rpm.

The air gap data was used to calculate volume flow making a broad assumption of discharge coefficient. Air gaps are shown against longitudinal position in Figures 21a and b. The mean values used are plotted against rpm in Figure 22. Cushion pressures are plotted in Figure 23. To calculate flow, jet velocity is obtained from cushion pressure:

$$V_j = \sqrt{\frac{2}{\rho} \times pc}$$

and effective area from gap, perimeter and discharge coefficient

$$S_j = h_j c_j C_D$$

Hence volume flow  $Q = \sum_j S_j V_j = \sqrt{\frac{2}{\rho}} pc \times \sum_j h_j c_j C_D$

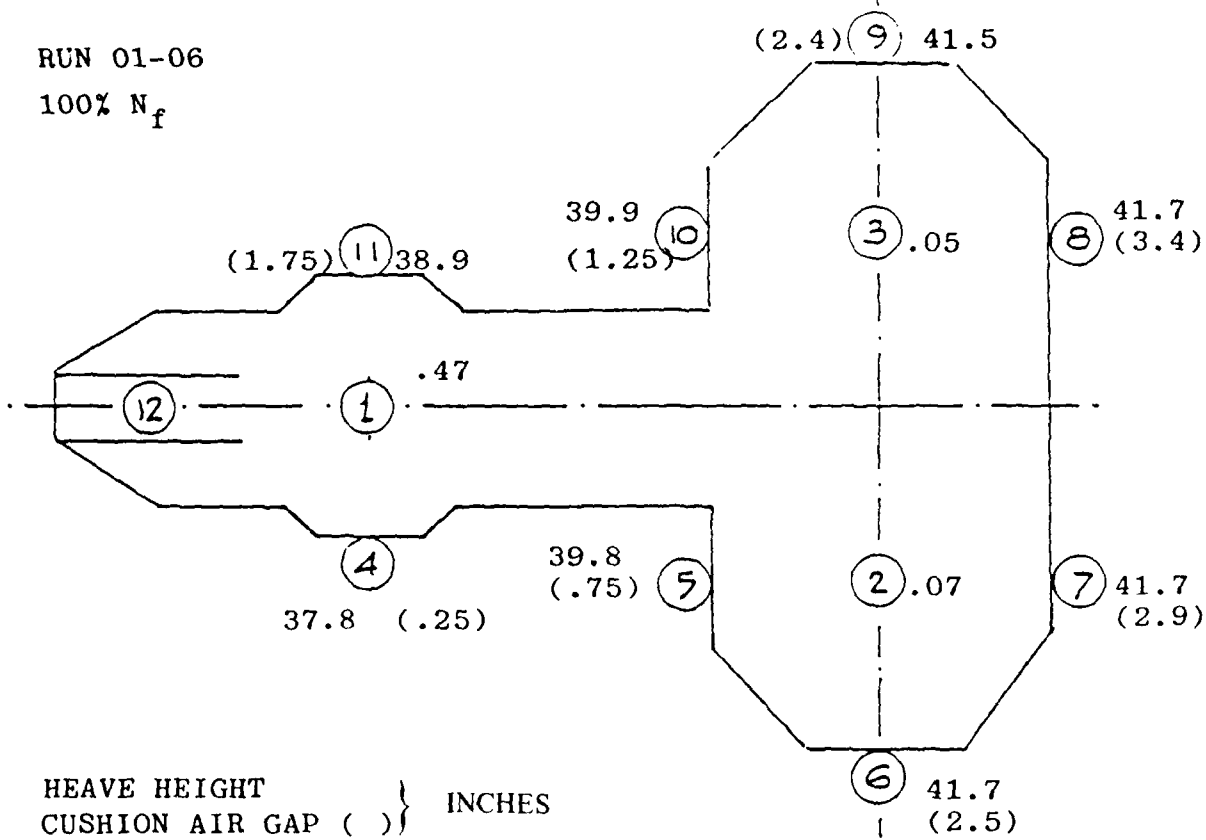
- Q = airflow, cu.ft/sec
- $\rho$  = density = .0025 slugs/cu.ft.
- pc = cushion pressure, lb/sq.ft.
- h<sub>j</sub> = measured jet height, ft.
- c = perimeter, ft.
- C<sub>D</sub> = discharge coefficient = 0.65

D

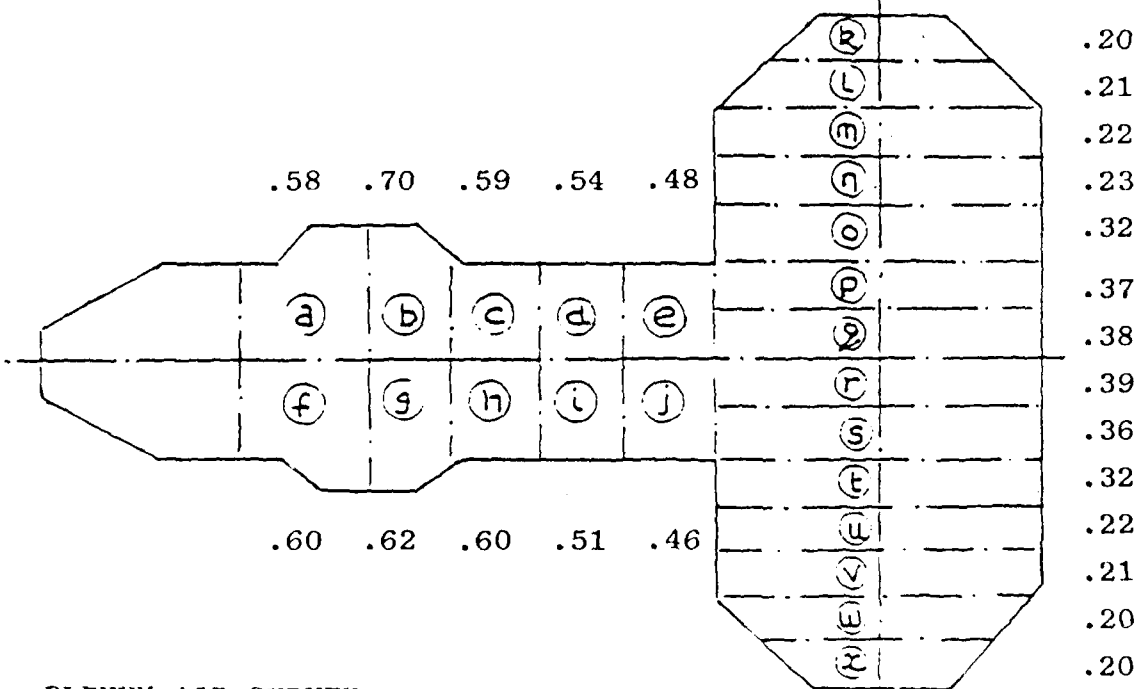
12. TEST DATA ACQUISITION POINTS

RUN 01-06

100%  $N_f$



HEAVE HEIGHT  
CUSHION AIR GAP ( ) } INCHES



PLENUM AIR SURVEY  
(P.S.I.G.)

Figure 20. Duct Pressure and Heave Survey

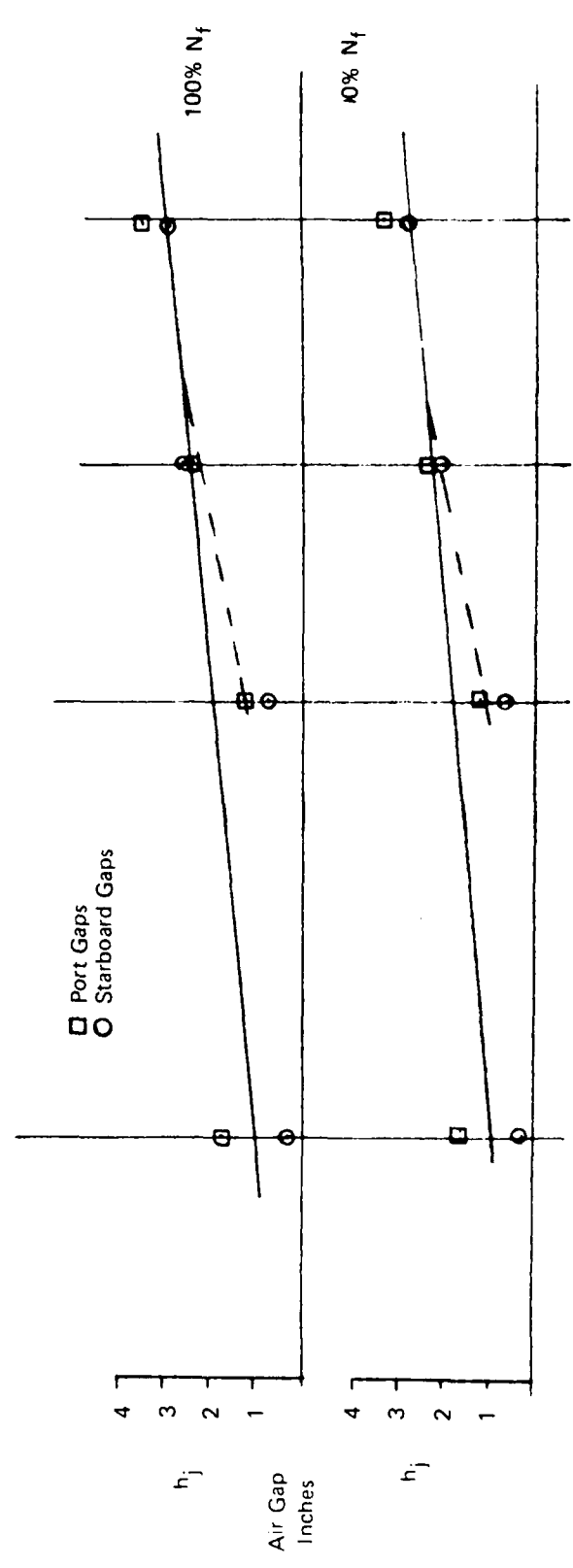
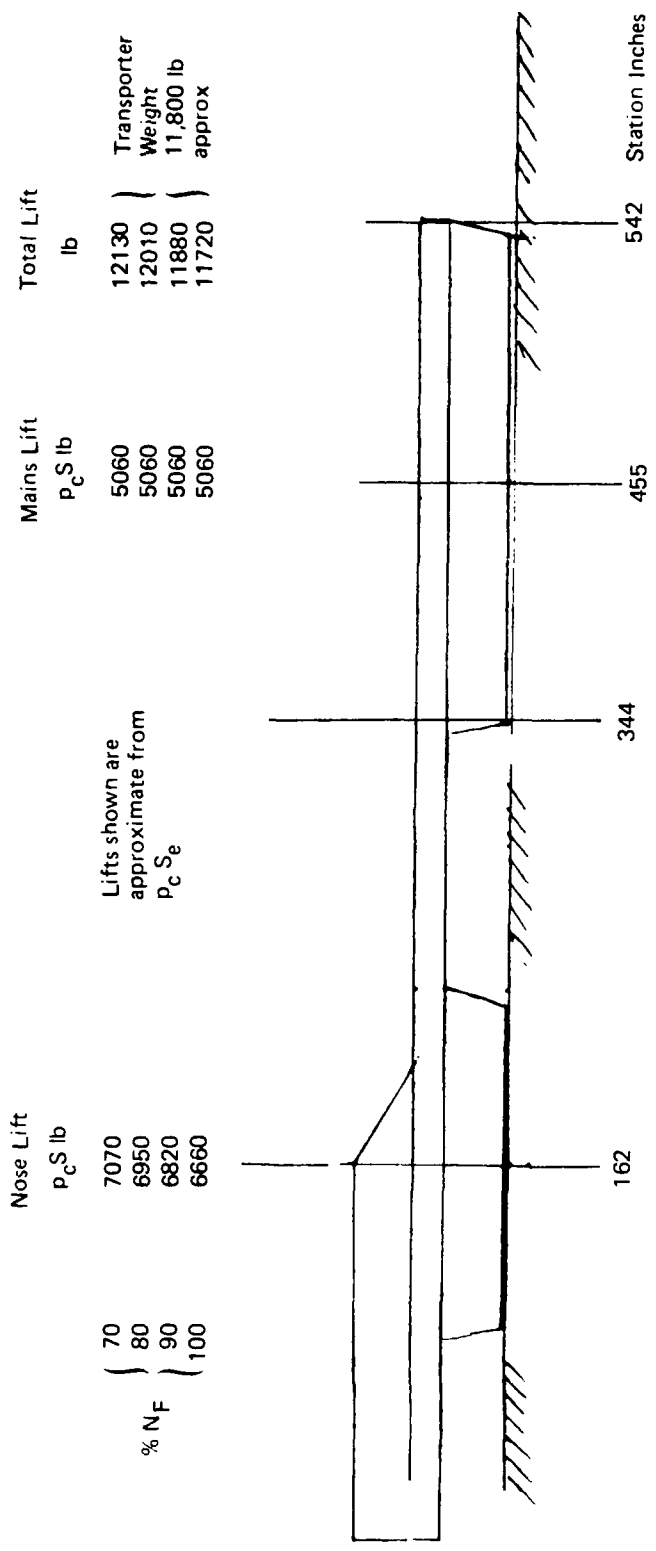


Figure 21 (A). ACHT Air Gaps at Skirt Stations (Plenum Skirts) Zero Payload: May 1983

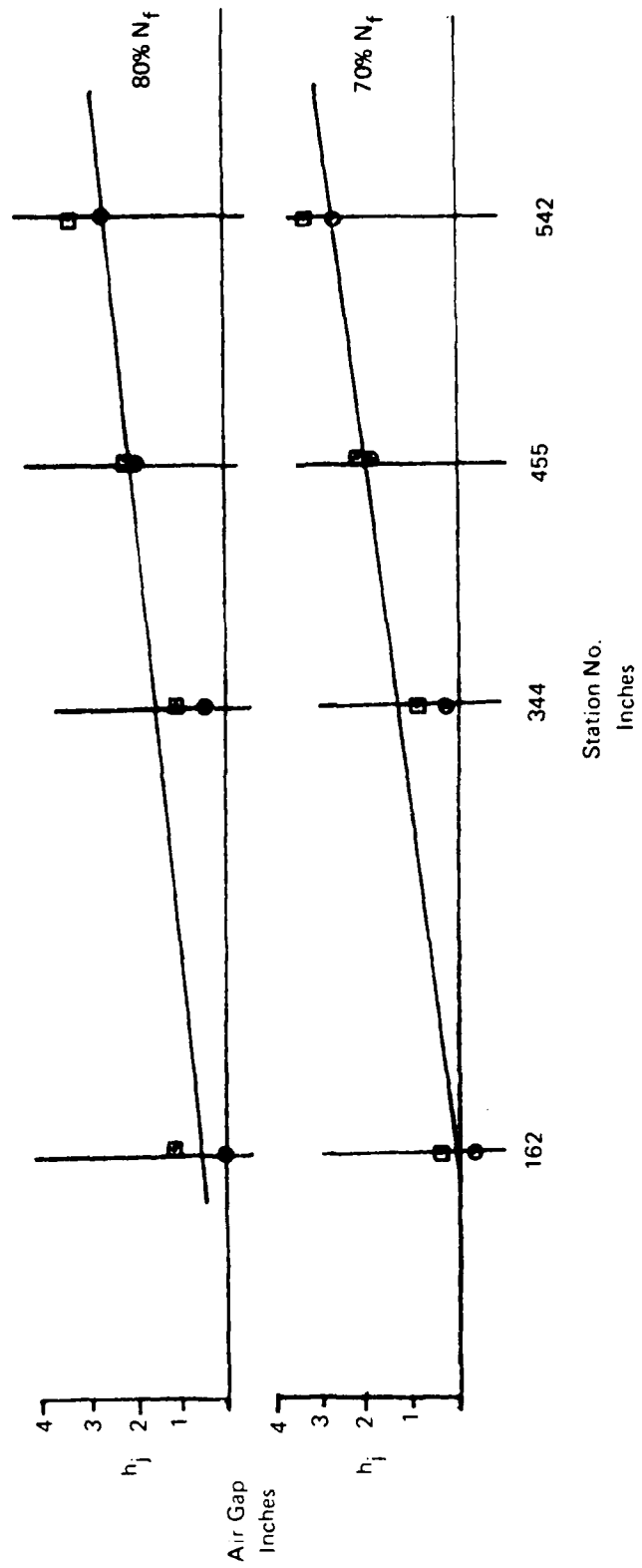


Figure 21 (B). Air Gaps (Contd)

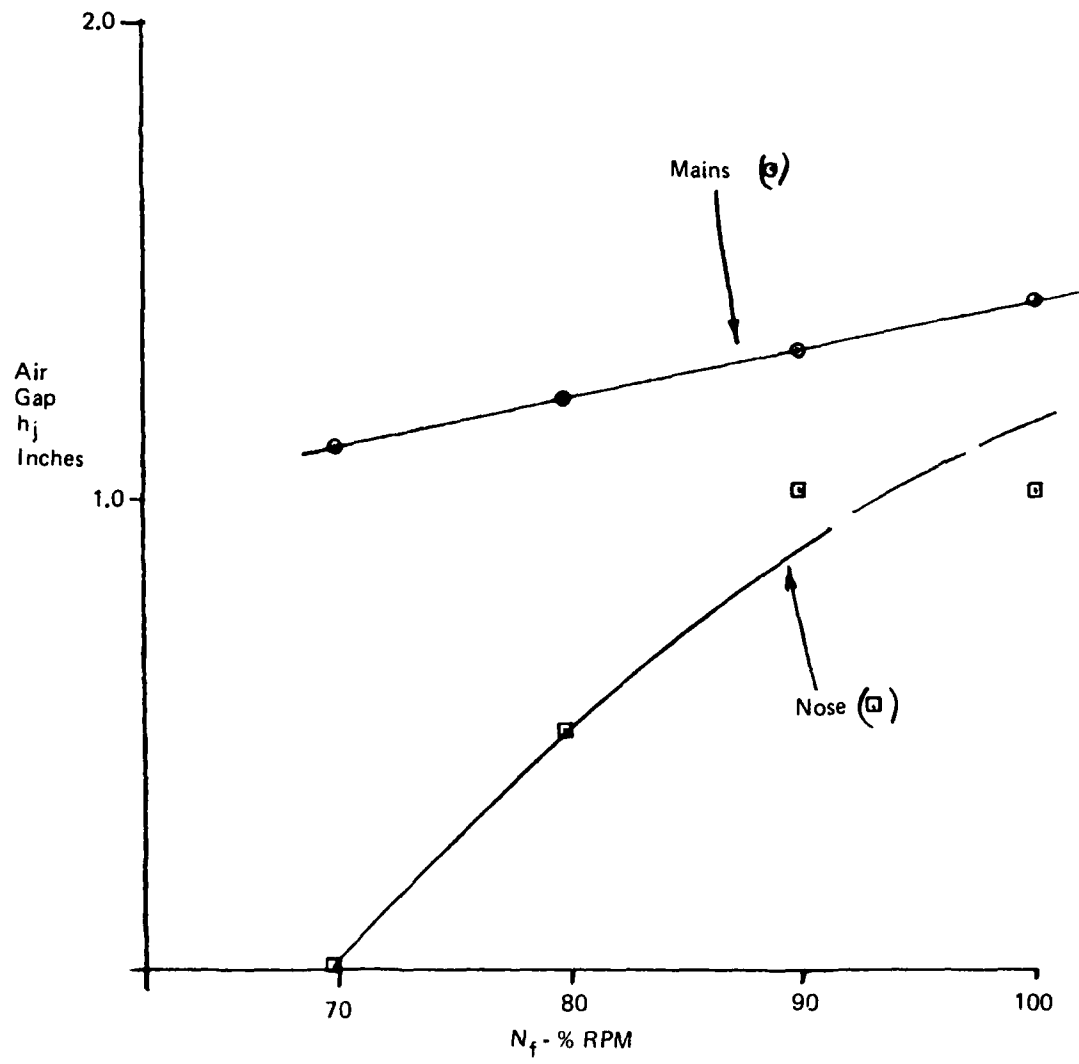


Figure 22. Variation of Air Gap With Fan RPM ACET Zero Payload

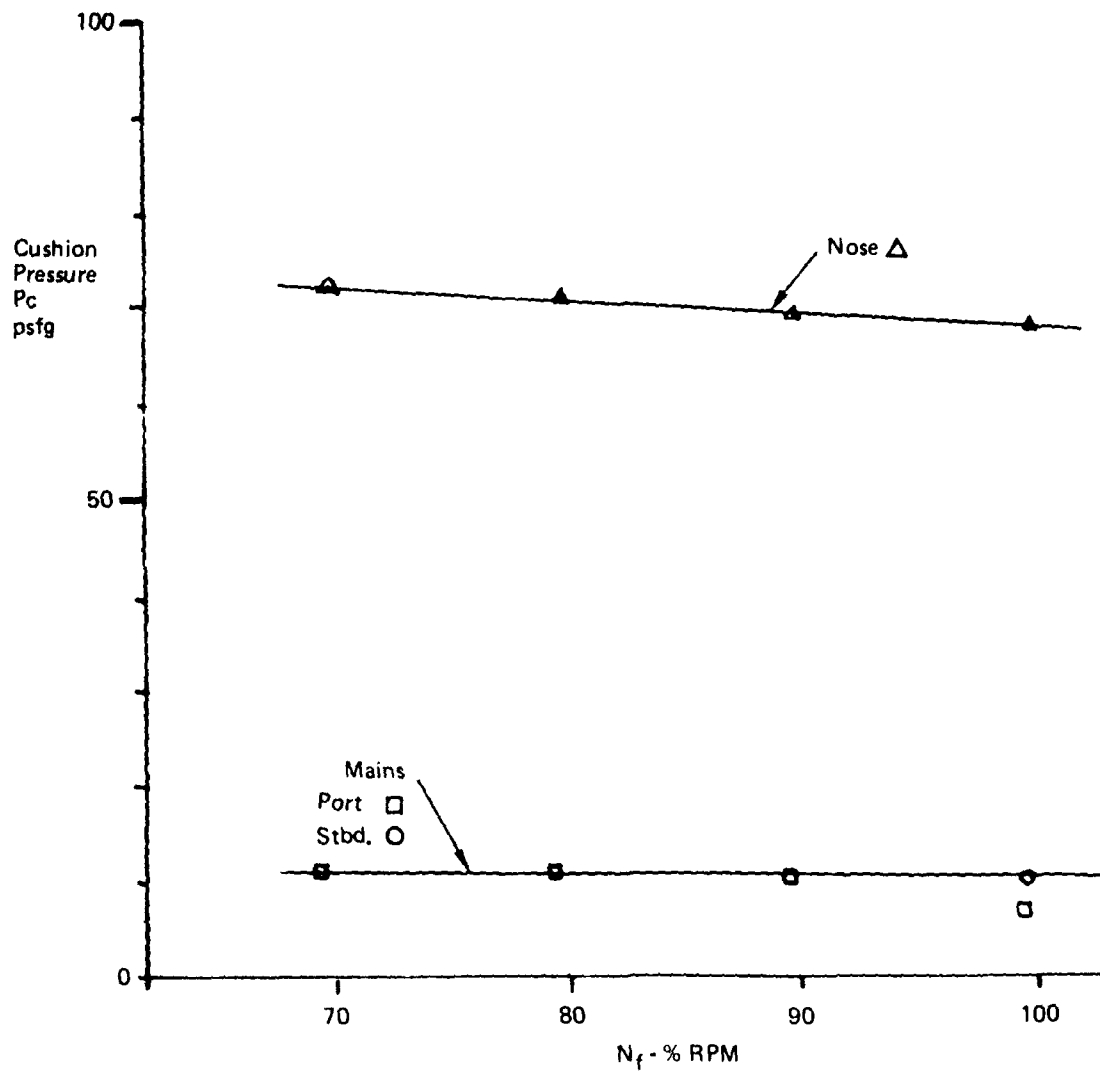


Figure 23. Variation of Cushion Pressure With Fan RPM  
ACET Zero Payload

A discharge coefficient of 0.55 was assumed in the design phase but 0.65 gives better correlation with test results. On this basis, flow is plotted against fan rpm in Figure 24 which also shows total flow against rpm after adding in ST-6 engine flow from the manufacturer's data shown in Figure 25.

Measured pressure drop through the system is given in Figure 26 from which fan pressure ratio is estimated after adding an initial diffusion loss in accordance with the estimate in Ref. 1 (this was not measured).

The flow pressure ratio and rpm for this zero payload case are then transferred to the known fan map. Estimated zero payload performance from Ref. 1 is also compared with the test data in Table 2. Fan rpm's on the fan map and estimated parameters in Table 2 are in good agreement with this analysis.

**TABLE 2**  
**COMPARISON OF AIR CUSHION CONDITIONS**

	Transporter		Cushion Pressures		CD = .65 Daylight Clearances		Jet Velocities		Cushion Flows	
	Weight lb	C.G. Ins.	pcN PSF	pcM PSF	hjN Ins.	hjM Ins.	VjN Ft/Sec	VjM Ft/Sec	QN CFS	QM CFS
Estimate	11,600	297	64.2	11.5	1.07	2.45	225	95	460	1380
Initial Test	12,130	282.5	68.0	10.5	1.15	2.4	240	97	520	1390

The pressure losses in Figure 26 show a maximum loss of 66 psf for the duct compared to the estimated 84 psf which is approximately 20% lower than the estimate. The variation of loss is found to be proportional to the square of the flow ratio as expected, providing some confirmation of these flow values. The following table shows this:

**TABLE 3**  
**INTERNAL PRESSURE LOSS AND FLOW**

NF % RPM	Flow CFS	Loss 'b' to 'k'	Loss Ratioed to 70% N
70	1220	.355	.355
80	1275	.40	.39
90	1330	.42	.42
100	1388	.46	.46

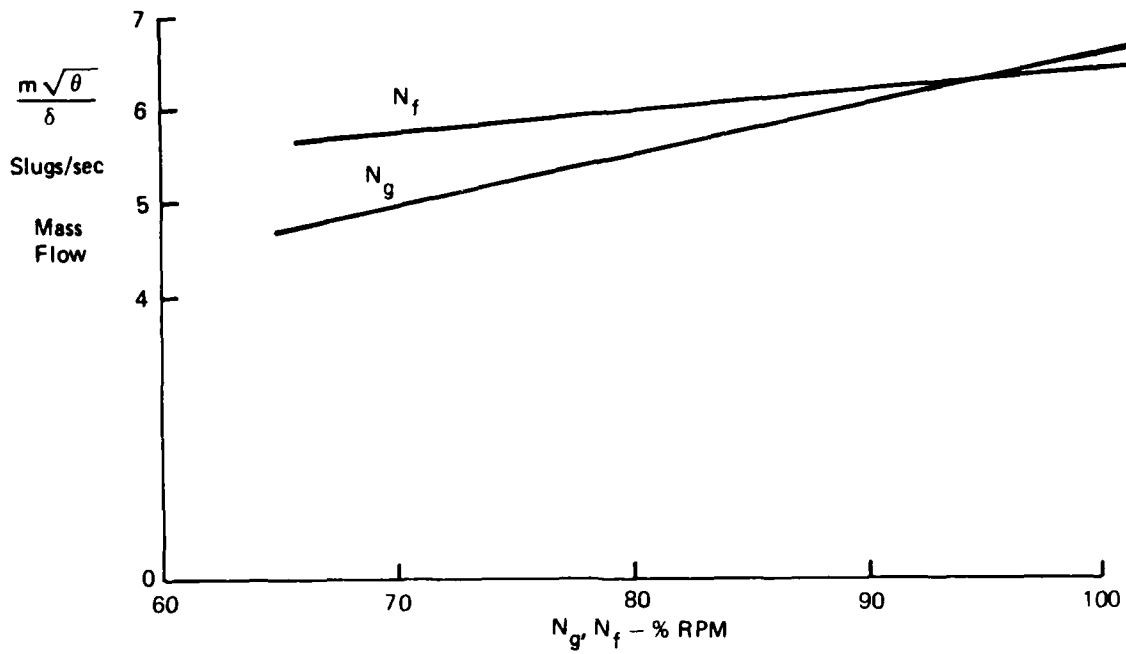


Figure 24. Volume Flow Versus Fan  $N_f$  and Compressor  $N_g$  % RPM

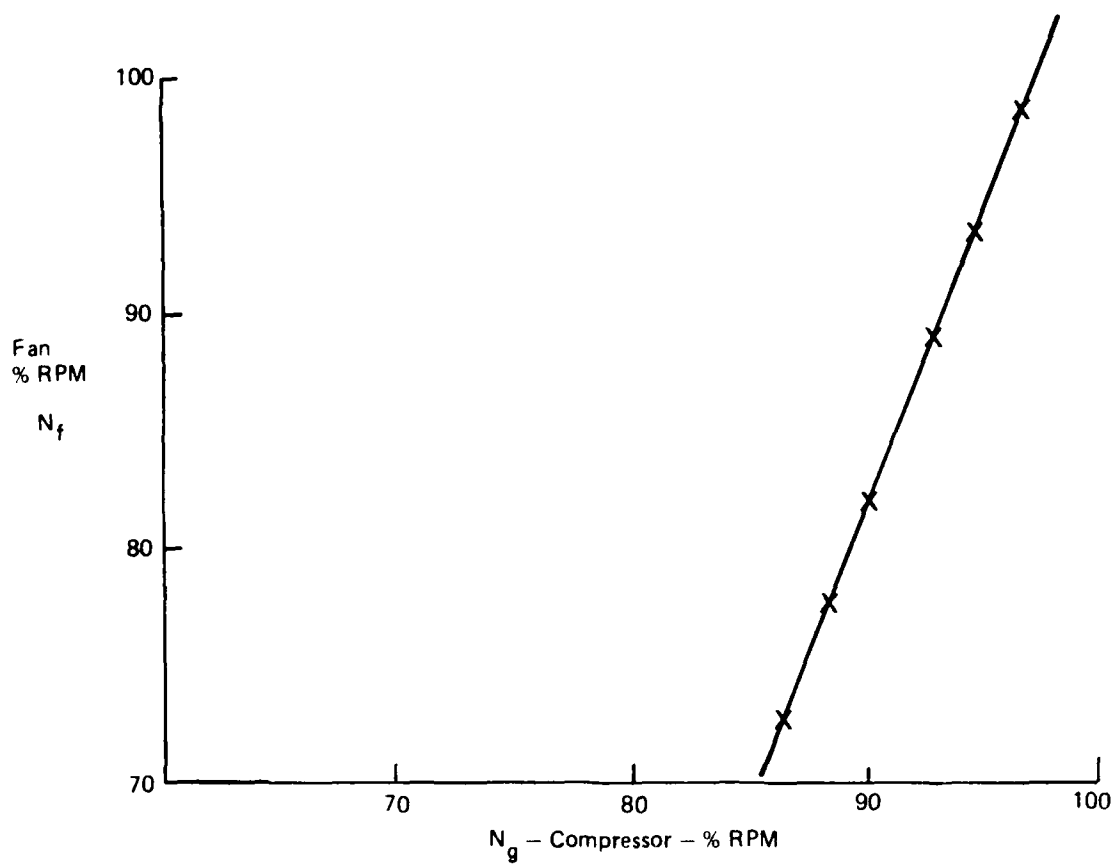


Figure 25. ST-6 Engine Flow Data  $N_f$   $N_g$

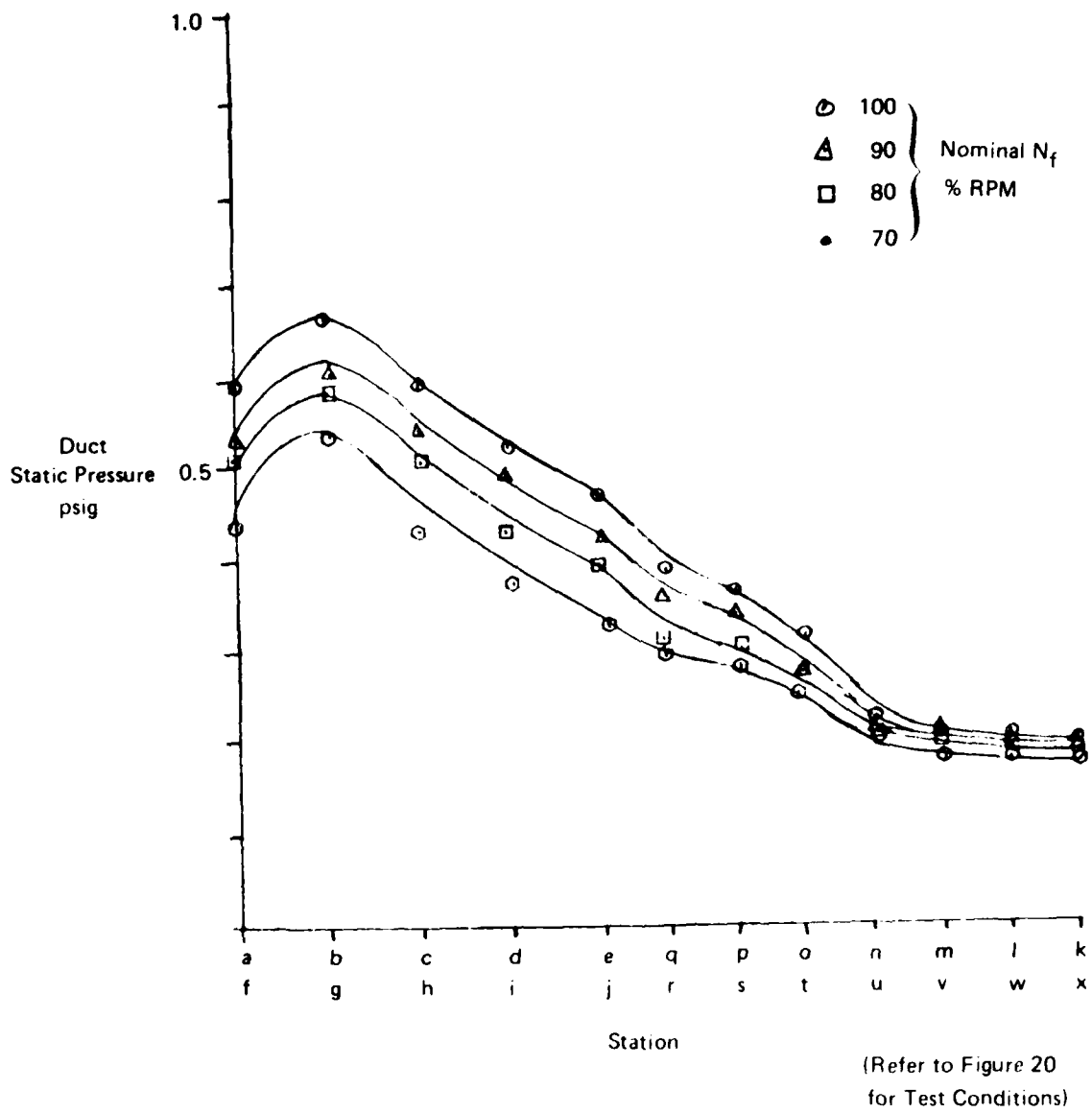


Figure 26. ACET Internal Duct Pressure Survey

## SECTION IV CONSTRUCTION PHASE

### 1. CONSTRUCTION

Construction was simple and straightforward and the ACET was built in 3-4 months. A single jig (Figure 27) was used for the basic structure to hold panels in place during welding operations and avoid distortions. Each module in turn was built on this jig. Panels were prepared at Bell's Niagara Falls Operations using the automatic welding equipment developed for LACV-30 (Figure 4). All panels were made from the same thickness aluminum hollowcore planks so that there were no different types to complicate matters. The panels were either 9 or 10 planks wide, six being required for basic decking with an extra one for internal members. The design was based on the completed 9 or 10 panel widths so that no width trimming was needed. An open box without the top deck was first prepared and completely welded, including cap extrusions on all internal bulkheads. Inside welding of the top plating was not possible because of the shallowness of the structure (15 in.). This was therefore fastened with "Huck" bolts through the caps, using an 1/8 in thick reinforcing plate on the outside to take the bucking pressure.

After all modules were completed they were individually rolled over to top-side up and assembled to each other (while supported on 50 gallon drums) by bolting them together with splice plates as shown in Figure 5. To complete the structure, the wheel tracks were then assembled. These were constructed as separate sub-assemblies concurrently with the modules. The wheel tracks are bolted in place to Z-sections which are welded to the modules. The main tracks cross the rear module splice and the nosewheel track crosses both splices, and both additionally tie the structure together.

Ahead of the platform proper the structure consists of a box beam, approximately 30 in square cross-section, from which the engines are hung, one each side. Air is ducted through filters (both barrier and momentum) within the beam to feed the engines. The same mounting parts as were used on the XC-8A were used on ACET to mount the engines, one either side of the box beam. Inside the beam at appropriate locations, diagonal truss bulkheads built from 2 in x 4 in rectangular cross-section aluminum tube are welded in place to support the mountings which consist of cradles with drag struts and V-strut stays (see Figure 28).

It remained to install skirts and other detail systems such as fuel, winch, etc. The skirts were fabricated in the BACT skirt shop by developing the necessary flat patterns for the fingers on mylar, cutting the material (which is done on a flat bench with an electrical machine knife manipulated by hand) and riveting to form the finger (which requires no special tooling).

From the foregoing, it is clear that the ACET construction was a straightforward task.



Figure 27. ACET Rear Module on Assembly Jig

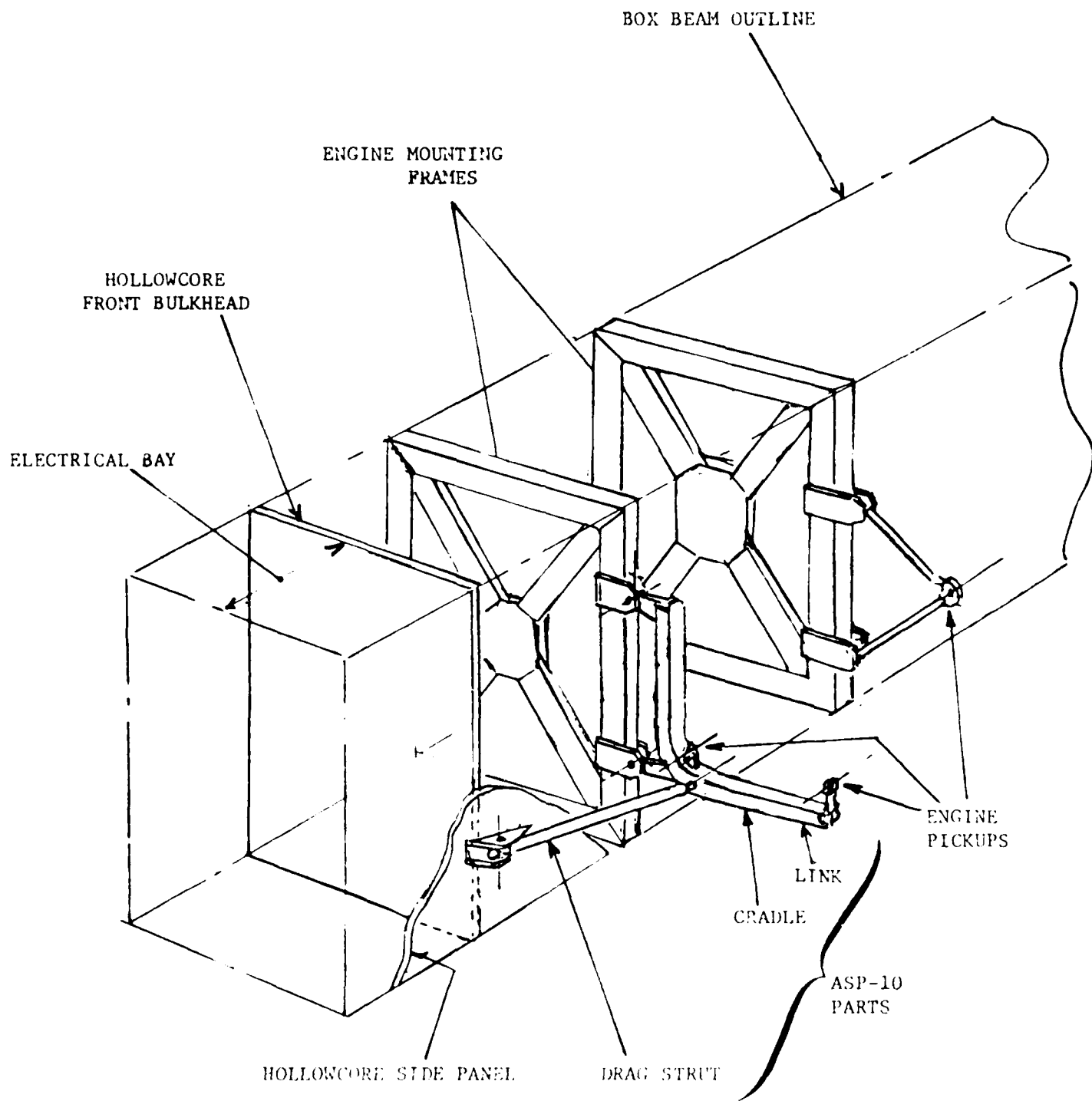


Figure 28. Perspective of Engine Mounting

## SECTION V

### DEVELOPMENT PROBLEMS

The initial test phase included the static flow and cushion performance measurements discussed earlier; partial rough grass operation (one cell over the grass); operation across the simulated crater, including traverse of a considerable area covered with 1/2in. pebblestone; mounting and dismounting the aircraft and operation over blacktop; and negotiating turns at 15 mph in winds gusting to over 30 knots.

Both major and minor development problems were identified/rectified in this phase.

#### 1. MINOR PROBLEMS

a. The PT6-70 engines forming part of the ASF-10 engine fan combination are configured with dual exit jet exhaust ducts. These ducts were selected for the engines to suit their installation on the XC-8A aircraft. Located in the vertical plane the ducts are less than ideally positioned for application on the ACET, since the lower duct is only six inches above the ground when the engines are run at idle rpm. The prospect of changing the ducts to a single outlet configuration similar to that employed on the PT6T-76 engines was examined. Implementing this change was prohibitively costly in terms of both money and time and the simple more cost effective method of providing a diverter duct to eject the lower exhaust gases out and to the side of the vehicle was adopted.

b. It was found that starting engines independently was not desirable due to high loads being placed on the second engine starter. Since both engines feed air into a common plenum, when only one engine is run, excess air escapes through the fan of the inoperative engine, driving it in the reverse direction, necessitating the starter motor having to perform the function of a brake to arrest the reverse rotation before it can commence the start cycle. While this does not affect the automatic start system it does prolong electrical current draw by the starter motor leading to overheating. To preclude the possibility of damaging the starter motors, simultaneous engine starts were made. These are quite practical with adequate ground power and were adopted as standard practice.

c. The fan screens were sucked in after becoming clogged with long grass. This is a familiar problem with an unfamiliar but nonetheless convenient solution found later. After a period of running on the type of surface that generates the problem, the ACET is paused and IDLE selected on one engine. It spools down and the fan eventually stalls and the backflow from the pressurized plenum clears the screen of grass buildup. This is then repeated for the other engine and the ACET is ready to proceed. It is noted that this blockage problem would not occur if a type of fan sufficiently tolerant to omit the screens were used.

d. In the initial towed tests with the single trailing wheel assembly, the trailing wheel assembly broke away after sustaining a lateral impact on a six inch high ridge. This incident occurred in a slipping turn in a 30 mph cross wind with the aircraft mounted on the transporter at the light gross weight. A simple modification to the method of securing the ramp was devised and subsequently incorporated into the design of the twin wheels ramp arrangement.

e. Despite the screens, slight fan blade damage was observed after traverse of the gravelled area. Additional screen fences were added later but no effort was made to explore their efficiency by deliberately risking further fan damage. The original screening as seen in Figure 6 was retained and the added fence can be seen in Figure 29.

## 2. MAJOR PROBLEMS

The major development efforts were related to the skirt system, stability augmentation and rapid mount-dismount. These items required considerable rework and some retest and the program had to be restructured to include them.

### a. Skirt System and Stability

Initial runs with the first skirt set and the aircraft at 30,475 lb. gross weight were satisfactory. From then on the skirts deteriorated, apparently because they stretched and it was concluded this was contributing to the dynamic instability heave problems which arose. Thus, skirt development and dynamic stability improvements run parallel. A second set of skirts was fitted with the design changed to increase the inward taper angle. Thicker material was also used to prevent unwanted skirt stretch. The second set was not very much more successful than the first and the craft was plagued by a violent oscillation at 6 Hz which occurred in unpredictable circumstances, but always over a hard surface. It was also evident that the inflation capacity of the skirts was defeated by a ridge of swept blacktop pieces. The problem of loose blacktop pavement may be discussed here relative to ACET operational use. As a problem, it is important not to overstate it. First, if the ACET primary mission is to transport aircraft off runway and deposit them at a strip of remaining high quality concrete, there will be no encounter with this type of surface. Secondly, for the problem to arise (and it has been experienced in the past with other ACV's) the surface must have a sufficiently deteriorated condition to allow the cushion air to pump beneath it. The runways and taxiways at Grand Bend are old (WWII) blacktop with weeds and grass growing in the cracks (Figure 30). This surface can be traversed by the ACET substantially without damage although a prolonged hover over a weak area may cause the problem. In the tests with the F-101 the worst conditions were created by the initial damage to the surface caused by the aircraft's high pressure (200 psi) tires.



Figure 29. Nose of ACT F Showing Inlet Fence and Exhaust

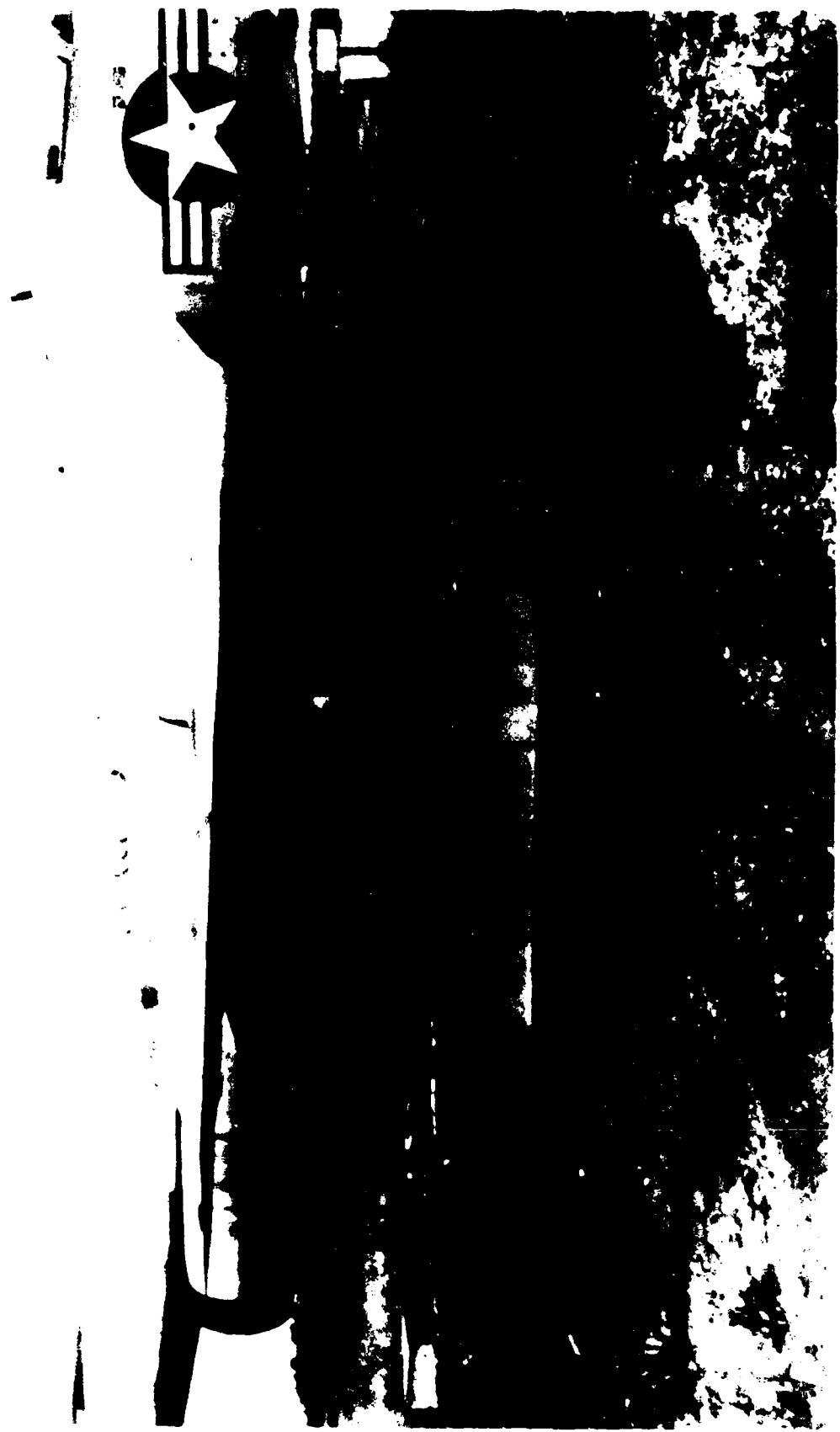


Figure 30. Typical Grand Bend Runway Surface with ACFT and F-101B

Efforts were made to use the steel load spreaders seen in Figure 31 but this was not always possible and greatly complicated mount/dismount procedures. On several occasions (at high weight particularly) the tires sank 8"-12" into the surface. Tow out soon becomes impossible and the aircraft must be jacked. Further traverse of the damaged area by the ACET then soon accelerates the problem (Figure 32), and it was sweep-up of this type of loose material inside the ACET skirts (to which the plain skirt would not conform) which gave the strongest indication that full depth fingers were required.

The system for passive cell venting identified in Appendix A was tried in combination with the second set of skirts. Improvement appeared to have been made and the vent doors actively responded to a 2 Hz oscillation, which was relatively mild. They did not, however, effectively correct the problem. It was realized that the system is basically wasteful with a deliberate constant bleed of cushion air occurring. Parallel development of an active system applied at model scale reported in Reference 1 has demonstrated the practicality of such a scheme. It is confidently expected that the ACET as it stands could be effectively damped in heave by such a system. Meanwhile the 6 Hz oscillation not predicted by the Appendix A analysis still occurred. The passive vent system was ineffective to control this and in any case a detailed analysis showed that the material frequency of the vent doors was of the same order as the oscillation.

The source of the 6 Hz oscillation is still not clear. It is presumed to be related to some phenomenon not included in the analysis. Candidates are the twin engine/fan installation which was only modelled mathematically as a single unit, the spring force of the trailing wheels which was not modelled, and the modal characteristics of the ACET/aircraft combination.

The stability in heave was generally of the same character when the finger skirts were fitted, with two oscillatory modes persisting:

- (1) A gentle limit cycle float of small amplitude at about 2 Hz.
- (2) A violent limit cycle divergence at about 6 Hz.

It was realized that the real need was to effectively desensitize the cushion pressure to height change. In all probability the use of a centrifugal fan with a flat pressure/flow characteristic would result in a radical improvement but this was not practical for the ACET prototype. A vent system at the base of the finger skirts was therefore indicated. Consideration was given to trimming the bottom of each finger to an arch, which had been reported as effective in some model tests, but the more positive method of punching a hole pattern in the front face (skin) of each finger was preferred. This has adequately suppressed the 6 Hz divergence which has not been observed since in



Figure 31. F-101B On ACET Showing Load Spreaders



Figure 32. Damage Caused by F-101B Wheel

tests up to full payload of 60,000 lb. and over the full range of power and fan rpm. The hole pattern adopted is a compromise providing a similar vent area (approximately 1 sq. ft. effective area/main cell) by using fairly large (1.0in.) holes in every fourth finger. The holes also provide a measure of air lubrication on a flat surface. This could be optimized by the use of smaller holes, venting every finger for the same total area.

b. Rapid Mount/Dismount

The modification to improve the mounting of the aircraft was the introduction of the folding main ramps. This proved successful, but the inadequacy of the winch to haul the aircraft was still in evidence. In the earlier tests a number of winch failures occurred, thought to be largely due to structural deflection of the winch mounting structure. This structure was drastically reinforced but the winch was still marginal for mounting the aircraft at maximum gross weight even with the lower ramp angle. Efforts should be made to replace the existing unit with a more powerful one. A mounting load of approximately 7000 lb. was measured, corresponding to the calculated value for the ramp angle of 7°.

The modification to improve dismounting was the introduction of the skirt lift system to provide a roll-off angle. The skirt lift system was marginally successful, difficulty being experienced in achieving the necessary angle to start the roll-off. This is due to insufficient retraction of the fingers with failure to ground the rear of the ACET on the rear landing pads. Two solutions appear to be practical.

(1) Increase the depth of the front skirts 3 in. This would increase the slope of the deck by 1% for an additional force component of 1% of the aircraft gross weight. An increase of the roll-off force of the order of 50% would be achieved. The slight attitude change is not expected to affect transport operations.

(2) Improve the finger retraction. Two developments are thought to be necessary.

(a) Change the cable runs for more effective lifting. Recent model experiments indicate a possible method is to use two lift points on the finger, one on either side of the center line on the rear closure panel. (Only the fingers with rear closures need to be lifted.) These lines may then run laterally across to the front face and through to the outside of the shin of the knee shaped finger and around the knee before being joined together, being retained in position by eyelets fastened to the fingers. Figure 33 displays this method. It is emphasized that alternatives are easily conceived, the point being that a satisfactory method can only be reached by full scale experiment, which should be guided by model test.

(b) Double the size of the retraction cabling. The selection of cable weight is judgmental. Minimum weight is

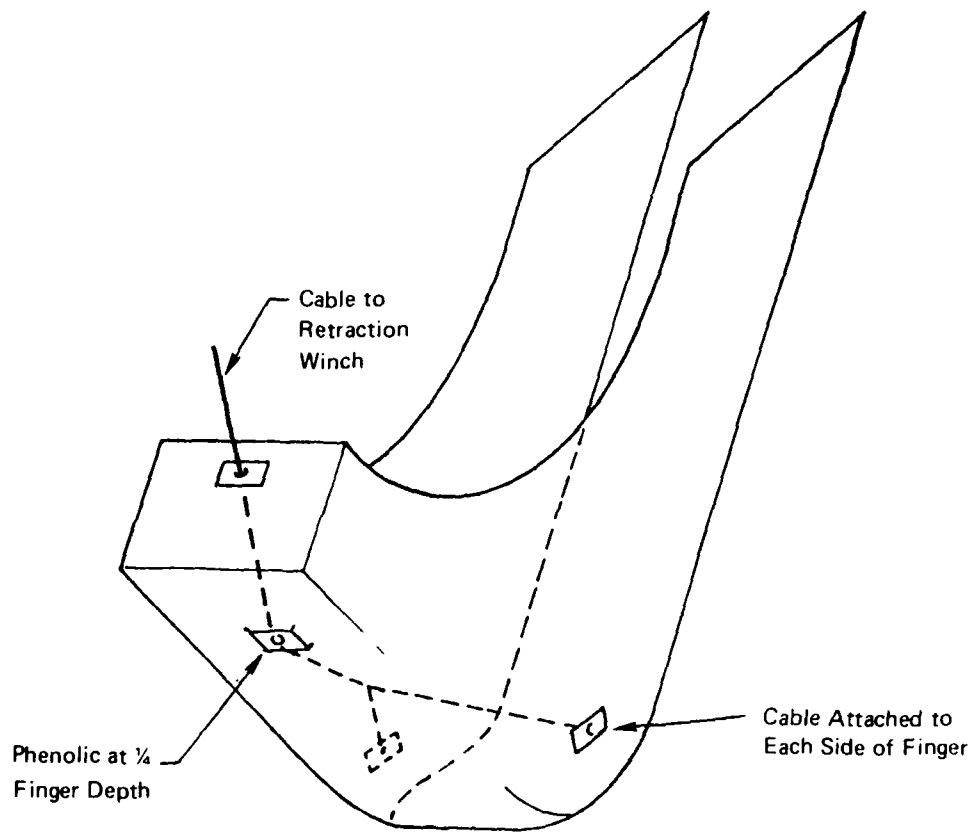


Figure 33. Recommended Skirt Lift Cable Run

desirable but the gauge initially selected can be broken without applying unreasonable force to the hand winch. This inhibits the ground crew from applying maximum winch effort.

c. Mount/Dismount Procedures

In the early test phases, mounting and dismounting the aircraft on/from the ACET was a cumbersome and time-consuming exercise. Initial tow-on of the F-101 at light weight was straightforward except that the 16° angle of the main ramps required that the tow lines be rigged to pull the main gear directly, to avoid overloading the nose gear attachments to the aircraft. It also required the use of 1/2 in cable on the drum which restricted the number of wraps and length of line which could be accommodated, and proved to be unsuitable for the winch used and liable to jam.

For dismount the aircraft was originally towed off. This required considerable coordination between the winch operator and the tow driver. If the winch lock was released, the aircraft would run too rapidly down the ramps and if not, the automatic brake prevented smooth operation. This led to jerking loads on the rig and a snapped cable. Snubbers in the line and a manual brake on the winch were fitted to overcome these problems but the inconvenience of transferring the tow vehicle and line from front to back and forward again was very apparent. A further problem arose because the aircraft's hydraulic system was disabled. The nose wheel was free to caster and in running backwards, was unstable, would attempt to reverse direction and jam in the track. This was corrected by locking the steering arms.

Additional delay in the operation was caused by having to remove the ACET trailing wheels from the nose wheel ramp for mounting/dismounting the aircraft. Although this only required removing four bolts it was operationally unacceptable.

Techniques for operating the mount/dismount were gradually developed and the following procedures outline the methods finally adopted.

Mounting

(1) Start ACET and tow vehicle. Disconnect ground power. Tow to aircraft location.

(2) Back-up ACET, approaching from one side of aircraft preferably on a curved path and pivoting on approach to line up the aircraft nose wheel with the center ramp. The tow vehicle center line remains at an angle to the ACET and aircraft (Figure 34). Reduce power to idle.

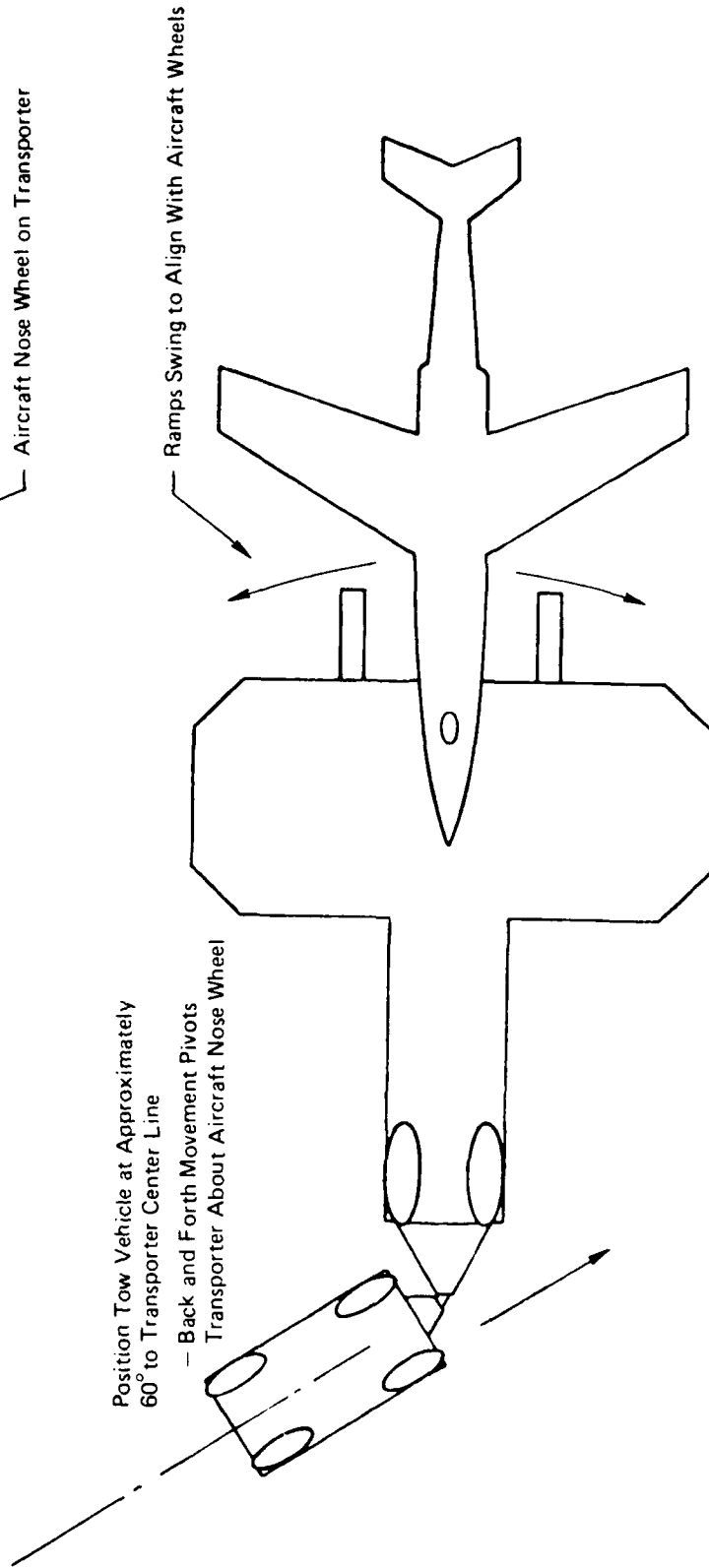
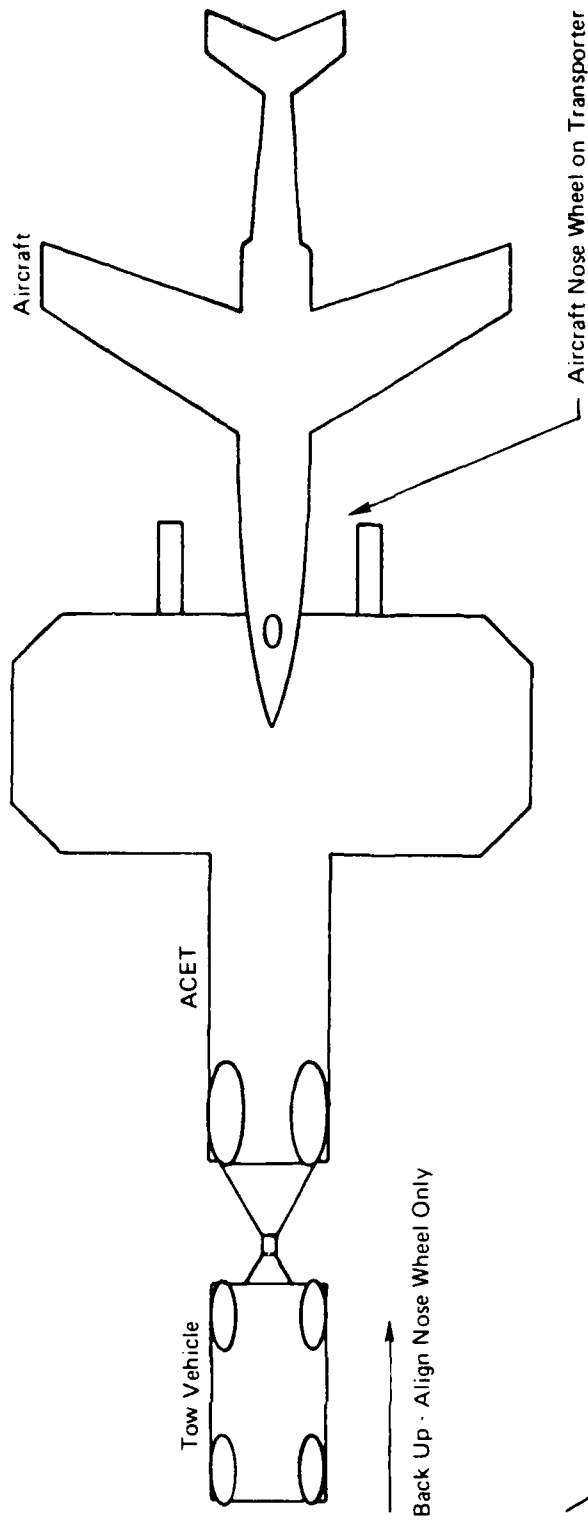


Figure 34. Aircraft Line-up Technique

(3) Close stop cock to retain accumulator bottle pressure and release wheel load pneumatic actuator pressure (dump). Unfold main ramps and set nose ramp in place.

(4) Connect the winch hook directly to the nose wheel and winch it up ramp on deck.

(5) Observe the line up of the aircraft main wheels (man on deck) and correct by going ahead or reversing the tow vehicle to rotate the ACET. At the same time double the winch cable and connect the pulley block (already on the line) to the nose wheel. Hook the cable end at the winch location.

(6) Winch on the aircraft. Put chocks in place behind main wheels. Re-fold the main ramps, stow the nose ramp on board the ACET. Recharge wheel load actuators. Press RUN button to return to predetermined cushionborne RPM. Tow away.

#### Dismounting

(1) Stop at dismount location and press IDLE, both engines. Release actuator pressure, unfold main ramps, and set nose ramp in place. Wind skirt lift winches to fully up position. Set pot to maximum rpm, press RUN.

(2) Release winch allowing aircraft to roll back until just before the main wheels reach the ramp ridges, and apply winch brake. Press IDLE. Release brake and slowly increase rpm until aircraft main wheels roll over ridge and down ramps.

The skirt lifting mechanism was designed for the jupe skirt and provided the necessary cushion exhaust area to create the slope of the deck to permit the aircraft to roll backwards. In changing the skirt to the all fingered type the method of collapsing individual fingers to achieve the desired cushion vent was not as effective and provided only marginal cushion venting. Additional modifications are necessary if the desired vent area is to be achieved with the fingered skirt.

(3) Disconnect winch cable from nose wheel, tow ACET ahead to run off nose wheel and to one side to clear aircraft. Press IDLE.

(4) Release skirt lift, fold main ramps and recharge wheel load actuators, stow nose ramp on board, reel in winch cable and press RUN. Tow away ACET.

## SECTION VI

### ACET AND F-101 AIRCRAFT WEIGHT AND C.G. SUMMARY

This section summarizes the weight and center of gravity characteristics of the fully developed ACET, the F-101B aircraft at three ballast conditions, and the combined ACET/aircraft as tested under various geometries.

#### 1. ACET

When originally weighed, the ACET was measured at 11,800 lb. Since then, modifications have been made which increase the total weight of the transporter by 961 lb. to 12,761 lb. Contributing to the weight increase were the addition of twin wheel ramps, fingered skirt, extended exhaust ducts, F.O.D. screens, increased winch cable capacity, mechanical cushion vents, improved winch mount, skirt lift mechanism and reinforced fuel tank mounting frames.

#### 2. F101B AIRCRAFT

The empty F101B aircraft was weighed upon receipt at Grand Bend using a Cox and Stevens Electronic Aircraft weighing kit. The weight of the aircraft was 30,475 lb. The CG was at the aft limit of station 502 in. This weight is the aircraft minimum weight for the purposes of the test program.

W<sub>min</sub> = 30,475 lbs. at Aircraft Sta. 502.0 in.

To achieve intermediate and maximum gross weight conditions water ballast was pumped into the empty aircraft fuel tanks using a Foreman Fuel Bowser equipped with a Neptune model 433 flow meter. Changes in aircraft weight were effected by completely draining the aircraft tanks and refilling with the required quantities of water.

The intermediate aircraft condition was achieved by adding 13,100 lb. water evenly over the extent of fuselage tanks 1-5, on a c.g. of approximately station 524.5 in.

The resulting intermediate weight configuration is:

W<sub>int</sub> = 43,575 at Aircraft Station 506.9 in.

The maximum aircraft weight condition was achieved by adding approximately 25,000 lb. to the EMPTY aircraft weight of 30,475 lb. (c.g. STA 502.0 in.

This was distributed as:

- a. 375 Imperial gallons each drop tank
- b. top off fuselage tanks from intermediate weight
- c. add remainder in wing tanks

This is estimated based on printed tank capacity data total of 2500.6 Imperial gallons to virtually fill all tanks and lines and results in an aircraft maximum weight condition of

W = 55,475 lb. at Aircraft Station 493.5 in.  
max.

Finally, for the last terrain testing at the maximum aircraft weight, 8 x 450 lb. water barrels were installed on the ACET at ACET Station 467 in.

Summarizing:

Developed ACET (including fuel)	13,822 lb. at St. 313.1 in. (ACET)
Min. Weight Aircraft	30,475 lb. at St. 502.0 in. (Aircraft)
Int. Weight Aircraft	43,575 lb. at St. 506.9 in. (Aircraft)
Max. Weight Aircraft	55,475 lb. at St. 493.5 in. (Aircraft)
External Ballast	3,600 lb. at St. 467 in. (ACET)

These figures were used for all estimates of combined transporter/aircraft weight-c.g. conditions.

Note that the four combined weight conditions are 44,297, 57,397, 69,297, and 72,897 lb.

Figure 36 indicates the variation of combined transporter/aircraft center of gravity with aircraft main wheel station on the transporter for the min., int. and max. aircraft weight conditions.

(Note that aircraft station of main wheels is Station 524.78 in.) (Reference Figure 35.)



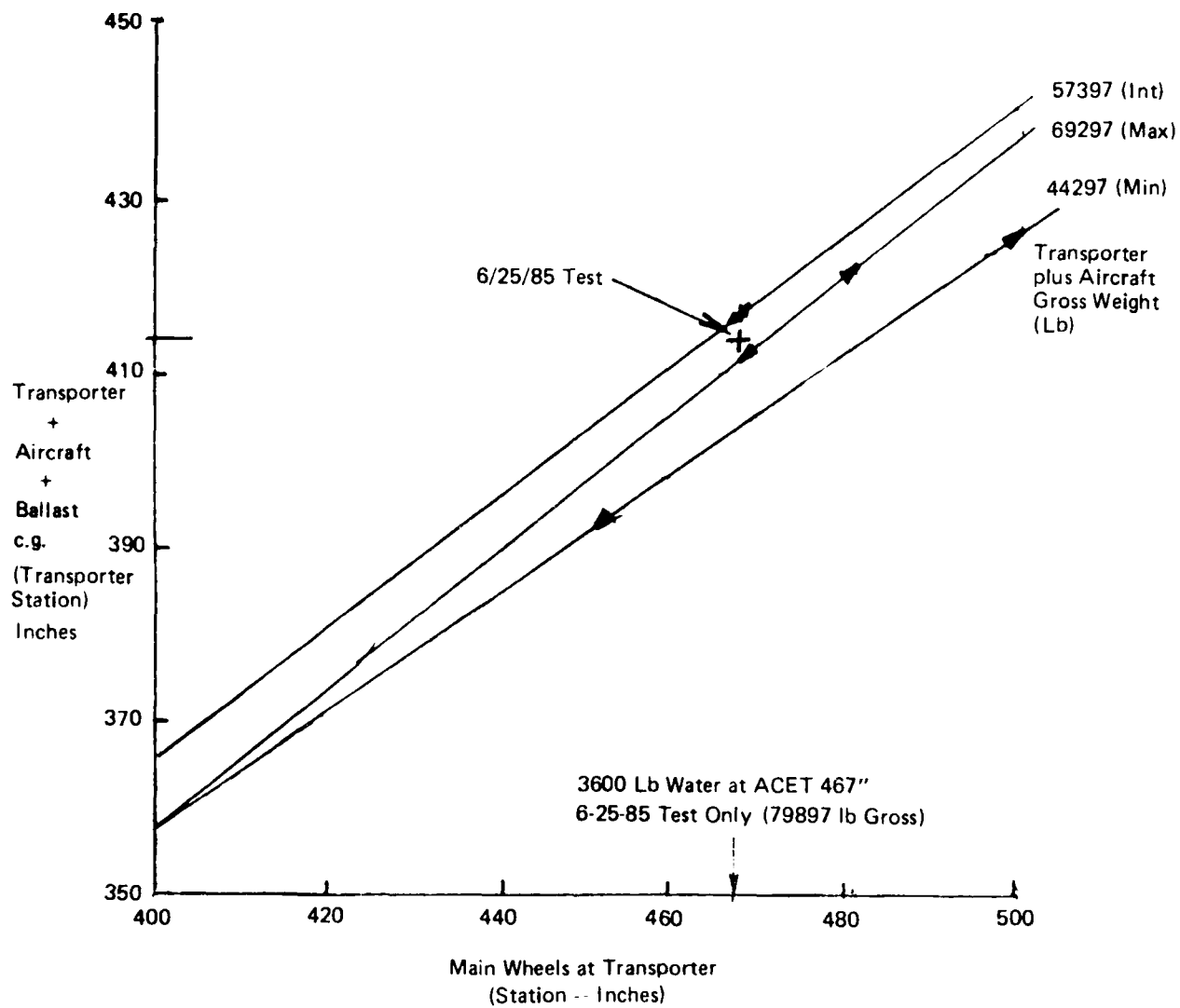


Figure 36. Combined C.G. Variation With Aircraft Position (Arrow Heads on Lines Show Limits of Position Tested)

## SECTION VII

### STATIC HEAVE AND STABILITY SHAKE-DOWN TESTS

Tests on heave height, and heave, pitch and roll stability were conducted over the period May 15 to 29, 1985. The ACET was configured with the fingered skirt system for these tests. Specific tests are described briefly in chronological order.

- a. 5-15-85 Test 04-03 - Transporter On-Cushion -  
No Payload

Heave attitude and air gap were observed over a range of power settings. The rear cells became fully inflated at 61% engine speed (Nf), the forward cell at 90% Nf. The transporter was very stable at all power settings. Transporter weight was 13,827 lb., c.g. at station 313 in.

Air gap and heave height are presented in Figures 37 and 38. Note that a 10 mph wind at about 50° off the starboard beam caused a very slight roll to port (1/2° max.) and a rather more significant asymmetry in air gap (approaching 1 in. larger on the windward (starboard) side). No flatness survey of the test site was conducted, so that some of the asymmetry may be attributable to hardstand irregularities.

In this weight condition the transporter c.g. (without aircraft) is much further forward than with the aircraft, so that the nose down heave development due to rear cell inflation preceding forward cell inflation is expected.

- b. 5-16-85 Test 05-01 - Pitch Dynamic Stability -  
No Payload

Dynamic pitch stability of the unloaded transporter was evaluated at 3 power settings. Two 1100 lb. masses symmetrically placed at the transporter trailing edge just inboard of the aircraft main wheel tracks were simultaneously "tipped-off", to apply an impulsive heave and pitch input to the transporter.

An oscillation of roughly one-half inch (double amplitude) decayed in approximately 3 visible cycles, suggesting damping of the order of 0.15 critical. No pitching frequency was estimated. Average power settings were Nf = 42%, 75%, 97%.

- c. 5-16-85 Test 06-01 - Roll Stiffness - No Payload

Roll stiffness of the unloaded transporter was evaluated at a range of power settings and roll moments. Six water filled barrels were placed so as to be centered at various lateral outtock lines along the span of the port rear cell. (LBL's of 55, 105, 140 and 195 inches.) Cell pressures, air gaps and heave heights were measured at various power settings for each ballast position.

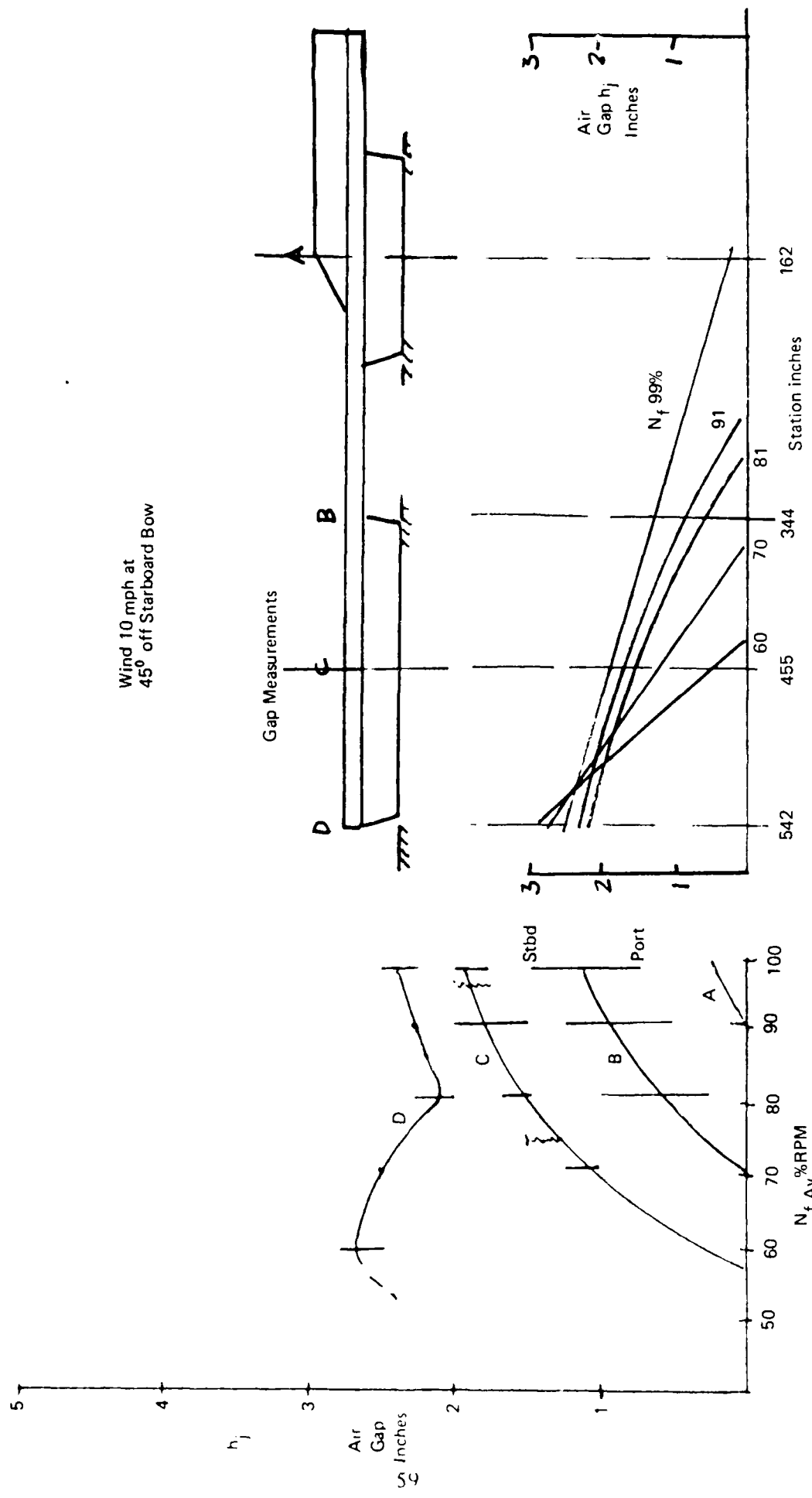


Figure 37. Cushion Gap Variation with Power ACET; Weight 13,827 lb at cg 313 in.

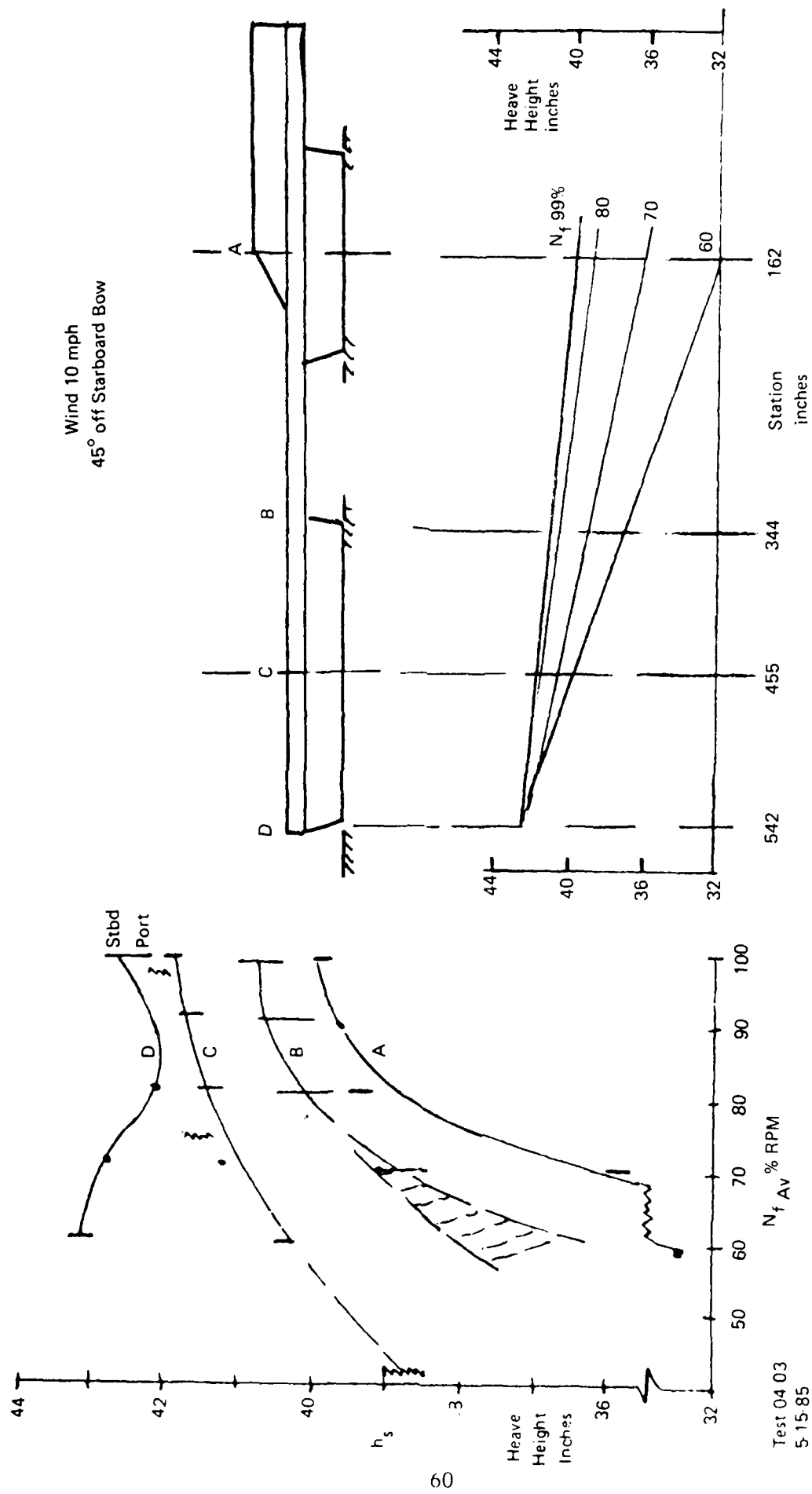


Figure 38. Heave Height Variation with Power ACET; Weight 13,827 lb at CG 31.3 in.

Heave height and air gap at the outboard rear cell positions are plotted on Figures 39 and 40 for the ballast and power ranges.

Rolling moment-roll angle is presented in Figure 41 for various power settings. From this is deduced the static rolling stability stiffness derivative C.P.<sub>g</sub>, which is defined and plotted on the same figure. The zero-roll value is 0.09 to 0.10 and weakens with roll angle.

d. 5-16 & 17-85 Test 04-04 - Transporter Plus Aircraft On-Cushion

Initial tests were conducted on 5-16 bringing the transporter-aircraft combination on cushion with the aircraft at a weight of 30,475 lb. at a C.G. of 502 in. The gross weight of the combination was 44,297 lb. at a C.G. of 397.5 in. (transporter).

On raising power to full cushion support a coupled pitch-heave oscillation occurred, the amplitude of which increased with turbine speed. The test was terminated since further operation was considered impractical.

On 5-17, the test was repeated with the aircraft moved 36 in. aft to give a C.G. position of STA 423.5 in. A limit cycle oscillation of about 6 Hz in heave was encountered, as power was increased. Flexing of the vehicle splice joint at Station 344 was also noted and the test was immediately terminated.

e. 5-20 to 28-85 - Transporter Lift System Modifications

Heave stability improvements were attempted by progressive steps.

(1) May 20, 21

1.1 Fifteen 1/2 in. holes were cut in every fourth finger of the aft cells. They were arranged in a triangular pattern - see Figure 10.

1.2 The door springs for regulation of aft cell cushion pressure were adjusted to 220 lb/3/8 in. opening.

1.3 Door dampers were adjusted to position 2 on the indicator.

(2) May 22

The aircraft was repositioned to the most forward position (combined weight 44,297 lb. at 397.5 in.).

The system was brought on cushion up to full power. All three cells participated in a small limit cycle oscillation at approximately 2 Hz. Air gap distribution was

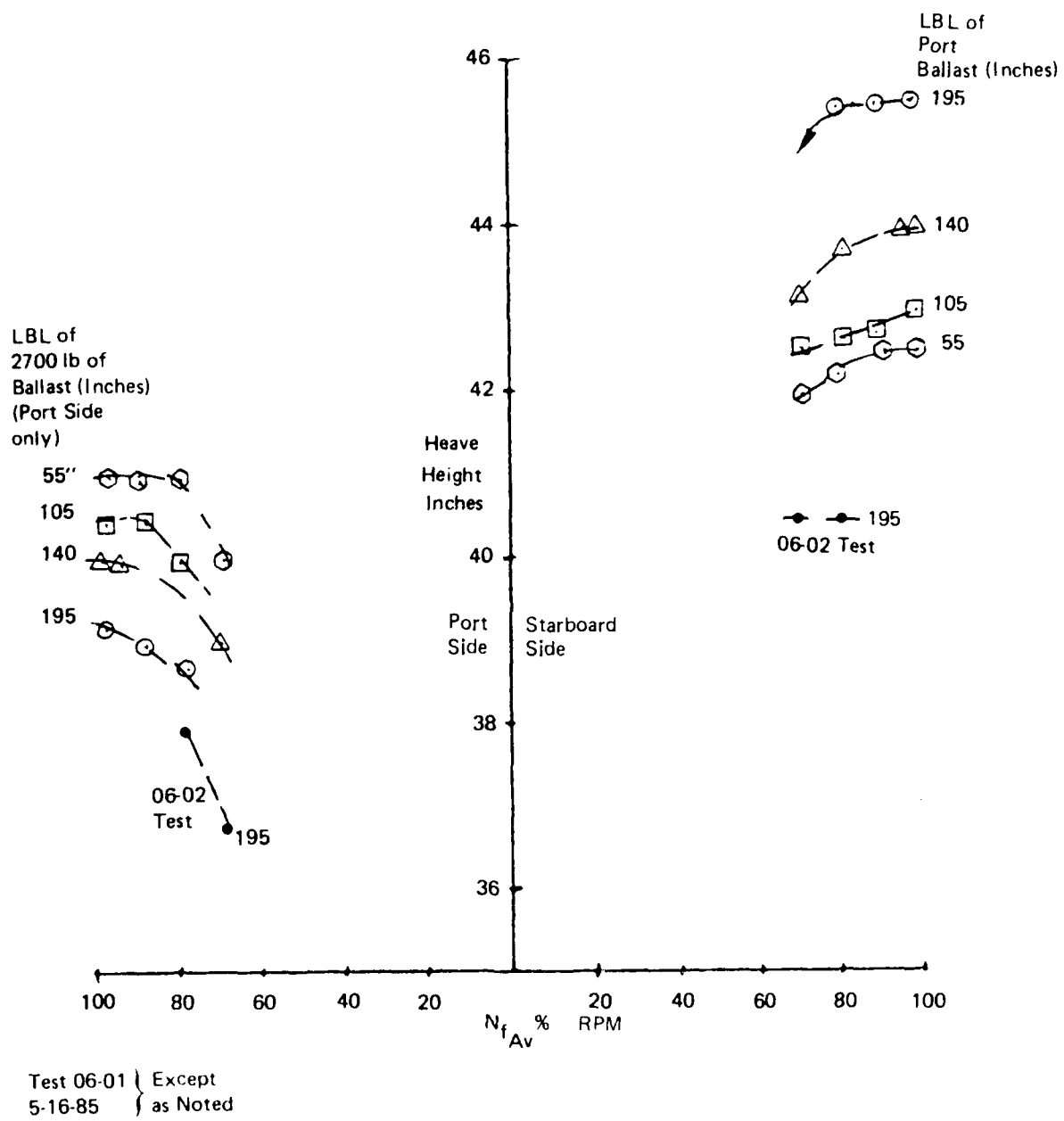


Figure 39. Heave Height (Rear Cell Outboard) Power-Roll Stiffness Tests

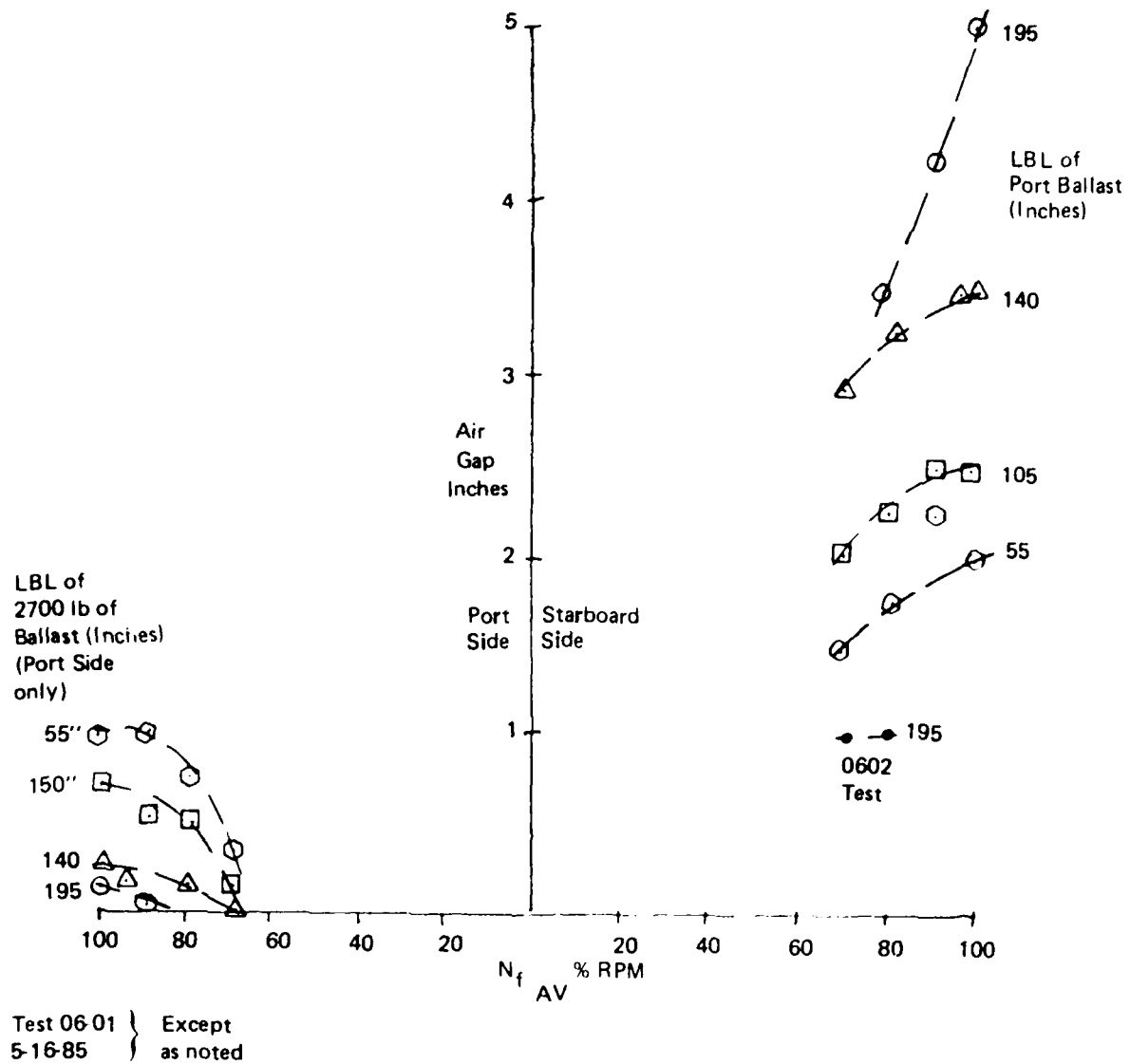
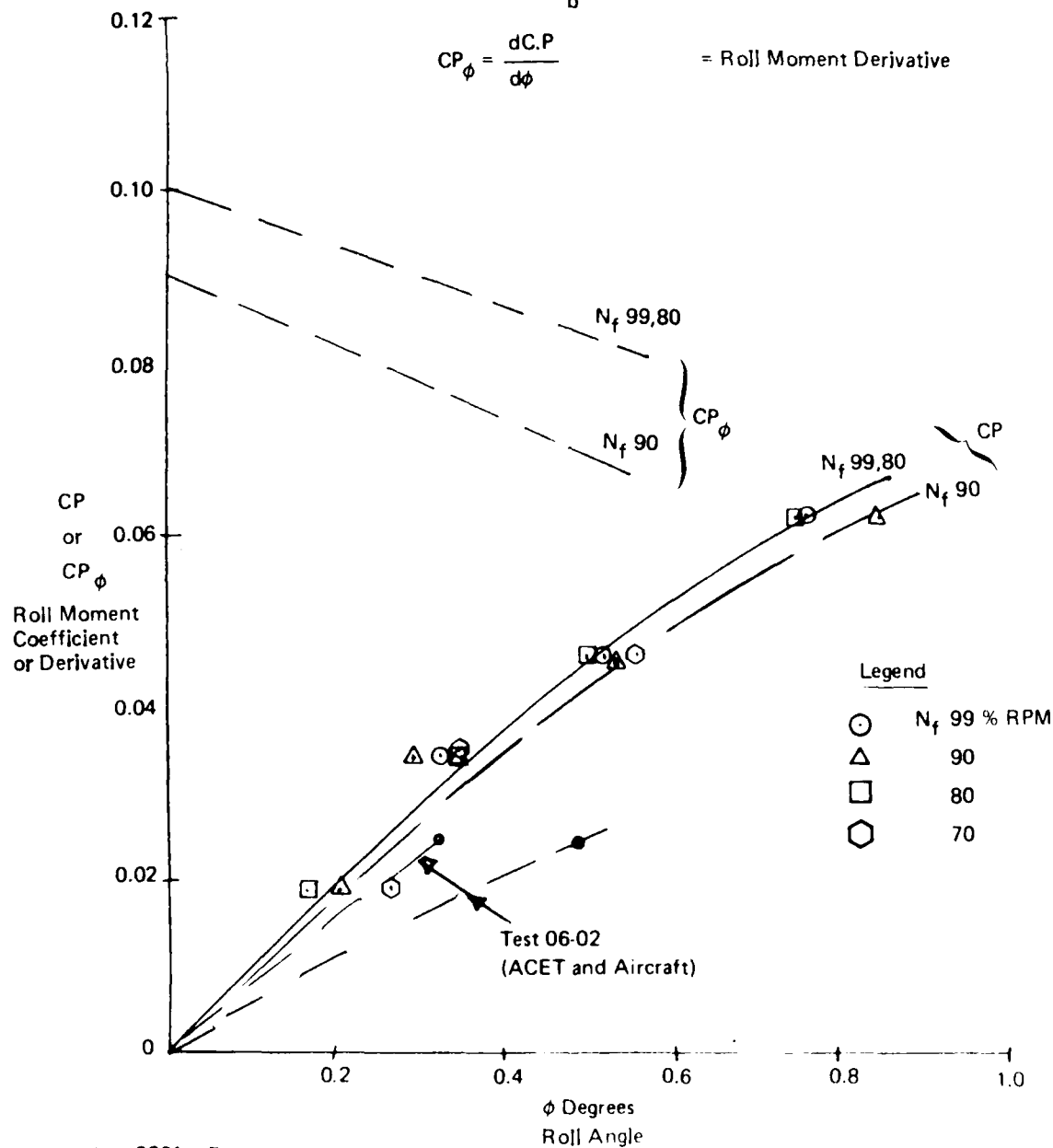


Figure 40. Air Gap (Rear Cell Outboard) Power-Roll Stiffness Tests

$$\text{Roll Moment Coefficient } CP = \frac{W_{\text{Ball}} \times (LBL)_{\text{Ball}}}{(W_T + W_B) b} = \frac{\text{Rolling Moment}}{\text{Weight} \times \text{Width}}$$

$$\phi = \frac{(H_t)_{\text{St}} - (H_t)_{\text{Port}}}{b} = \text{Rolling Angle}$$

$$CP_{\phi} = \frac{dC.P}{d\phi} = \text{Roll Moment Derivative}$$



Test 0601 Except as  
5-16-85 Noted

Figure 41. Roll Stiffness and Derivative

roughly 1/4 in. front cell, 1/8 in. forward side of rear cells and zero at rear. Aft cell doors were opening at the oscillation frequency. Front cell doors were inactive.

The aircraft was repositioned 36 in. aft (44,297 lb., C.G. at STA 423.5 in.) and the system brought on cushion to full power.

While air gaps were relatively unchanged, the limit cycle was now constrained to the front cell. Door behavior was unchanged.

The front door springs were now readjusted so that on each door, one spring was totally relieved and one "snug" (closed at no tension).

At full power on cushion, minor front cell oscillations and phased door action were observed. Power was reduced until the oscillation disappeared. At this point, the system was very easily moved forward and backward about 3.0 feet with no significant drag in evidence.

It was concluded that the cushion venting provided by the series of 1.0 in. dia. holes in every fourth finger in the two aft cells was of more significance in reducing the oscillation than door/spring action, even though heave height and air gap were reduced. To confirm this a further run was made with the main cell relief doors loaded firmly shut. No movement of the relief doors occurred and the behavior of the craft appeared to be unchanged.

An auxiliary test conducted at this time was to explore the variation of trailing wheel ground reaction with ramp angle and accumulator pressure (so that vehicle balance could be correctly assessed). For this test the transporter was supported on barrels. The tires were suspended level with the landing pads at 0.75 in. tire compression. Wheel reactions were recorded at various ramp angles and accumulator pressures. Results are presented on Figure 42.

(3) May 23

The fifteen hole triangular pattern was incorporated in every 4th finger of the front cell. Calibrations were also conducted by load cell tests on aircraft main and nose wheel legs.

f. 5-28-85 Test 04-04 Transporter Plus Aircraft  
Initial Test

With the aircraft installed at the most forward position in the minimum weight condition, (Gross w = 44,297 lb. at STA 397.5 in), the system was raised on cushion and run from idle to maximum rpm. A gentle limit cycle heave oscillation of about 2 Hz was evident at approximately 80% power. Amplitude was observed to be  $\pm 0.5$  in.

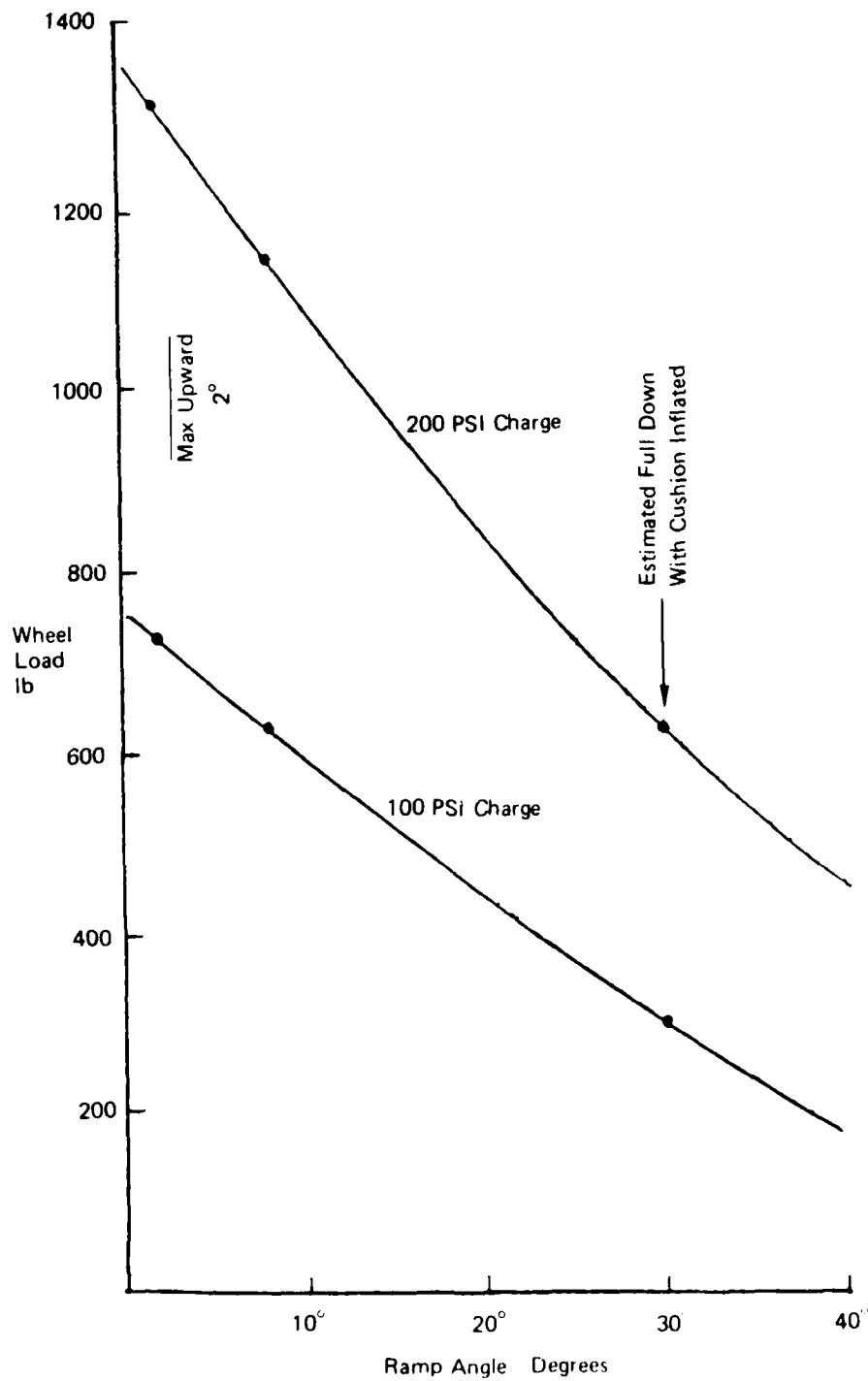


Figure 42. Rear Wheel Ground Reaction

Decisions were taken to continue with stability testing.

g. 5-29-85 Test 06-02 - Heave Height and Roll Stiffness, Transporter/Aircraft

Following modifications described above, cushion performance and roll stiffness tests were conducted with the aircraft forward at minimum weight (44,297 lb. at STA 397.5in.).

Roll "Moment" was applied by positioning water barrels (6 x 50 gal. of 450 lb. each, totaling 2,700 lb.) at port LBL 195. Roll attitude was measured at power settings of 70 and 80% N.

These results have been added to Figures 39, 40 and 41. It is noted that the roll stiffness derivative at this weight is reduced to approximately 0.07 at 70% power and 0.05 at 80% power from the ACET alone value of about 0.10. Heave height and air gaps are, of course, significantly lower.

h. 5-29-85 Test 06-03 - Heave Attitude as Function of Aircraft Position

Static longitudinal pitching stiffness of the transporter-aircraft combination was investigated. The aircraft at minimum weight (30,475 lb. at STA 502in.) was stationed on the transporter at 4 longitudinal positions. Heave height, gaps and pressures were recorded for two powers at each aircraft position.

Height is plotted against position and power on Figure 43 for stations 162 and 453. Note the disparity between rear port/starboard heights implying roughly 1/2° of roll/twist.

On Figure 44, pitch angle is plotted against aircraft position, and moment increment is plotted against pitch angle. From this latter we infer a static pitching stiffness coefficient C.P. of 0.044 based on a reference longitudinal length of 37.25 ft. (front of forward cell to rear of aft cell). This estimate is for a power of  $N_f = 60\%$ , which was a value generally common to all aircraft positions tested.

C.G./C.P. and lift/weight correlation are plotted in Figure 45. In this analysis, the cushion areas are modified assuming that the ground plane intersects the cell profile at a height determined by the measured average heave height of each cell. Average cell pressures are also used.

The lift/weight correlation exceeds unity by up to 15%. Observation of the cell behavior when not totally extended suggested that the effective cell area was less than the ground plane intersection assumption made above. This accounts for the overestimated lift. However, lift C.G./C.P. correlation is generally good when allowance is made for ramp reaction.

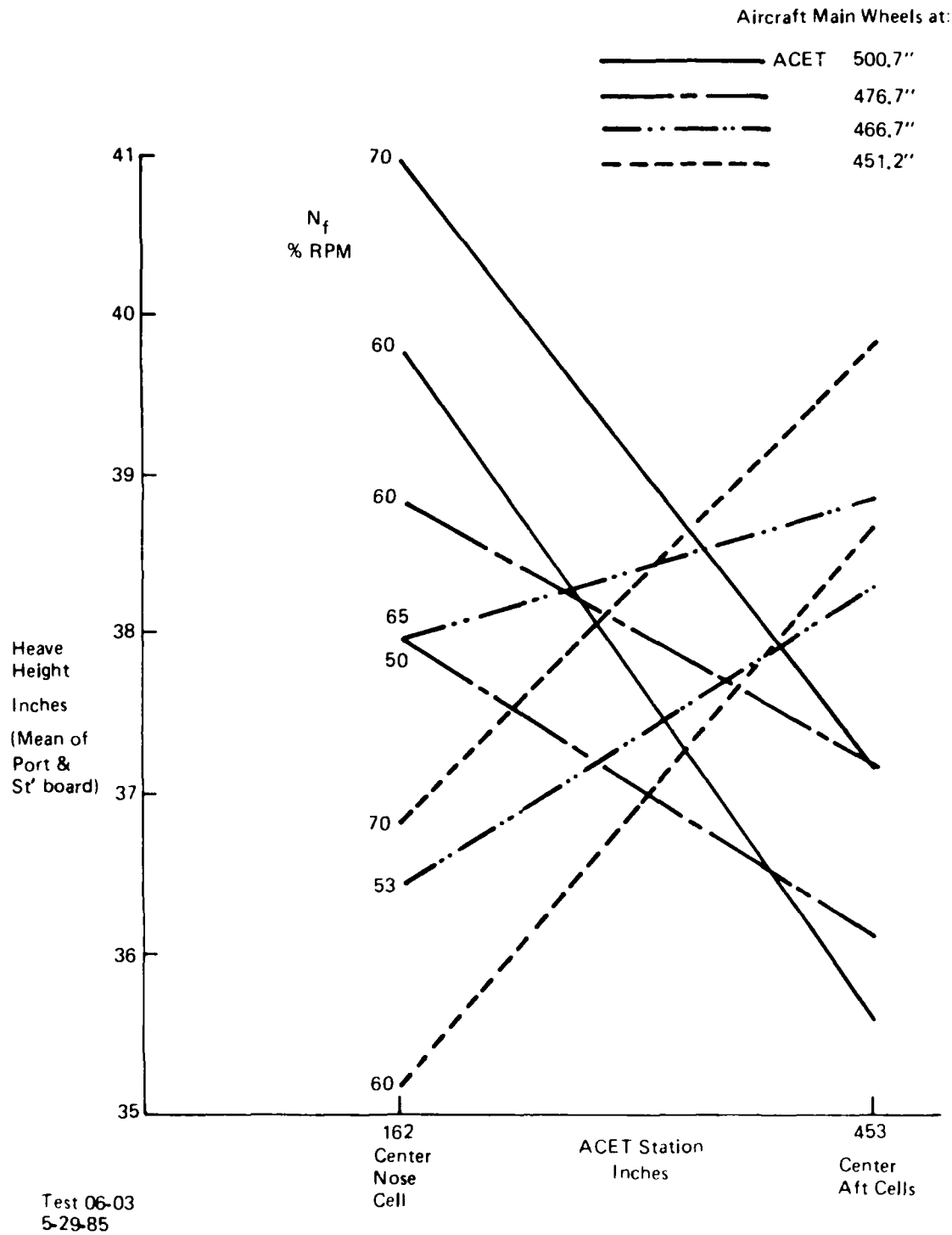
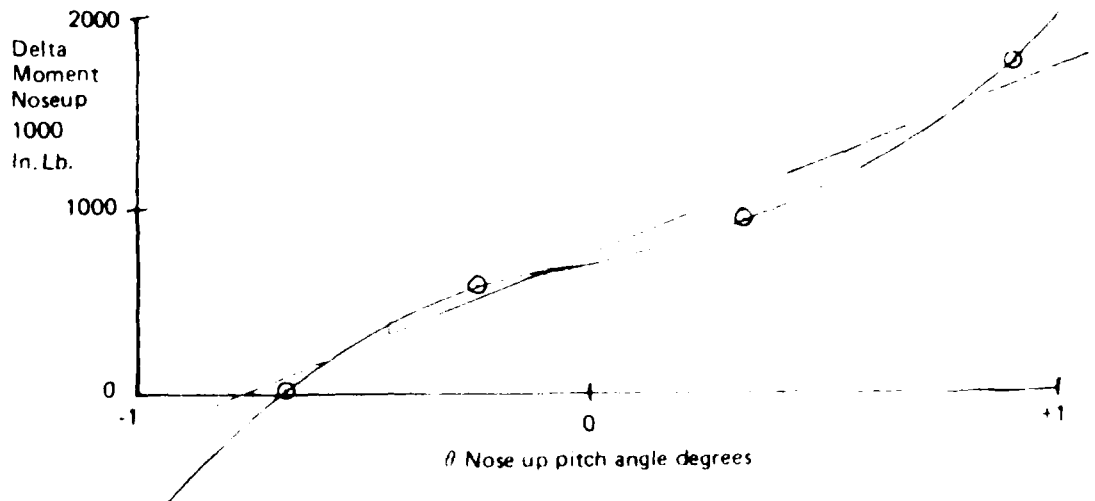
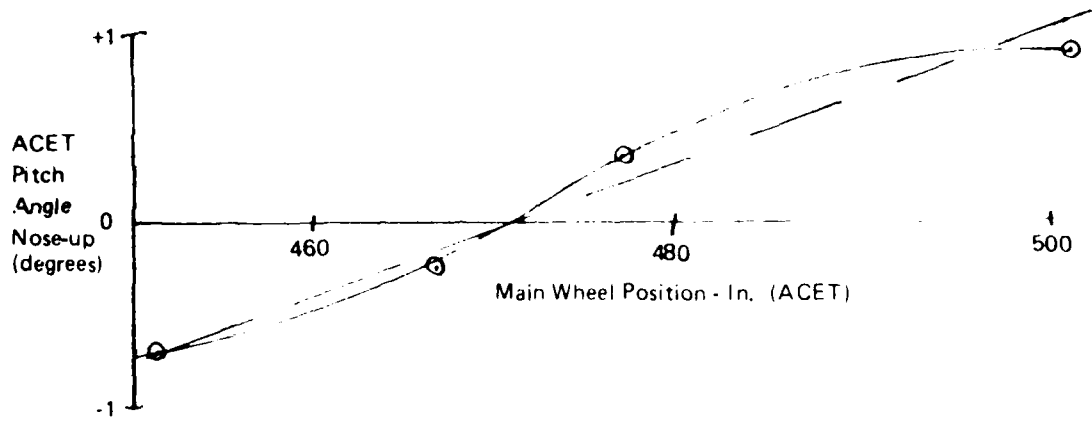


Figure 43. Heave/Pitch Attitude of Aircraft/ACET as Function of Main Wheel Position and Power (Aircraft at Minimum Weight)

Average Heights, Forward and Aft  
at 60% Power

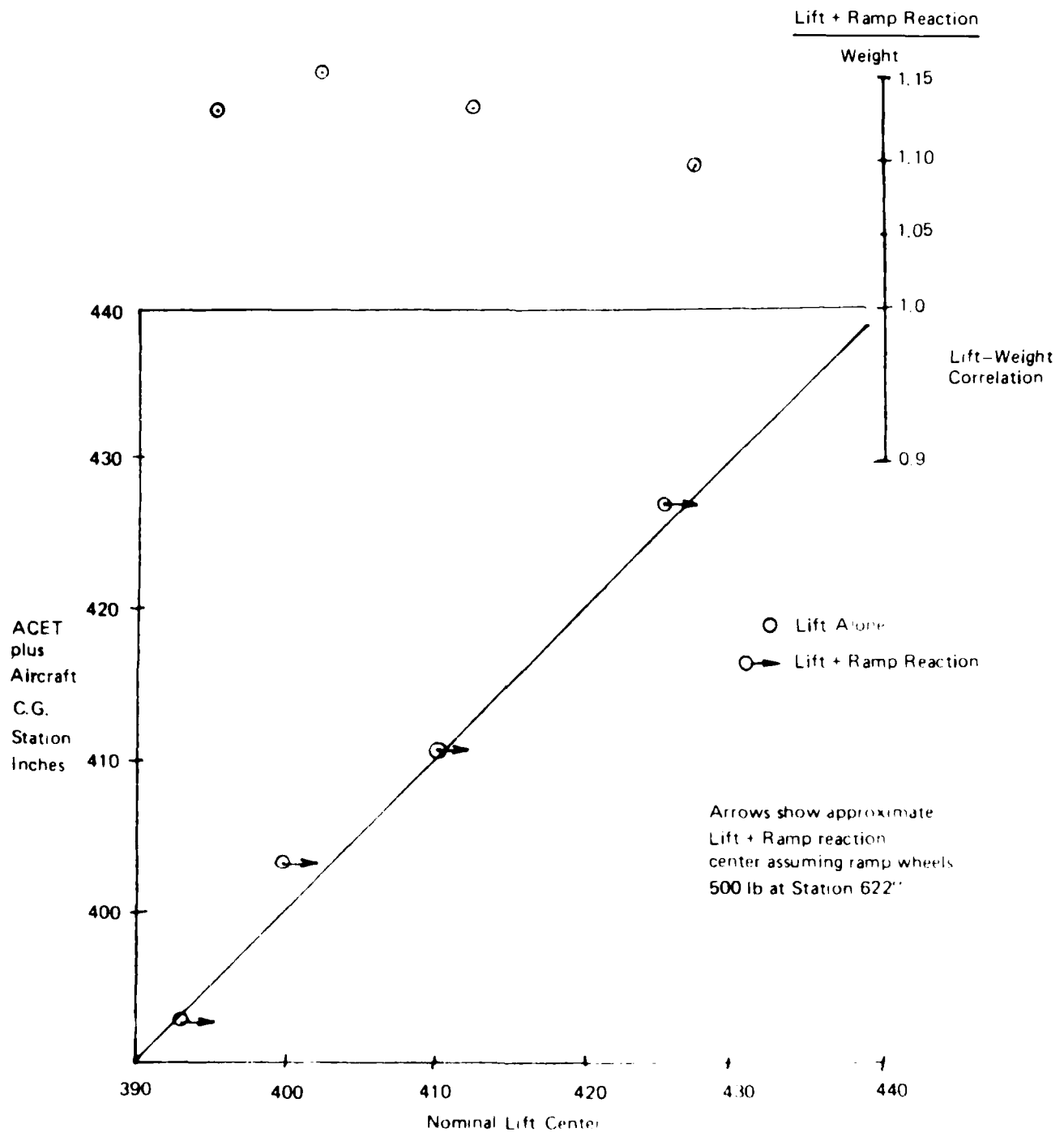


For  $W_{Total} = 44297 \text{ lb}$   
 Ref Length  $447'' = 37.25'$   
 (o/a cushion length)

$C_{P_{\theta}} = 0.044/\text{degree, av}$   
 $= 0.028/\text{degree at } \theta = 0$

Test 06-03  
5-29-85

Figure 44. Moment Pitch - Various Aircraft Positions on ACET  
(Derived From Figure 43 at 60% Power)



Test 06-03  
5-29-85

Figure 48 Lift Weight and CG/CP Correlation (Total Weight 44,297.15)

## SECTION VIII

### TERRAIN TESTS

#### 1. GENERAL

These tests, listed in Table 4 were intended to evaluate the dynamic performance of the transporter/aircraft over hard and soft surfaces, slopes and irregularities (such as a crater). Vehicle motions, tow and aircraft gear forces, air cushion systems, engine and atmospheric parameters were to be recorded at various total weights, powers, speeds and maneuvers (Table 5). Continuous data recordings were made and coordinated with hand data records where possible.

#### 2. TESTS DESCRIPTION

a. 5-30-85 Test 07-02. Breakaway, tow, on asphalt and grass at aircraft minimum weight (transporter and aircraft 44,297 lb. at STA 407 in. (main wheels @ 467 in.)).

Breakaway tests on asphalt were conducted at "start-up" (50-55% power) and at 68, 75 and 80% average powers. Breakout forces were in the range 410-675 lb. power on, and 1000 lb. at start-up/shutdown. A minor limit cycle oscillation of about 0.2g peak to peak at the transporter C.G. and 1.8 Hz frequency occurred at the highest power. About 2000 lb. peak to peak force was registered as a nose wheel fore/aft loading. Cell pressure oscillations were of the order of 0.2 psi peak to peak and skirt gaps roughly 0.7-0.8 in.

Breakaway tests were conducted on grass at 70 and 80% power. Tow force readings in the cab (taken on a separate load cell in series) were recorded at 700-1000 lb. A spike of 6000 lb. on the full data record is probably due to a force "reversal" and backlash/impacting in the tow system. Minor limit cycling was observed in the rear cell pressures and on the nose wheel drag force.

A field tow was conducted at about 90% power traversing a roughly elliptical track. Rear cell pressures were 0.6 psi, and the drag observed in the cab averaged 300 lb., with slightly higher spikes on the rougher parts of the terrain. The ellipse was about 100 x 100 feet. One burst of limit cycle oscillation was observed on the data record, possibly at a hardtop crossing.

All these tests were conducted in 10-20 mph wind at 70°F.

TABLE 4

## TERRAIN TESTS - CHRONOLOGICAL

Date	Test No.	Brief Description
5/30/85	07-02	Backup and tow, asphalt, grass
6/3/85	08-02	Backup, asphalt & grass, field run, crater
	07-03	Backup, tow asphalt
6/4/85	08-03	Breakaway, grass and field tow
6/5/85	07-04, 09-04	Breakaway, tow, asphalt, field and crater run
	07-04	Same, door springs at 270 lb.
6/7/85	08-02	Asphalt, down and uphill on grass
6/16/85	No no.	Asphalt, hill, field crater traverse
6/25/85	No no.	Asphalt, grass, field, water

TABLE 5  
SUMMARY OF TEST PARAMETERS - PROCEDURE AND PRACTICE

Procedures Parameter	Static Tests	Dynamic Tow Tests	Comments
Heave Height Gauge	X	X	Approx. since surface flatness uncertain
VCR	X	X	Video tape record
Cushion Pressure Probes	X	X	Use sometimes questionable
Cushion Air Gap Gauge	X	-	
Cushion Pressure Front	?	X	Generally not taped
Cushion Pressure Port	X	X	
Cushion Pressure Stbd	X	X	
Cushion Air Gap Front	X	-	
Cushion Air Gap Port	X	-	
Cushion Air Gap Stbd	X	-	
Atmos. P & T	X	X	
Wind Direction/Velocity	X	X	
Port TGT, $N_f$ , $N_g$ , QD	X	X	
Stbd TGT, $N_f$ , $N_g$ , QD	X	X	
Transporter $x, y, z$	-	X	Of generally insignificant nature.
Aircraft $x, y, z$	-	X	Mostly not recorded.
Transporter	-	X	
Nose Wheel $F_x, F_y, F_z$	-		Generally not recorded
Main Wheel $F_x, F_y, F_z$	-		
Tow Force	-	X	
Transporter Vel, Direction	-	?	Nominal records
Mass Flow Port	-	X	
Mass Flow Starboard	-	X	
CBR	-	X	Not measured

b. 6-3-85 Tests 07-02/08-02. Backing on asphalt and grass, field/crater run (gross 43,575 lb. at STA 407 in.)

Aircraft main wheels were at Station 467". Backing on asphalt at 70% power required about 500 lb. (1800 lb. shock spike). On grass at the same power, a steady 450 lb. was required. One limit cycle burst occurred (the usual 1.8 Hz). During a run on the field and over the crater at 80%, tow force generally varied from 450 lb. to 600 lb. No significant variations occurred on tape throughout the run. (Note - It appeared from tests generally up to now, that cabin cell pressure readings and tape playback did not correlate--tape calibrations are suspected.) Very slight random 1.8 Hz traces were detectable in cushion pressure and vertical acceleration.

c. Test 07-03. Backing/breakaway on asphalt, (gross weight 57,397 lb. at STA 417.2 in.)

Aircraft main wheels were at Station 467 in. Tests were conducted at five power settings from 50% to 97%  $N_f$ .

Heave height, fore and aft, is plotted against power on Figure 46A. Air gap was reported as zero throughout the tests, port and starboard, at stations 162 and 453. Limit cycle oscillations of about 0.16 psi peak to peak, 1.8 Hz, were steady at 80% and 97%  $N_f$ .

During backing maneuvers on broken blacktop, the port ramp jammed in a 6 in. hole, resulting in a broken weld on the tow bar. Repairs were made before further tests.

d. 6-4-85 Test 08-03. Breakaway tests on grass and "field run" (gross weight 57,397 lb. at STA 417.2 in.)

Aircraft main wheels were at STA 467.0 in. Breakaway tests were conducted at 5 power settings, with tow forces recorded in the cabin from 400-450 lb. Cushion pressure and fan flow data are plotted against power on Figure 47. Mild 1.9 Hz limit cycles occurred again at the high power levels.

The subsequent field run at an average 82%  $N_f$  was uneventful and characterized by low tow forces of 250 to 450 lb.

e. Tests 07-04/09-04. Breakaway tests over asphalt and field/crater runs (gross weight 69,297 lb. at STA 409 in.)

Aircraft main wheels were at STA 467.0 in. Breakaway tests were conducted at 4 power settings with tow forces recorded in the cabin ranging from a high of 500 lb. at 58%  $N_f$  to a low of 250 lb. at 90%  $N_f$ . Cushion pressure (hand) readings and fan flow data are plotted against power on Figure 47. Heave height is plotted against power on Figure 46B.

Limit cycle oscillations of 1.8 Hz were again detected in the starboard main cells.

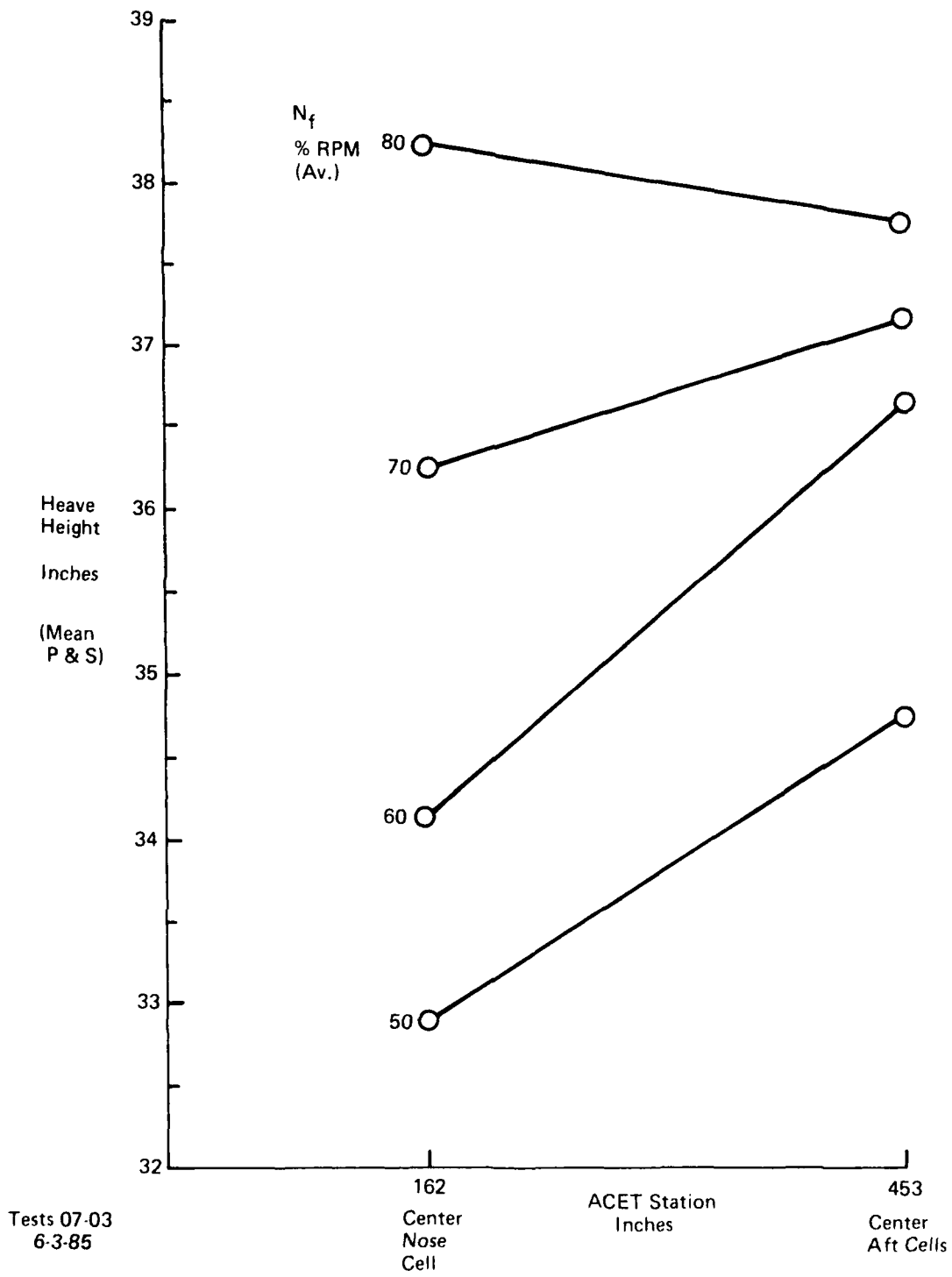


Figure 46A. Heave/Pitch Attitude of Aircraft/ACET as Function of Power - Weight 57,397 lb at 416.2 in.

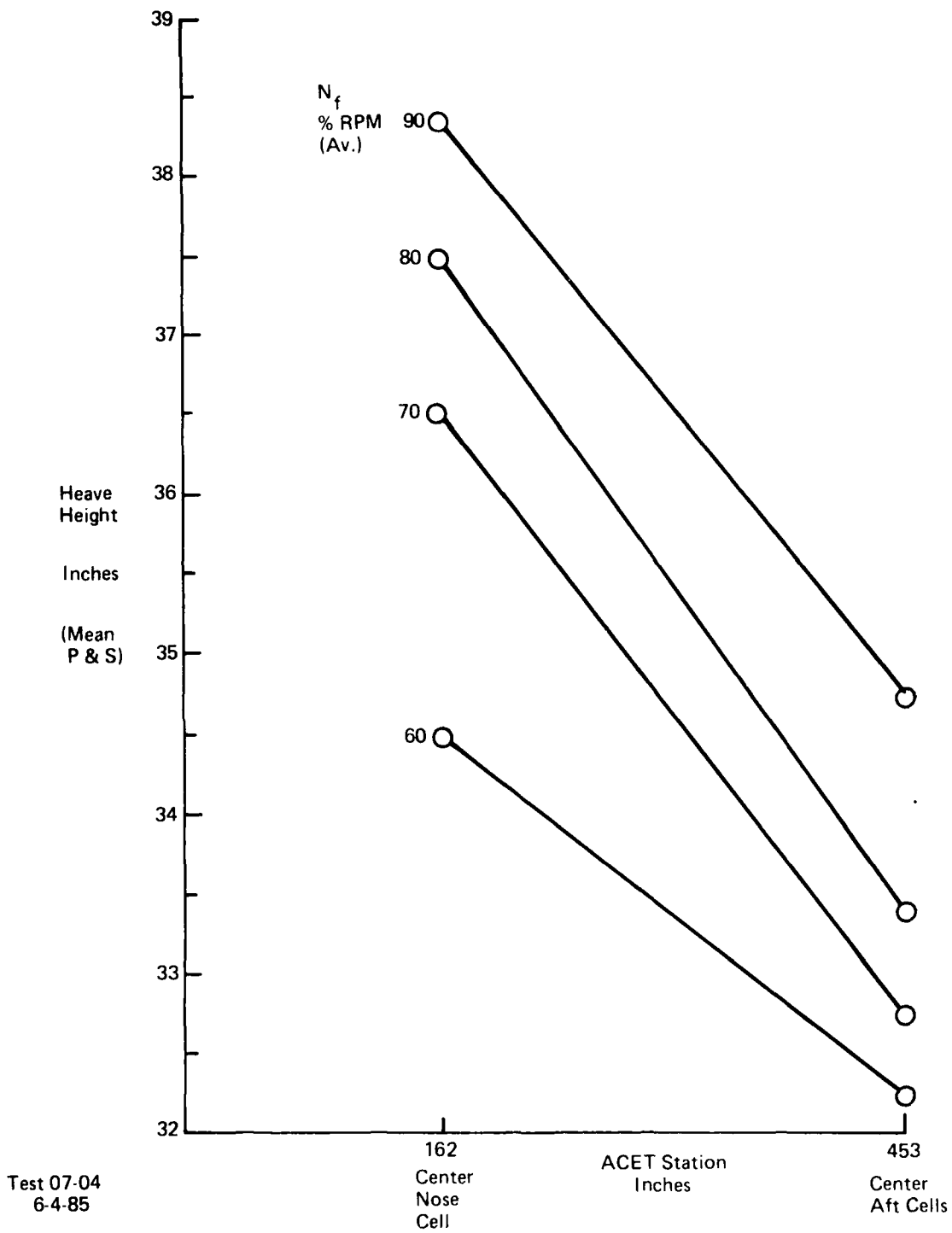


Figure 46B. Heave/Pitch Attitude of Aircraft/ACET as Function of Power - Weight 69297 lb at 411.5 in.

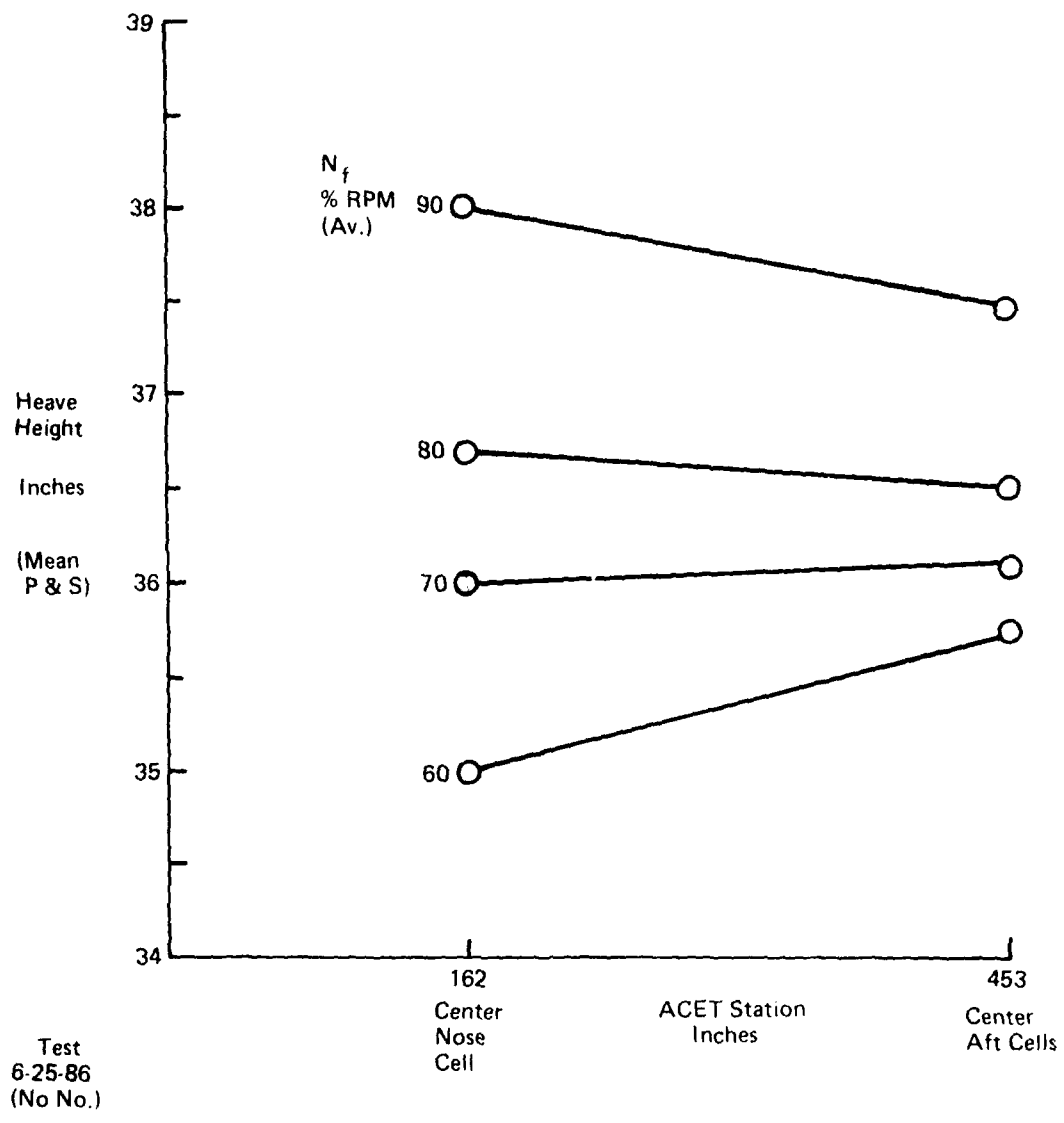


Figure 46C. Heave/Pitch Attitude of Aircraft/ACET as Function of Power - Weight 72897 lb at 414.0 in.

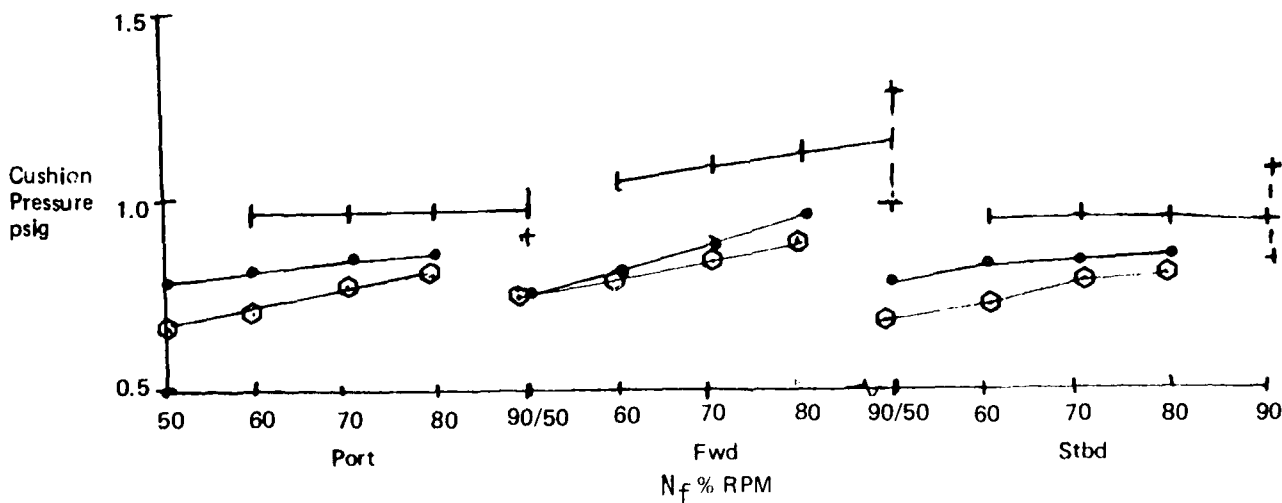
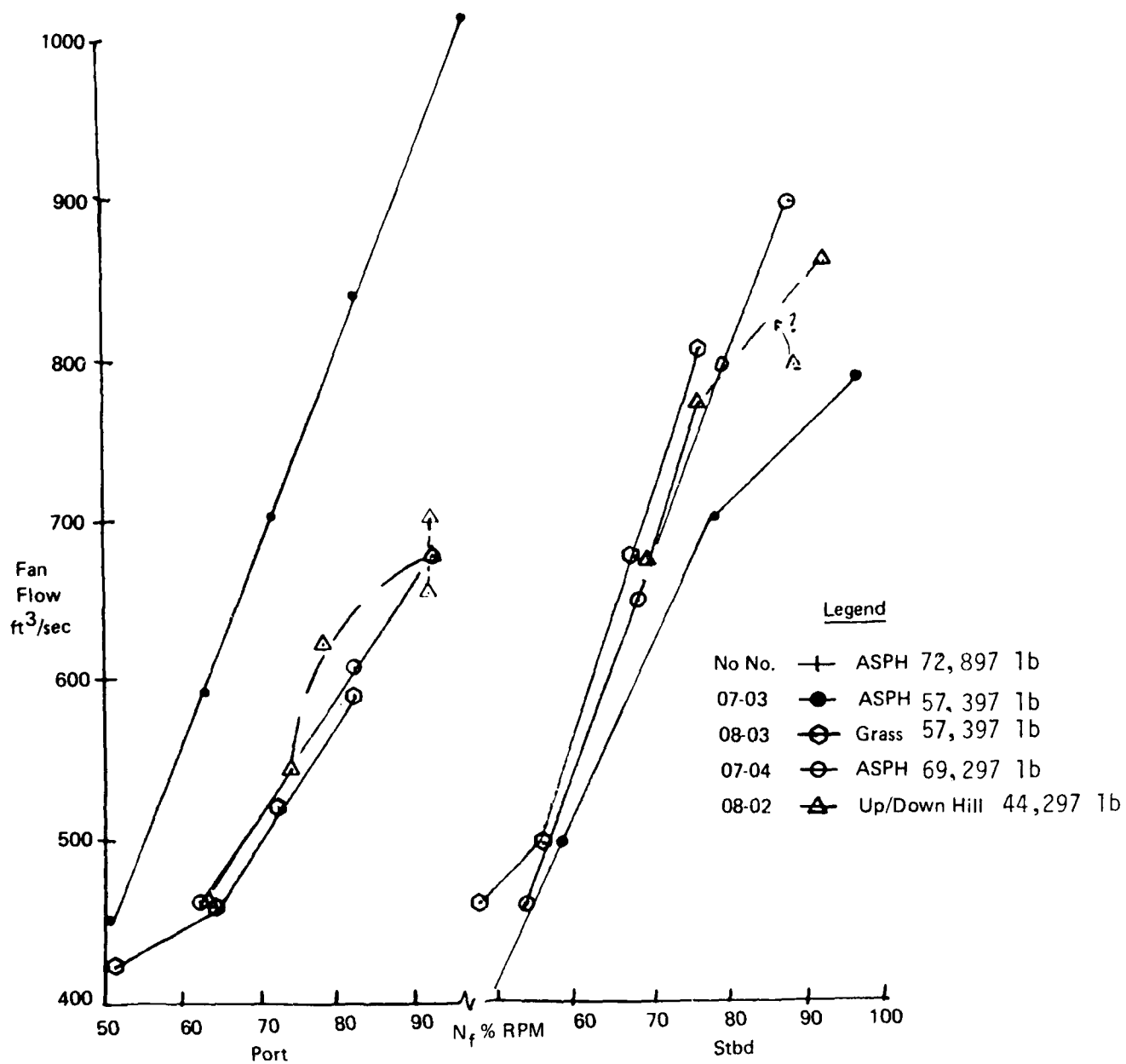


Figure 47. Fan Flow and Cushion Pressure Power Various Gross Weights  
(Not all Data Available for all Tests)

Again, using neave height to estimate effective cell areas, integrated lift pressures overestimated lift at all powers by 1800 to 4600 lb. and predicted lift centers from 401 to 405 in. compared with weight C.G. at 409.

An uneventful run was conducted over the field and crater at 98% N<sub>f</sub>. Drag readings ranged from 250 to 500 lb. Except for a spike in the tow record of 3,500 lb. peak, the tape records were uneventful.

f. 6-7-85 Test 08-02. Down/Uphill Circuits (Gross weight 44,297 lb. at STA 407 in.)

Main wheels were at station 467 in. This test consisted principally of runs down and up the sloping area adjacent to the Bell taxiway. A sketch of the route and a rough terrain traverse of the principal slope are given on Figure 48. Principal features of the tow force time histories are reproduced for four runs at various fan speeds on Figure 49. Fan flow data is included on the Figure 47 summary.

The normal round trip distance is approximately 800ft and very rough run times can be gauged from the tape playback. These are:

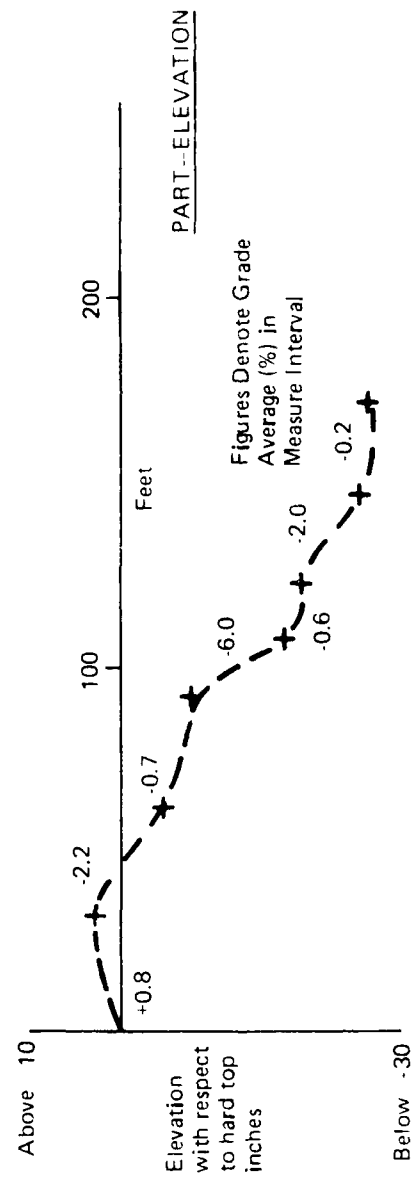
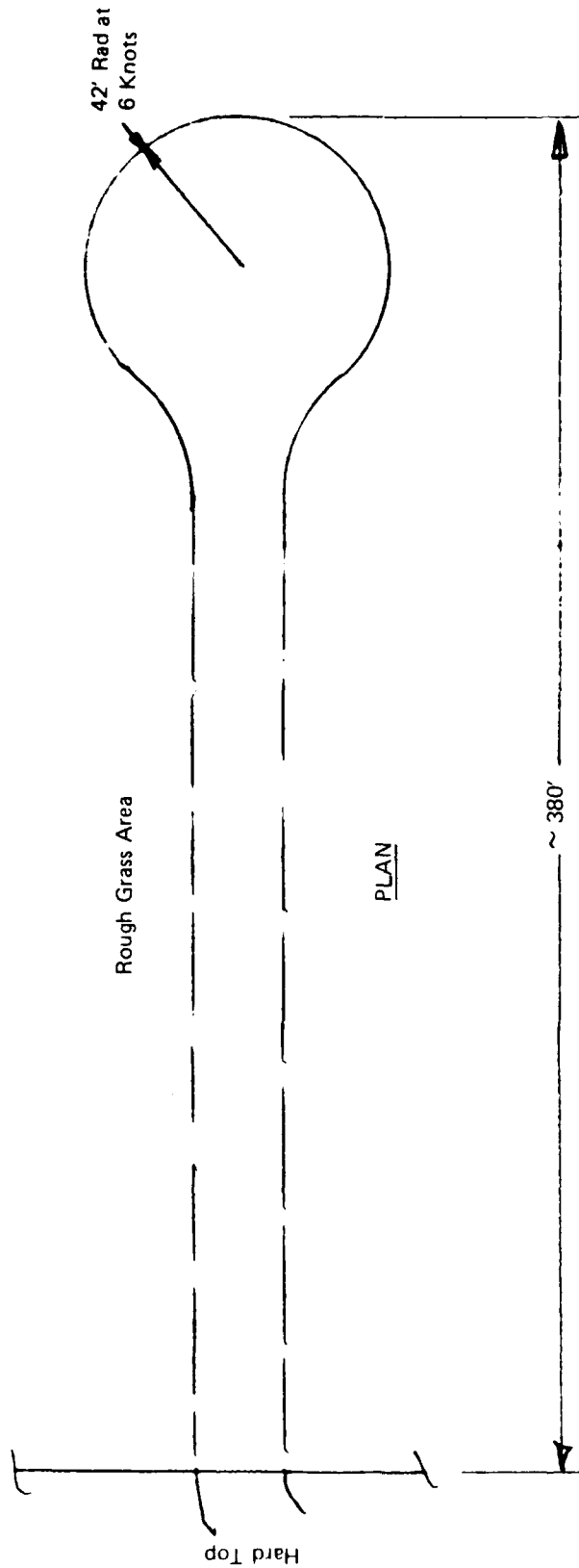
Run No.	N <sub>f</sub> % Speed		Time Sec.	Speed Knots
	Port	Stbd		
1	74	70	150	3.2
2	78	76	300	1.6
3	92	88	180	2.6
4	92	88	120	3.9

The speeds quoted are very approximate.

The gross features of the four records may be characterized as follows:

Run No.	N <sub>f</sub> % Speed		Max. Smoothed Pull lb.	Range of Largest Fluctuation lb.	Approx. RMS Fluctuation lb.
	Port	Stbd			
1	74	70	2500	900	200
2	78	76	4500	2000	700
3	92	88	2700	1300	800
4	92	88	5200	2200	900

Note that a maximum grade of approximately 6% occurs over a length of the order of 15 ft. maximum. This is approximately the diameter of the main cells which are also carrying 85%



Test 08-02 (6.7.85)

Figure 48. Down-Uphill Circuit Characteristics

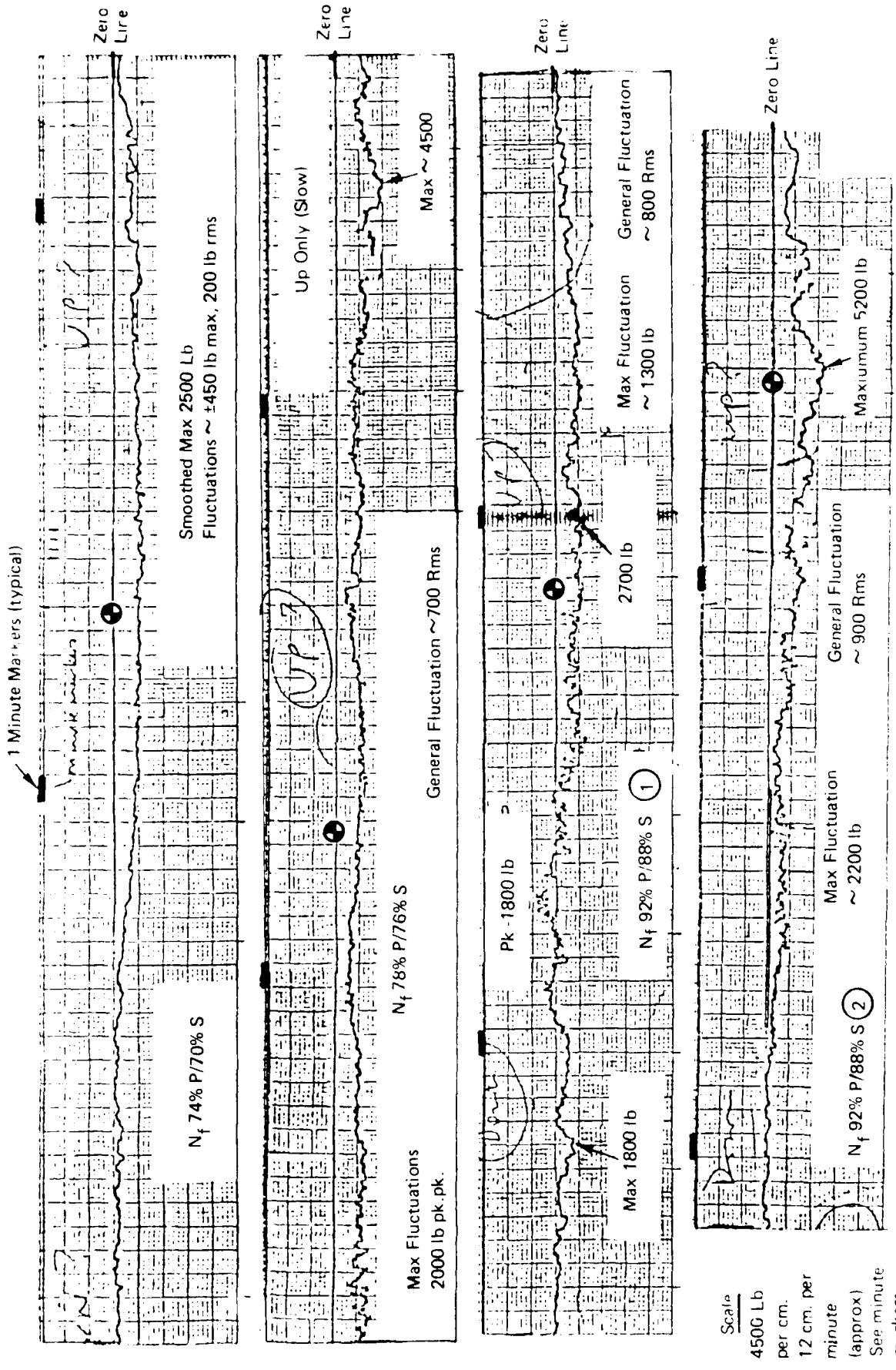


Figure 49. Down/Up Circuits (44,297 lb Gross at 403.3 in) Tow force Histories

Test 08-02  
6-7-85

of the weight. Thus, a maximum of 3% of the weight is recorded as tow force; i.e., about 1490 lb.

The tow drag force thus ranges from smoothed maximum of about 1000 to 3700 lb., since momentum drag can be neglected at these speeds.

g. 6-18-85 No Test Number. Circuit at Maximum Gross weight 69,297 lb. at STA 422 in., moved during circuit to STA 411.5 in. (Main wheels at STA 481 in. and 469 in.)

The circuit undertaken is sketched on Figure 50. Representative tow-bar time records are reproduced on Figure 51 and are selected, in order, from:

- |                                    |   |                          |
|------------------------------------|---|--------------------------|
| (1) Asphalt backup at 70% $N_f$    | } | Main wheels at STA 481   |
| (2) Downhill/grass at 80% $N_f$    |   |                          |
| (3) Uphill/grass at 80% $N_f$      |   |                          |
| (4) Tow on Wheatfield at 90% $N_f$ |   |                          |
| (5) Crossing crater at 90% $N_f$   |   |                          |
| (6) Crossing field (south)         |   |                          |
|                                    |   | - Main wheels at 469 in. |

Tow bar force calibration is 6000 lb/cm.  
Time scale is 12 cm/minute

Backing on asphalt required a mean push of about 1800 lb. with "jolts" to 6500 lb. and an rms fluctuation of about 1500 lb.

During the uphill tow on grass, a maximum pull of 8400 lb. was recorded in a trace that was steadily varying but showed little in the way of jolting.

On the flat field tow, values varied from 1500 to 4500 lb.

At the crater crossing, a fluctuating tow force peaked at 6900 lb. over a period of 2-3 seconds.

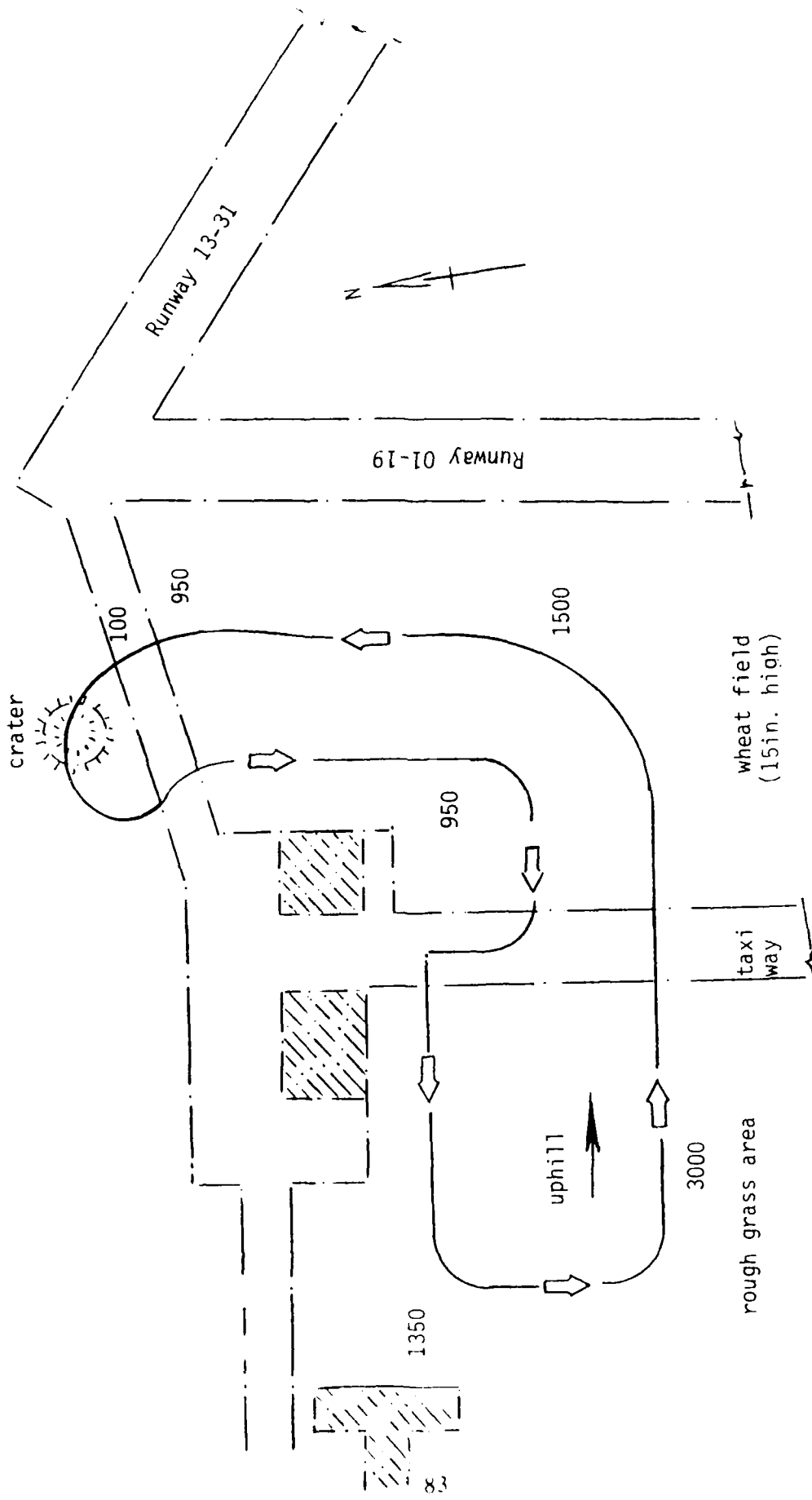
The south field traverse was generally similar to the north traverse, although one or two jolts of 3-4000 lb. occurred.

h. 6-25-85 No Test Number. No tape record. Gross weight 72,897 lb. at STA 413.8 in.

Aircraft was positioned with main wheels at STA 467 in. 6 x 450 lb. water barrels were also distributed symmetrically with their C.G. centered at STA 467 in.

Data available throughout these tests is very limited.

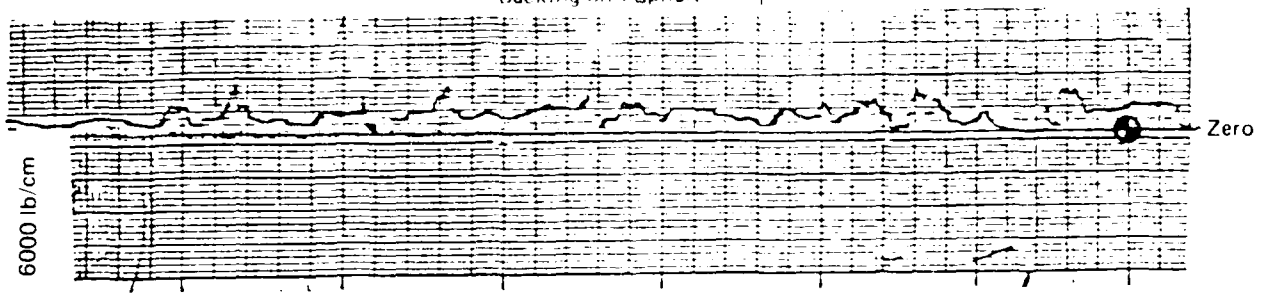
Breakaway tests were conducted on asphalt at 4 power settings. Only cushion pressure and heave height data is available and has been given on Figures 46C and 47. Using effective cushion areas based on heave height data, gross lift predictions



Note: Figures are noted grads of test of 6/18/85

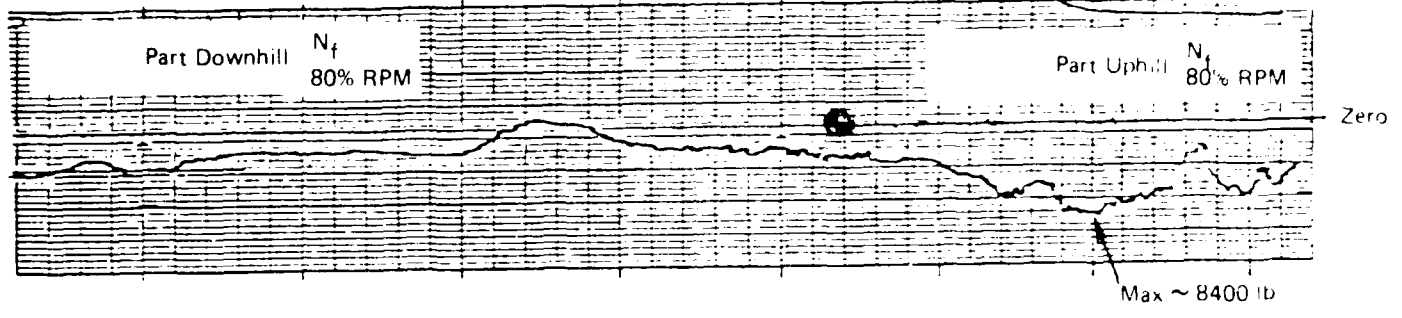
Figure 50. Plan of Typical Hardstand/Hill/Field/Crater Area of General Terrain Testing

Backing on Asphalt  $N_f$  70% RPM

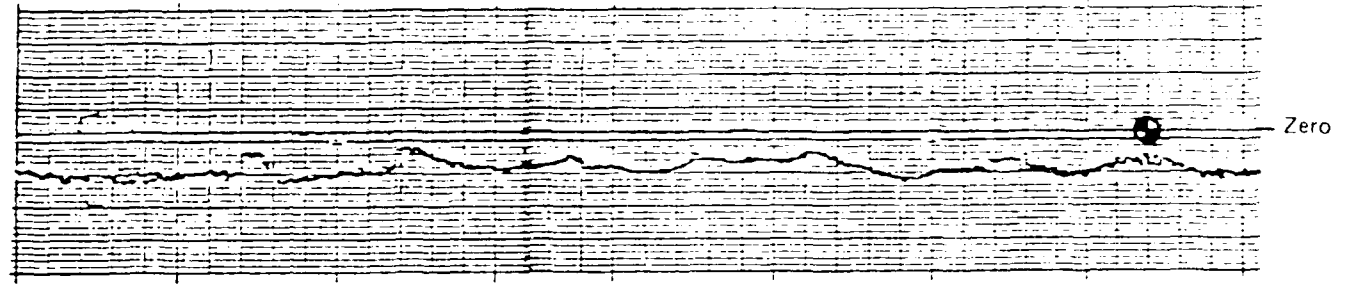


Part Downhill  $N_f$  80% RPM

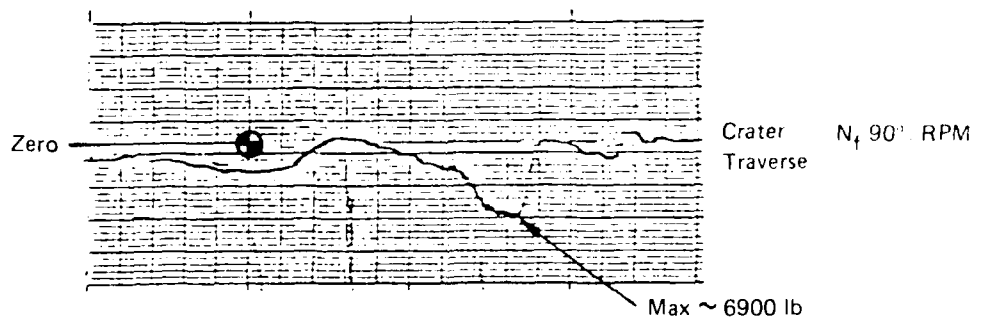
Part Uphill  $N_f$  80% RPM



Field Sample (→ North)  $N_f$  90% RPM



Scale  
6000 lb per cm  
12 cm per minute



Field Traverse South and West

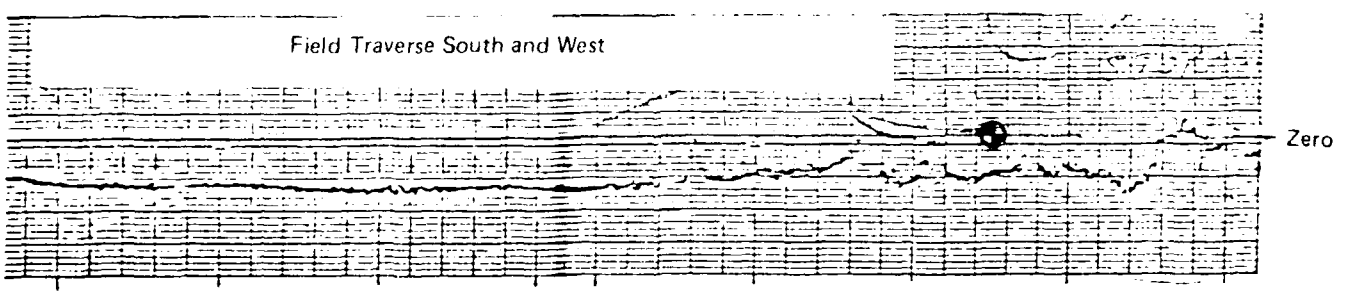


Figure 51. 69,297 lb Gross Weight Circuit-6/18/85

varied from 71,000 to 72,800 lb. with center of lift at STA's 397 to 398.5 in.

Subsequently, uneventful breakaway tests on grass and a field/crater circuit were conducted. Tow vehicle speeds across the crater up to 15 mph were achieved. No significant data was recorded during these test stages.

## SECTION IX

### CONCLUSIONS

The ACET has proved to be a highly maneuverable transporter capable of crossing snow, ice, rock, clay, and grass cover with very low drag, at weights to 75,000 lb.

Aircraft mounting and dismounting methods for rapid relocation over off-runway surfaces to/from a designated take-off and landing strip have been developed.

Violent heave divergences which can occur with stiff fans at high weight can be eliminated by introducing skirt vents. Except for a mild low frequency float in heave the ACET is a stiff and stable platform capable of carrying weight up to 60,000 lb.

## SECTION X

### RECOMMENDATIONS

In the prototype program, available ASP-10 engines were used for reasons of economy. In a production version, however, it would evidently be uneconomical to power the ACET with an expensive gas turbine. Further study followed by installation of an alternative power plant is recommended. Typically, this might be a diesel engine such as the DDA 8V92 TA mounted "inside" the box beam, driving a pair of centrifugal fans through a right angle gear box as shown in the sketch of Figure 52. Use of such fans may well eliminate heave stability problems. An extended analysis of stability is necessary to prove this.

Development of a better means for rapid mounting/dismounting of the aircraft is needed. The concept of venting the rear cushions to produce a reduction in heave height thus creating a deck slope of sufficient proportions for the aircraft to run backwards and thereby self dismount, proved practical. Venting the rear cushions with the fingered skirt was less than satisfactory and requires more work to simplify the mechanics of collapsing the required number of individual fingers. Solutions may be found in providing the transporter with a nose high attitude by increasing the depth of the forward cushion or by incorporating a permanent slope to the deck mounted wheel ramps (Figure 53). The deployment of the aircraft loading ramps is currently a time consuming manual operation. It is recommended that the deployment/retraction of these ramps be made by either pneumatic or hydraulic means.

To provide for a wide range of aircraft types to be loaded on ACET, it is recommended that the main wheel track be of lateral displacement to accommodate the main wheel track of a range of aircraft types. This would necessitate varying the position of the aircraft loading ramps but the ramps should be conveniently arranged and housed on a suitable structure to ease of placement.

The escaping cushion air creates a high velocity flow and the entrainment of airborne particulate matter which could be directed into the ACET and the equipment it is intended to protect. This is a critical area. To preclude this, it is recommended that a spray skirt be provided for each of the three cushions. The weight of such a skirt could be restricted to vital areas where the high velocity air is generated by the cushion air flow. This problem should be addressed.

The main wheel track should be adjustable to allow the transporter to traverse a range of deck heights. It is recommended that the main wheel track be adjustable to allow the transporter to traverse a range of deck heights.

AD-A188 369

AIR CUSHION EQUIPMENT TRANSPORTER (ACET) TESTING VOLUME 2/2  
2(U) BELL AEROSPACE CANADA TEXTRON GRAND BEND (ONTARIO)  
T D EARL ET AL OCT 86 7624-928882-VOL-2

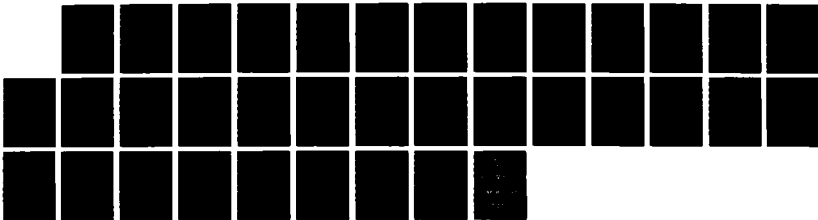
UNCLASSIFIED

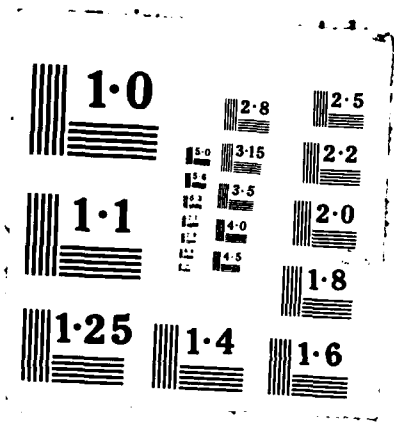
AFMAL-TR-86-3888-VOL-2

F/G 13/6

NL

4





1.0

1.1

1.25

2.8  
3.15  
3.5  
4.0  
4.5

1.4

2.5

2.2

2.0

1.8

1.6

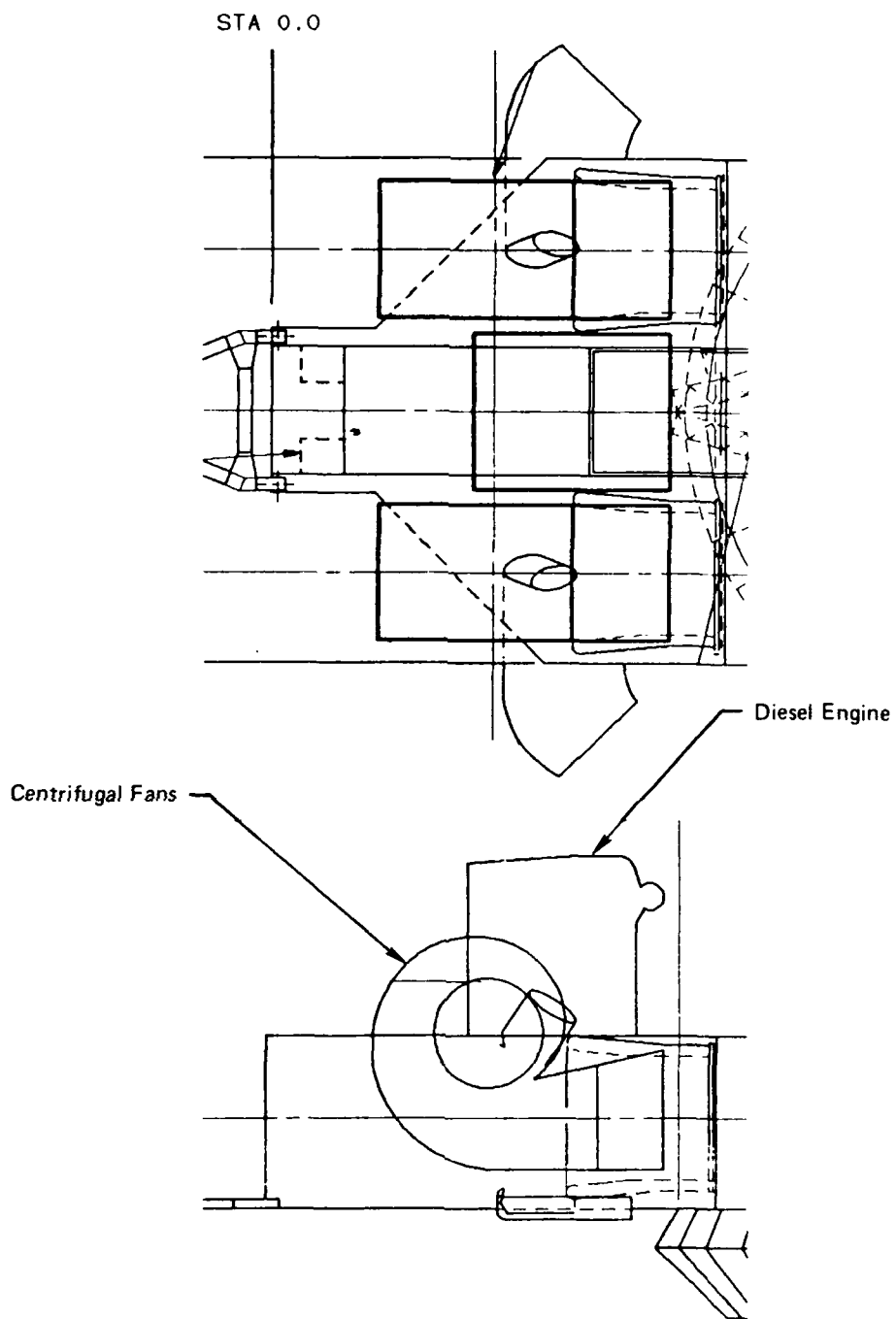
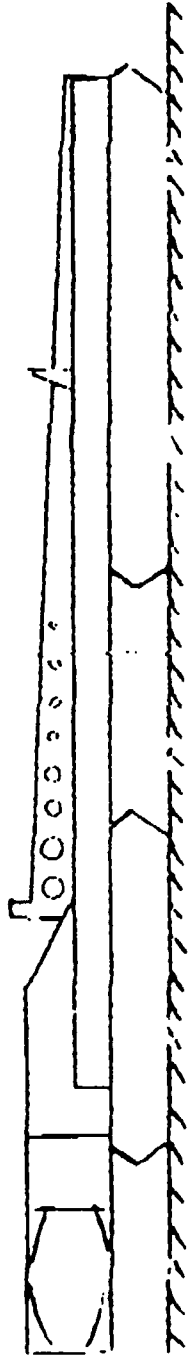
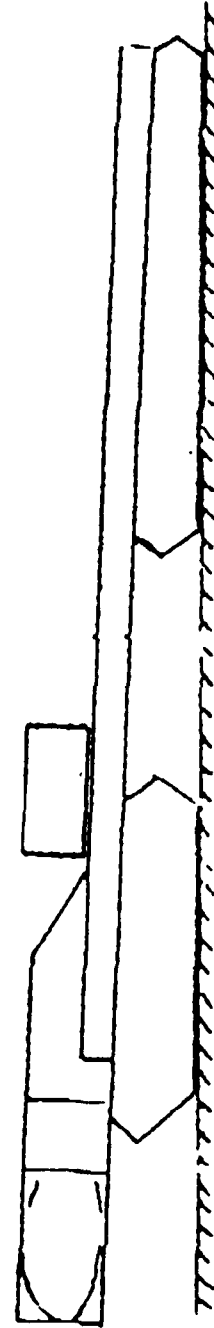


Figure 52. DDA 8V92 TA Diesel and Centrifugal Fan Installation



Stopping wheel tracks

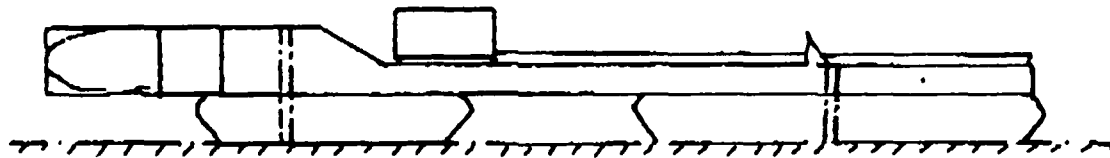


Increased depth forward cushion

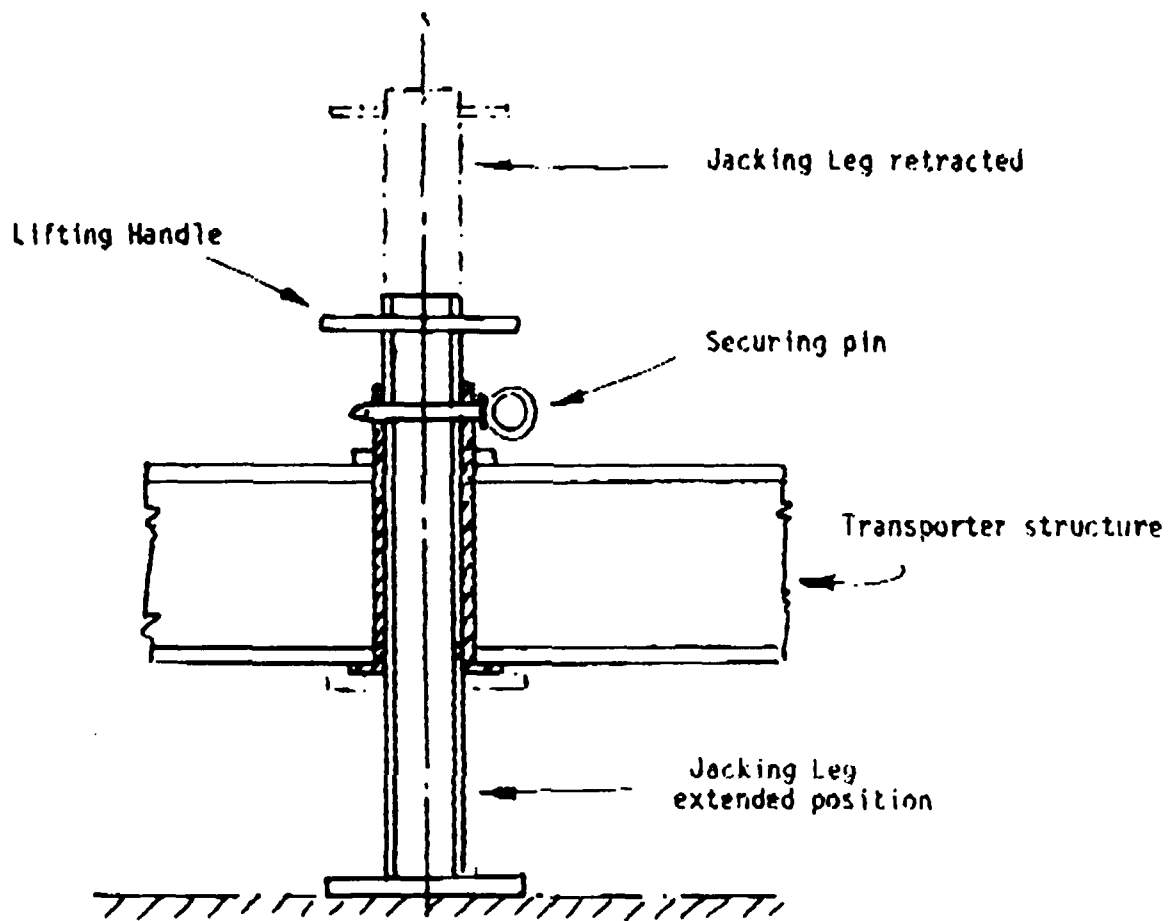
Figure 53. Methods of Providing Sloping Deck

system to a minimum. Prolonged running of the transporter over concrete surfaces inflicts heavy wear on the fingers. Consideration should be given to increasing the weight of the skirt material weight to 80 or 90 oz. The attachment of the fingers to the structure is not conducive to rapid finger replacement. This was not addressed in the initial design due to the necessity of securing the fingered skirt installation as early as possible. It is recommended that for future transporters consideration be given to designs for the rapid removal and installation of the fingers.

For skirt maintenance it is recommended that future transporters be equipped with a simple through-deck jacking device which would permit elevation of the craft without recourse to a crane or other remote lifting equipment. This simple device would consist of three tube assemblies manually extended and retracted when the transporter was on hover, being held in the desired location by a pin (Figure 54).



Location of jacking points



Transporter is placed on cushion and jacking leg is extended and secured in place. Transporter is then taken off hover and lowered onto jacking legs

Figure 54. Proposed Method of Vehicle Jacking

ACET HEAVE STABILITY ANALYSIS

J. J. Potter  
S. M. Warren

Report Date :  
August 1984

PREPARED FOR:

Bell Aerospace, Canada, Textron  
P.O. Box 160  
Grand Bend, Ontario  
Canada

IN RESPONSE TO:

Bell Aerospace Purchase  
Order Number 509828-3A

Boeing Military Airplane Company  
P.O. Box 3939  
Seattle, Washington 98124

### ACET Heave Stability Analysis

A heave stability analysis of the Air Cushion Equipment Transporter (ACET) was performed for Bell Aerospace Canada by the Landing Systems Group of The Boeing Military Airplane Company during July and August of 1984. The analysis was performed to size stability vents which are designed to prevent the heave instability that was exhibited by the ACET during full scale field tests. The field tests indicated that the instability is a function of weight. Undamped heave oscillations occurred (as explained by Bell) when the combined ACET and aircraft (F-101) weight was increased from 30000 pounds to 35000 pounds.

The objectives of the stability analysis described below were to (1) study the general nature of the instability exhibited by the ACET/aircraft system in the air cushion hover mode and (2) size stability vents to eliminate undamped heave oscillations of the ACET/aircraft system. The EASY air cushion computer models and programs developed by Boeing to study the Alternate Aircraft Takeoff System (AATS) were used during the analysis. The program input data were modified to incorporate characteristics of the ACET and F-101. In addition, a stability vent model based upon the Bell Aerospace recommended vent design (see Figure 1) was incorporated in the ACET model.

#### Computer Simulations and Vent Model

The computer simulations used for the ACET stability analysis were modified versions of the AATS/F4 EASY simulation. Revisions included input data changes and modification of the stability vent model.

- 1) The fan map of the ACET air supply system was modified to reflect the change from single engine AATS to dual engine ACET configuration. The fan slope was changed from -3.14 to -1.57 cu.ft./sec/psf.
- 2) The weight and CG of the air cushion vehicle and aircraft were changed to agree with those of the ACET.
- 3) The models of the stabilizing vents of the nose and main air cushion skirts were revised to reflect the proposed ACET vent design.

Items 1) and 2) above involved modification of data only, while item 3) involved changes to the computer code to implement the proposed ACET vent design. The original (AATS) vent model added a vent area to each cushion as the cushion pressure increased:

$$A_v = A_{nom} + DADP * (P_c - P_{nom})$$

where,

$A_{nom}, P_{nom}$  = Nominal vent area and cushion pressure  
 $DADP$  = Change in vent area per change in cushion pressure  
 $P_c$  = Cushion pressure  
 $A_v$  = Vent area

The modified (ACET) vent model includes the dynamic behavior of the venting mechanism in determining the vent area. The steady state vent area is of the same form as that above, however, cushion pressure and vehicle vertical acceleration act as forcing functions to a second order model of the venting mechanism. The state equation used to model the vent mechanism is:

$$\ddot{A}_v + 2 \zeta \omega \dot{A}_v + \omega^2 A_v = (P_c - P_{nom})/M_1 + \ddot{z}/M_2 + \omega^2 A_{nom}$$

where,

$\ddot{z}$  = Vehicle vertical acceleration  
 $A_{nom}, P_{nom}$  = Nominal vent area and cushion pressure  
 $\zeta, \omega$  = Venting mechanism damping ratio and frequency  
 $P_c$  = Cushion pressure  
 $M_1, M_2$  = Generalized masses associated with cushion pressure and vertical acceleration  
 $A_v$  = Vent area

The AATS stability analyses performed in 1983 utilized two separate EASY simulation models. The first model was of a single rigid body vehicle supported by three air cushion skirts and having the inertial properties of the AATS launcher and the F-4 aircraft. This model was identified as the lumped mass model. The second model was an extension of the first with the aircraft rigid body dynamics separately modelled and with an interaction component to determine forces exerted by each vehicle on the other. This model was identified as the coupled vehicle model.

Early analyses utilized the lumped mass model. It was during these analyses that the heave instability was identified and the original stabilizing vent model was implemented. Subsequent analyses with the coupled vehicle model showed substantially greater stability margins than those determined from the lumped mass model. Stabilization vent areas were reduced as a result of these increased stability margins. The enhanced stability of the coupled vehicle model is believed to be due to increased system damping associated with relative motion between the two vehicles. The source of this damping is the friction of the aircraft shock struts and damping of the shock struts and tires.

Initial analyses of the ACET stability was made using the coupled vehicle model. Results of a linear analysis of this model showed the ACET to be stable in pitch and heave at a total weight of 65500 pounds. Elimination of the stabilizing vents, tire damping and shock strut friction and damping reduced heave and pitch damping to marginally stable values with modal frequencies of approximately 12 Hz in heave and 5 Hz in pitch.

Similar analyses with the lumped mass model predicted unstable heave response at weights above 48,000 pounds. Pitch and heave frequencies for this model were found to be approximately 1.5 and 3.5 Hz respectively.

Upon consultation with Bell, it was determined that the apparent instability exhibited during their testing was more consistent with that predicted by the lumped mass model than the coupled vehicle model. Therefore, it was decided that the remainder of the analysis and sizing of the vent mechanism would be performed using the lumped mass model.

#### Vent Sizing

The venting mechanism used for the stability analysis was assumed to be a hinged, spring loaded door positioned above each air cushion. The preliminary vent configuration provided by Bell is shown in Figure 1. At cushion pressures above that required to overcome the spring preload, the vent door is assumed to act as a second order dynamic system forced by cushion pressure and rigid body vertical acceleration. Dimensions of the main cushion vents were taken as those provided by Bell in Figure 1. It was assumed that the nose cushion would incorporate two 14 X 14 inch vents. Vent slopes (ratio of the change in effective vent area to the change in cushion pressure) were estimated to be the same as those established during the AATS analysis. Cracking pressure of the vents was set to correspond to a loaded weight of 35,000 pounds.

#### Stability Analysis

The analysis performed to assess the effects of the proposed stabilizing vents on the stability of the ACET consisted of the following four tasks.

- 1) Analyze effect of vents on ACET rigid body stability,
- 2) Analyze stability of venting mechanism,
- 3) Assess sensitivity of stability to vent design parameters,  
and
- 4) Verify stability analysis with time history simulations.

## Rigid Body Stability

Figures 2 and 3 show the results of small perturbation stability analyses performed as a function of gross weight with and without the incorporation of the stabilizing vents. As shown in these figures, the vents have a slight stabilizing effect on pitch response (Figure 2) and a substantial stabilizing effect on heave response (Figure 3). Heave damping at 70000 pounds is approximately equivalent to that at 35000 pounds without the stabilizing vents.

## Vent Mechanism Stability

The results of analyzing the stability of the venting mechanism is shown in Figures 4 through 6. These figures show the frequencies and damping ratios of the three modes associated with the dynamic responses of the venting mechanisms. It was determined that stable venting response requires minimum vent mechanism damping of 30% of critical.

Natural frequencies of the nose and main vent mechanisms were estimated from the vent sizes and spring rates required to achieve the desired vent slopes. Nose and main vent natural frequencies were estimated at 80 and 60 rad/sec respectively. Figures 7 through 11 show the system eigenvalues at 70,000 pound vehicle weight as the vent frequencies were varied by 50%. All conditions assume that damping of the venting mechanisms is maintained at 30% of critical. These results predict stable ACET dynamic behavior over the range of frequencies analyzed.

## Simulation Time Histories

The vent characteristics determined during the stability analysis were used to generate time history responses of the lumped mass ACET model at high and low weights and with and without the stabilization vents. Simulations were performed at the point of vent opening (35,000 pounds) and at maximum gross weight (70,000 pounds). All cases simulate a drop from a height of approximately 5 inches.

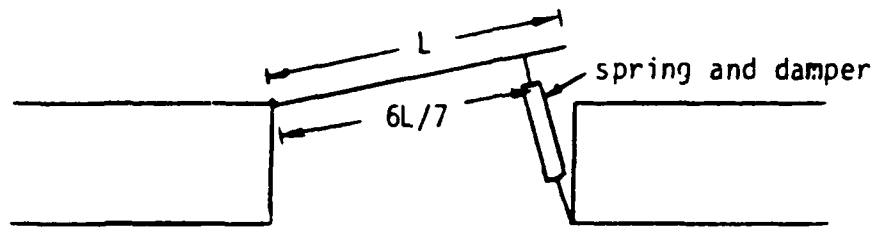
Figures 12 and 13 show time histories of pertinent simulation variables for the low gross weight condition without and with stabilizing vents respectively. Both conditions exhibit stable dynamic behavior. However, the addition of the stabilization vents does improve heave damping.

Figures 14 and 15 show the same data for the maximum gross weight condition. The ACET/aircraft system as shown in Figure 14 exhibits divergent heave oscillations without the stabilizing vents. The response shown in Figure 15 confirm that the incorporation of the vents produce stable dynamic behavior of the model.

## Recommendations

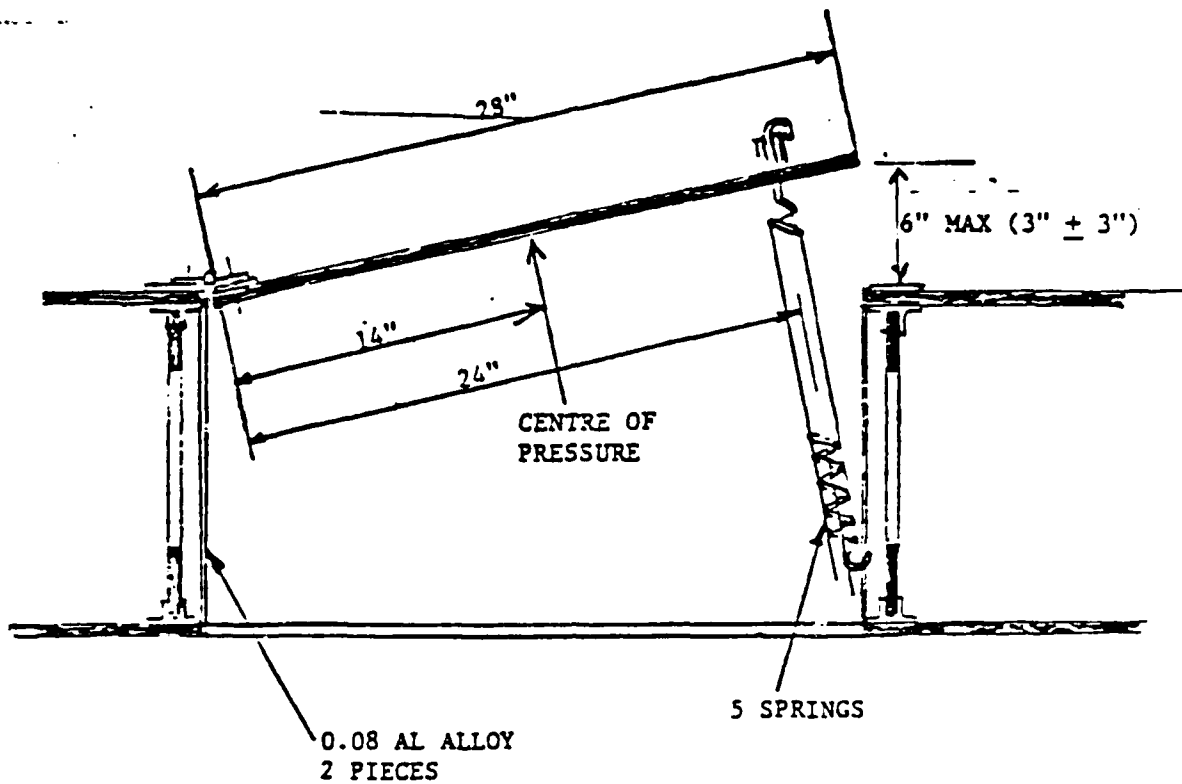
Based on the results of these analyses, it is recommended that the stabilizing vent design proposed by Bell be implemented on the ACET air cushion vehicle. Vent design parameters determined in these analyses are given in Table 1.

Table 1  
ACET Vent Design Parameters



The ACET vent design parameters presented below are based on calculations assuming the vent configuration depicted above having a square vent door with a uniform density of 3.6 lb/sqft.

Parameter	Nose (each - 2 required)	Main
Natural frequency $\omega$ (rad/sec)	80	60
Damping ratio $\zeta$ (nondim)	.3	.3
Discharge coefficient $C_d$ (nondim)	.85	.85
Vent dimension L (in)	14	28
Nominal effective area $A_{nom_e}$ (sq ft)	.292	1.076
Nominal pressure $P_{nom}$ (psf)	128.5	117
Effective vent slope $dA_e/dP$ (sqft/psf)	.004	.016
Spring constant $K_{spring}$ (lb/in)	38.25	75
Damping constant $C_{damper}$ (lb/in/sec)	.30	.75
Spring preload (lb)	53	193



CROSS SECTION LOOKING INB'D

ANALYSIS:

CRITERIA:

Vent area required at 68,800 lb. GW=1.0 sq.ft. (main cell)

Area rate of change  $\frac{dA}{dp_c} = 0.02$  sq.ft./psf

Design for  $\pm$  adjustments to these figures.

Vent door dimensions 28" x 28" (between bulkheads)

Pressure area = 5.44 sq.ft.

Vent gap nominal at maxim GW = 0.25 ft (3 in.)

Gross vent area =  $.25 \times 2.33 + 2(1.17 \times .25) = 1.17$  sq.ft.

Assumed discharge  $C_D = 0.85$

Nett vent area = 1.0 sq.ft.

Retaining springs total load =  $707 \times \frac{14}{24} = 412$  lb.

Area change per 1.0 travel at door edge  
 $= \frac{1}{12} \times 2.33 \times 2 \times .85 = 0.33$  sq.ft.

Spring extension for 1.0 travel =  $1.0 \times \frac{24}{28} = 0.86$ "

Pressure increment for this extension =  $\frac{0.33}{0.02} = 16.5$  psf

Load increment =  $5.44 \times 16.5 = 90$  lb.

Springs load increment =  $90 \times \frac{14}{24} = 52.5$  lb.

Assume 5 springs. Rate =  $10.5$  lb +  $0.86 = 12.2$  lb/in

Initial extension at max GW =  $\frac{412}{5 \times 12.2} = 6.75$  in.

Initial free length  $\approx 12$  in.

NOTES: 1. By use of a number of springs rate is easily adjusted by adding or removing them.

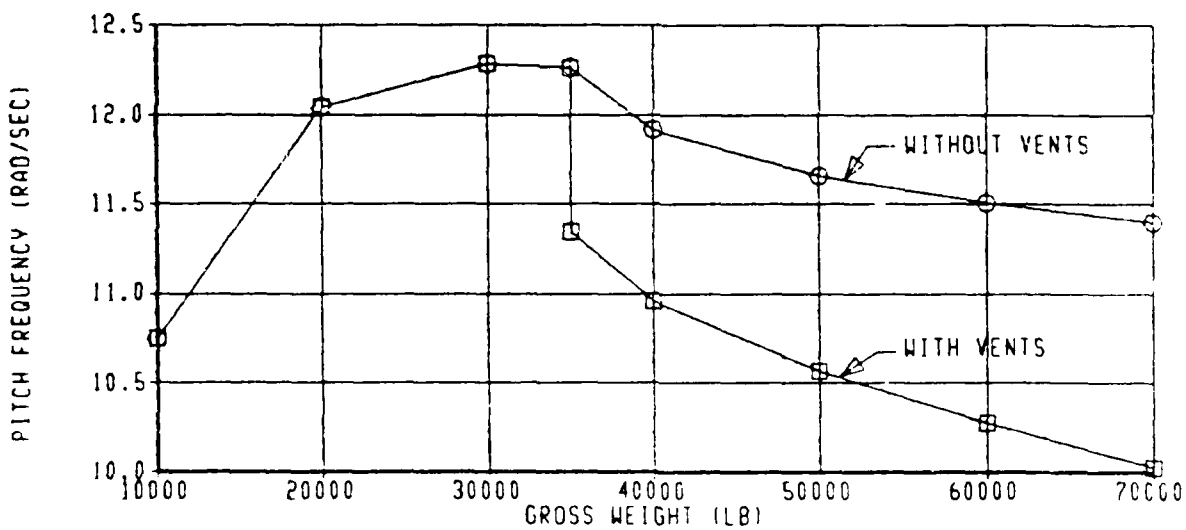
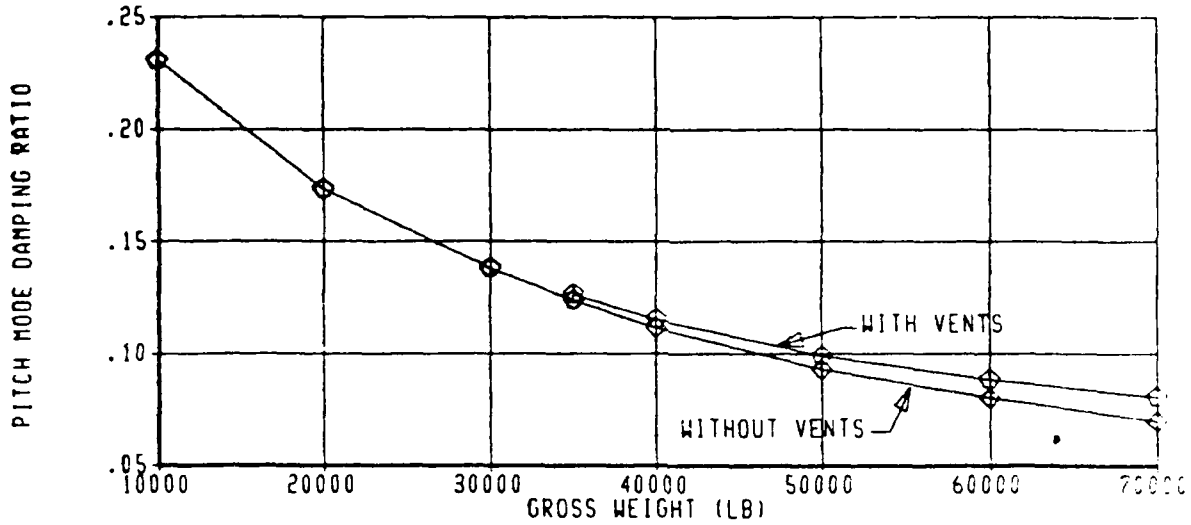
2. Nominal vent area is adjusted by tensioning the springs.

3. INERTIA OF DOOR CAN BE VARIED BY ADDING WT.

4. DAMPER WOULD BE NEEDED.

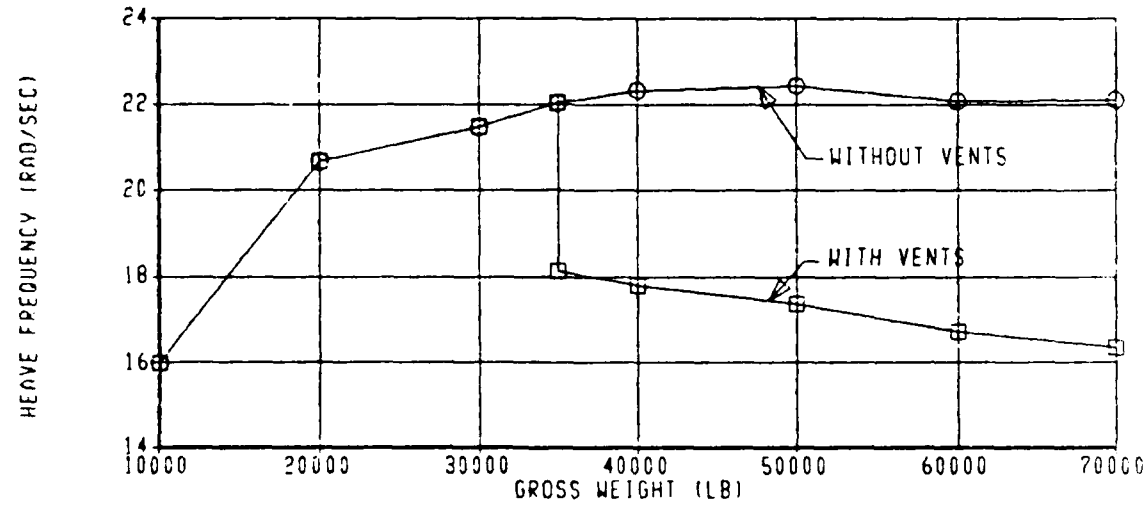
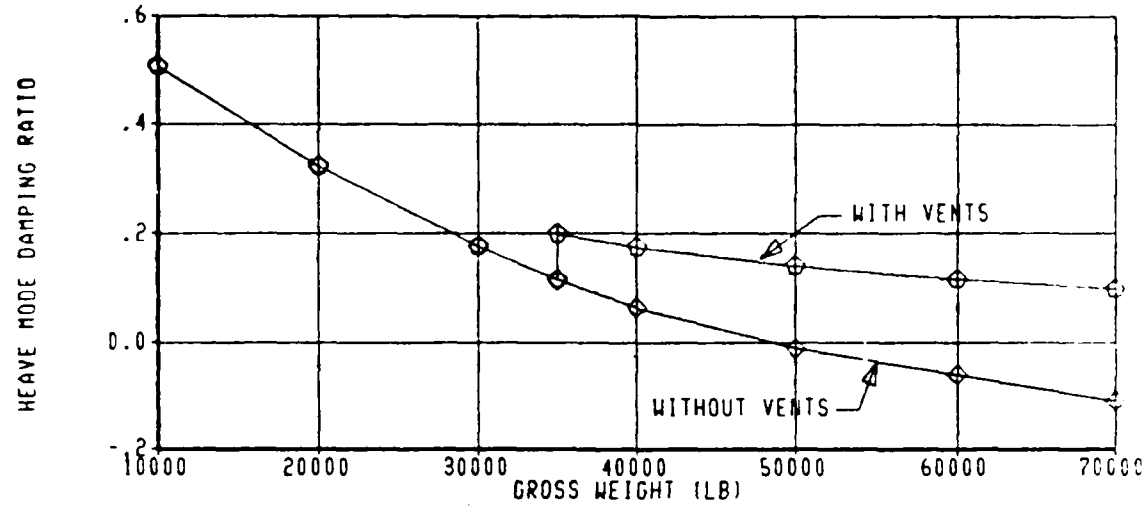
Figure 1 - Bell Aerospace  
 Proposed Main Cushion Vent Design  
 And Initial Sizing Data

EASY DYNAMIC ANALYSIS  
 LUMPED ACET/F-101 MODEL  
 STABILITY ANALYSIS



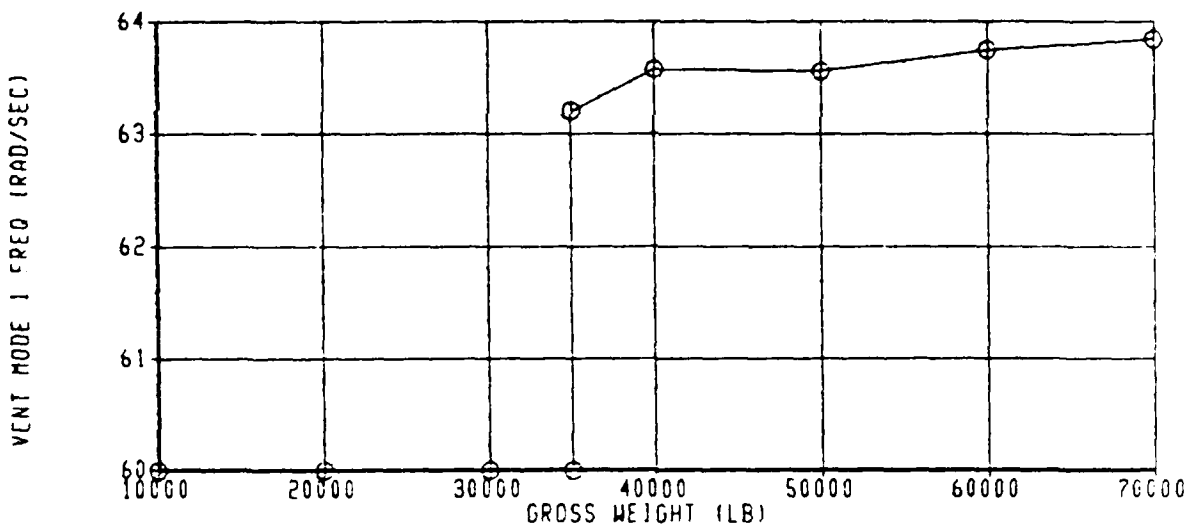
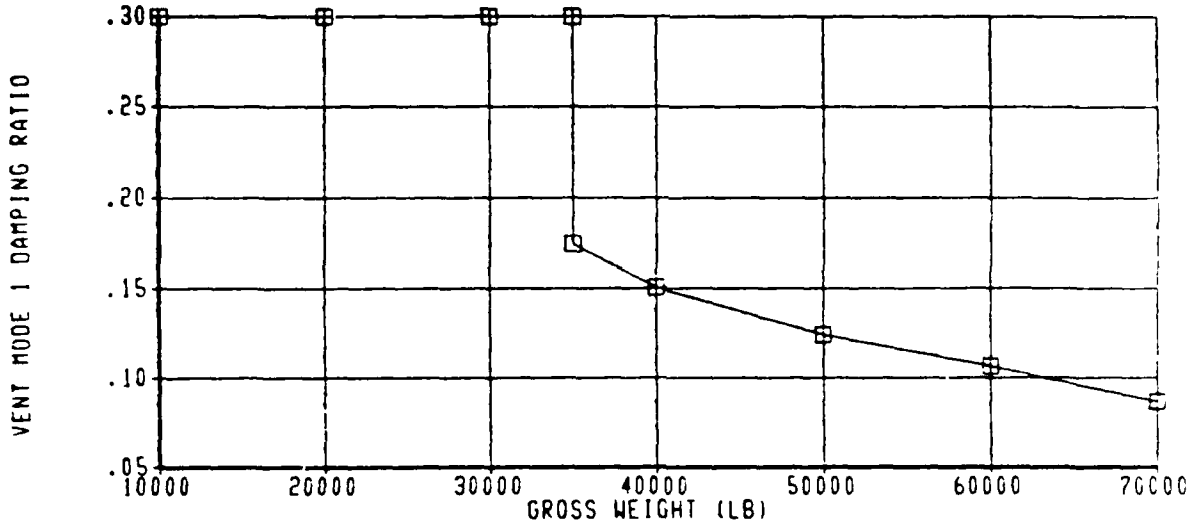
CALC	01AUG84	REVISED	DATE	ACET STABILITY ANALYSIS PITCH MODE FREQUENCY AND DAMPING WITH AND WITHOUT STABILIZING VENTS THE BOEING COMPANY	Figure 2
CHECK					PAGE
APPD.					
APPD.					

EASY DYNAMIC ANALYSIS  
LUMPED ACET/F-101 MODEL  
STABILITY ANALYSIS



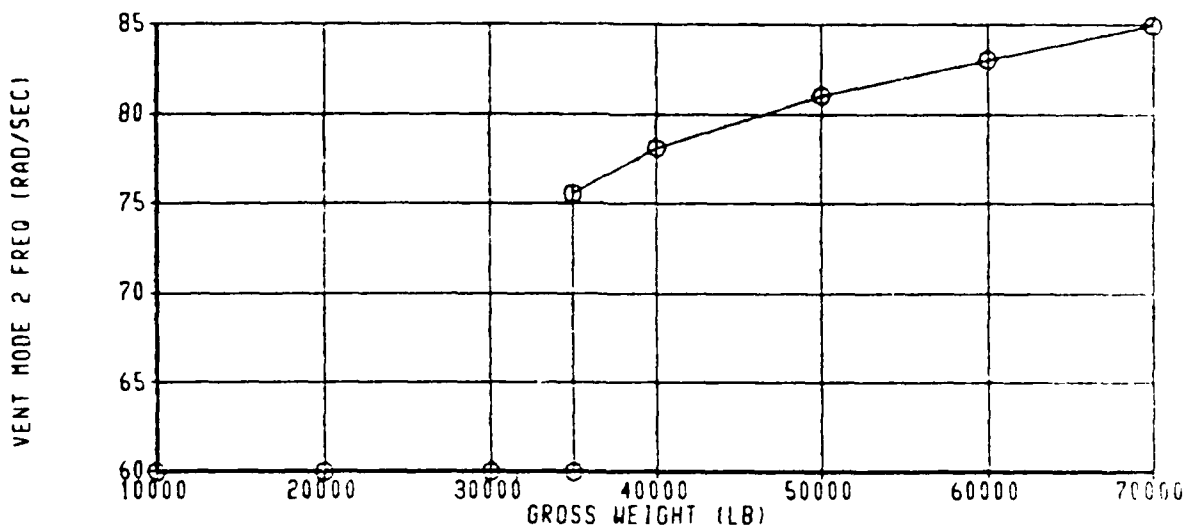
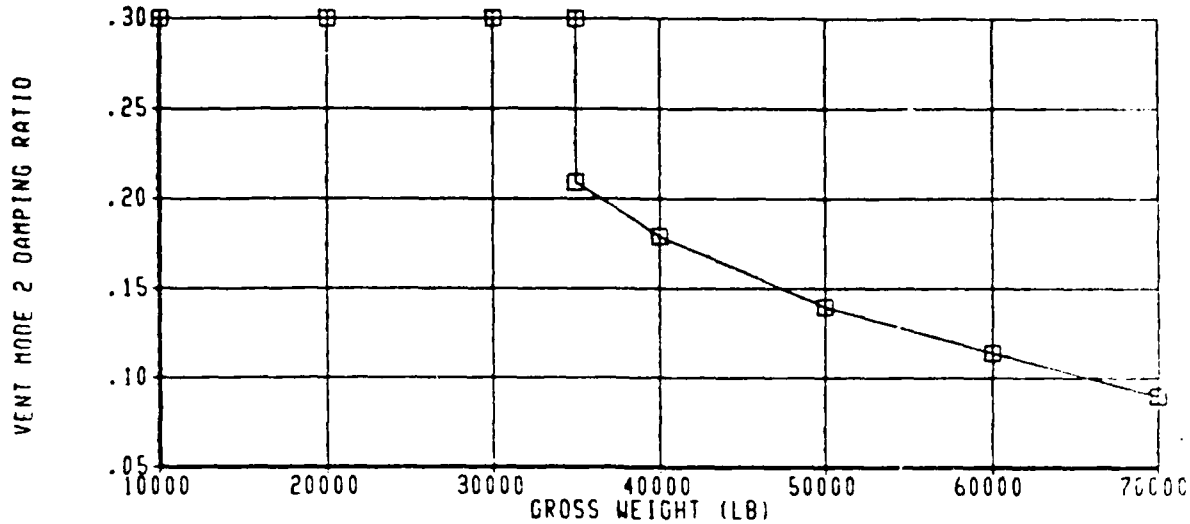
CALC	01AUG84	REVISED	DATE	ACET STABILITY ANALYSIS HEAVE MODE FREQUENCY AND DAMPING WITH AND WITHOUT STABILIZING VENTS THE BOEING COMPANY	Figure 3 PAGE
CHECK					
APPO.					
APPO.					

EASY DYNAMIC ANALYSIS  
LUMPED ACET/F-101 MODEL  
STABILITY ANALYSIS



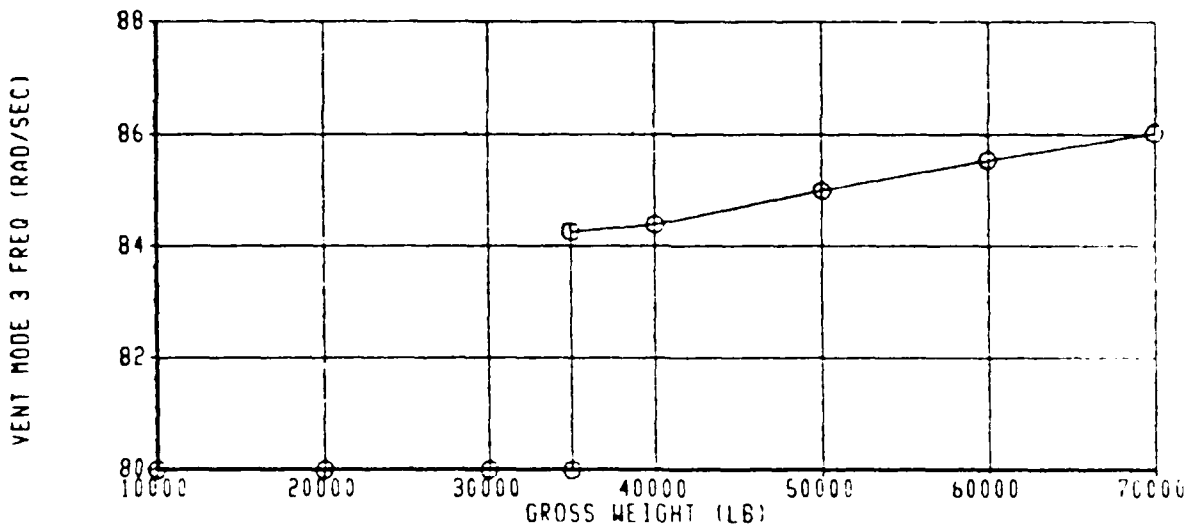
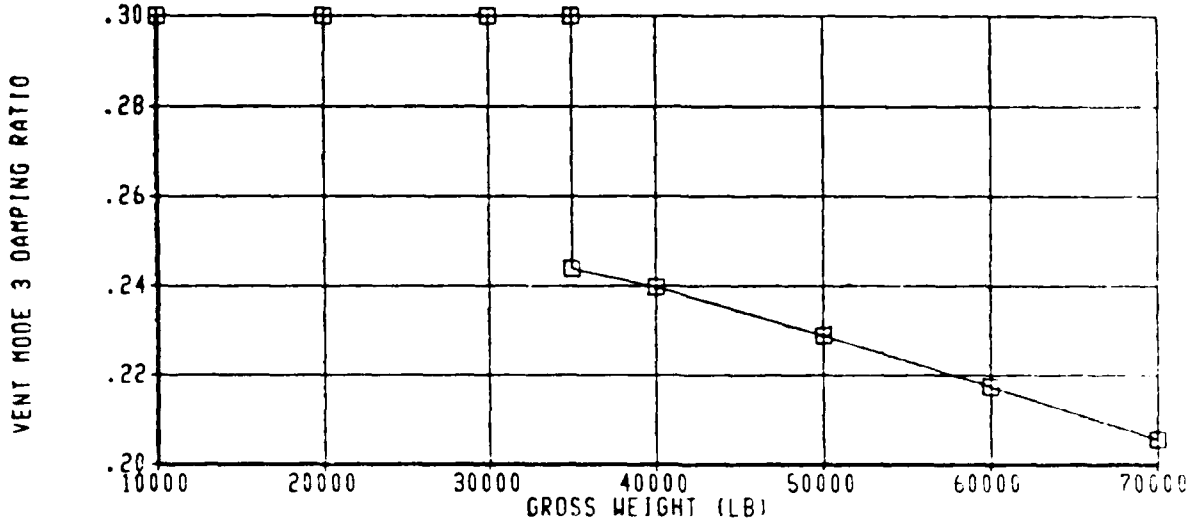
CALC	01AUG84	REVISED	DATE	ACET STABILITY ANALYSIS FREQUENCY AND DAMPING OF FIRST VENT MODE	Figure 4
CHECK					
APPD.					
APPD.					
THE BOEING COMPANY				PAGE	

EASY DYNAMIC ANALYSIS  
LUMPED ACET/F-101 MODEL  
STABILITY ANALYSIS



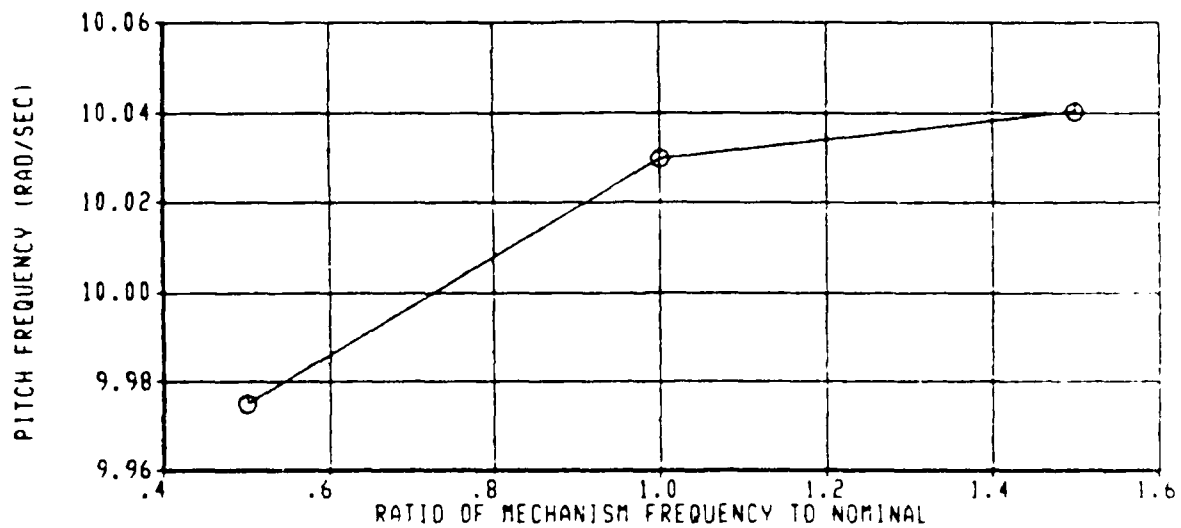
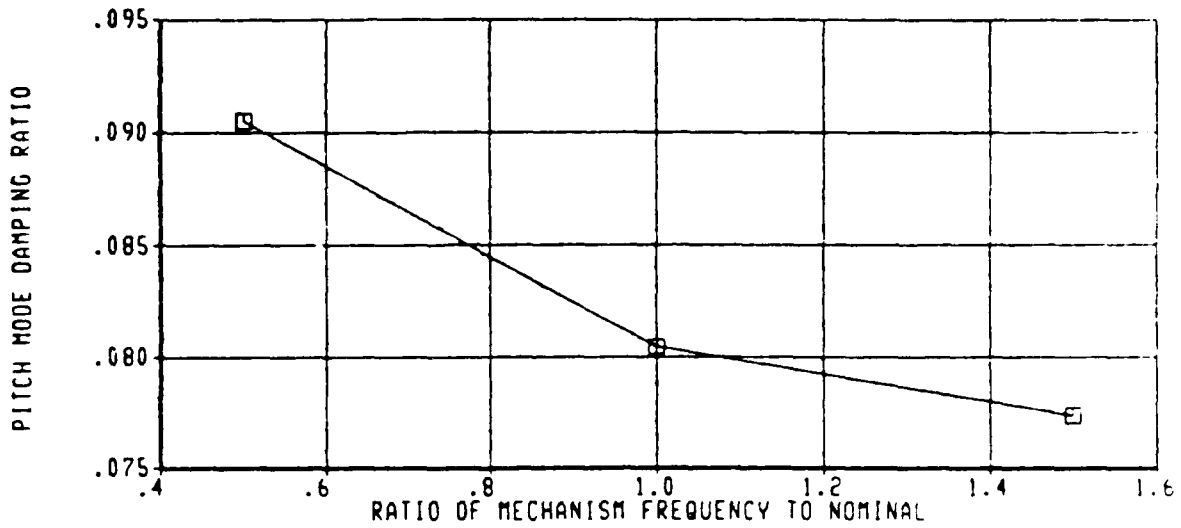
CALC	01AUG64	REVISED	DATE	ACET STABILITY ANALYSIS FREQUENCY AND DAMPING OF SECOND VENT MODE	Figure 5
CHECK					
APPD.					PAGE
APPD.					
				THE BOEING COMPANY	

EASY DYNAMIC ANALYSIS  
LUMPED ACET/F-101 MODEL  
STABILITY ANALYSIS



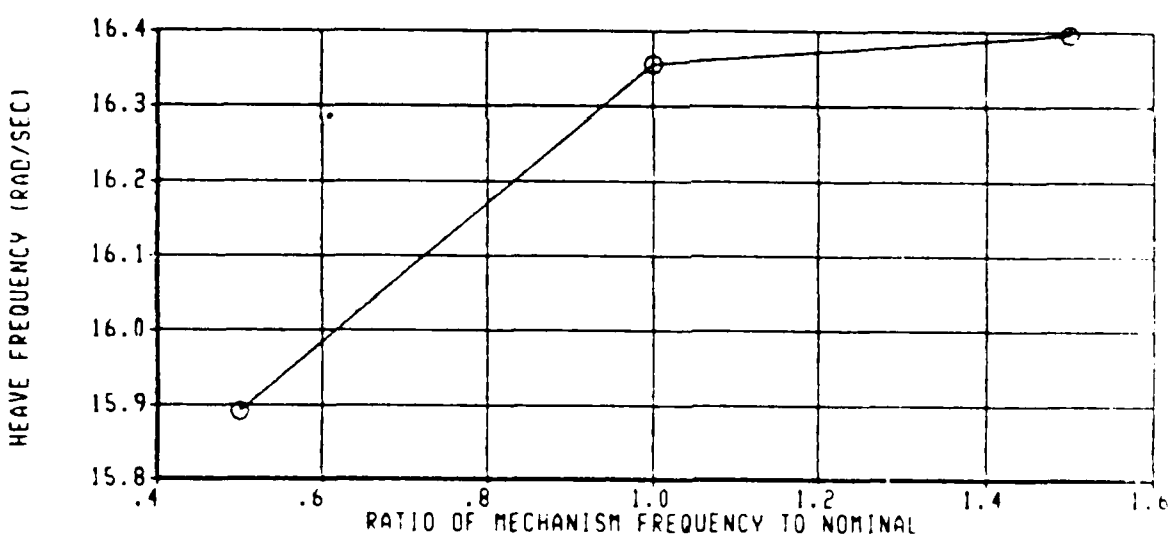
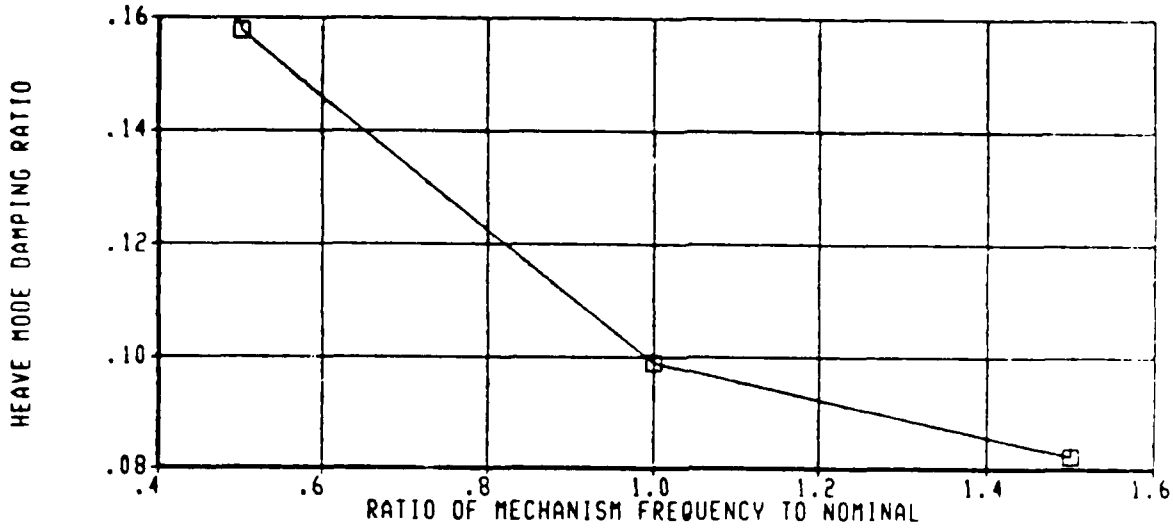
CALC	01AUG84	REVISED	DATE	ACET STABILITY ANALYSIS FREQUENCY AND DAMPING OF THIRD VENT MODE  THE BOEING COMPANY	Figure 6  PAGE
CHECK					
APPD.					
APPD.					

EASY DYNAMIC ANALYSIS  
LUMPED ACET/F-101 MODEL  
STABILITY ANALYSIS



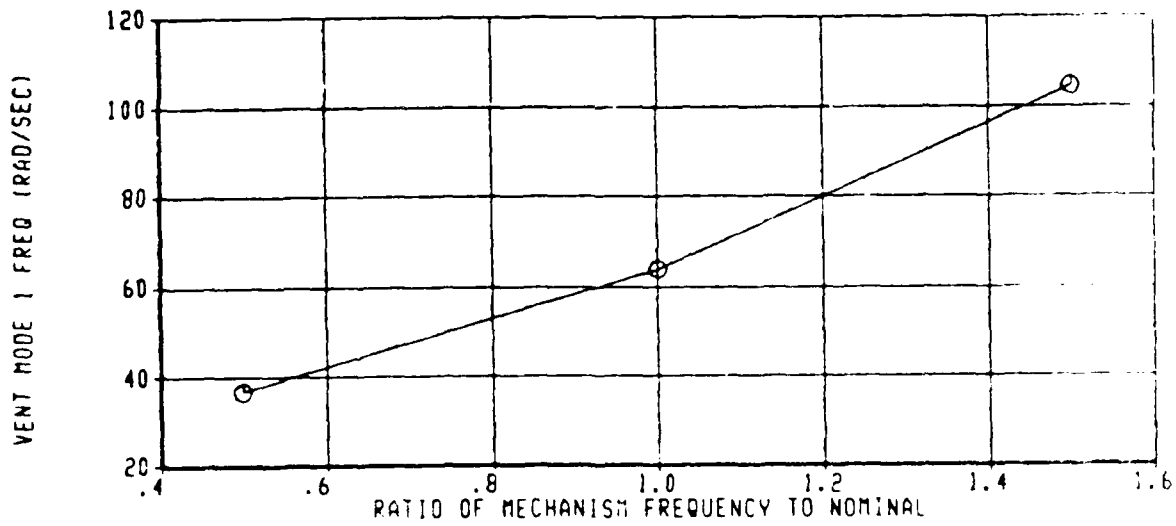
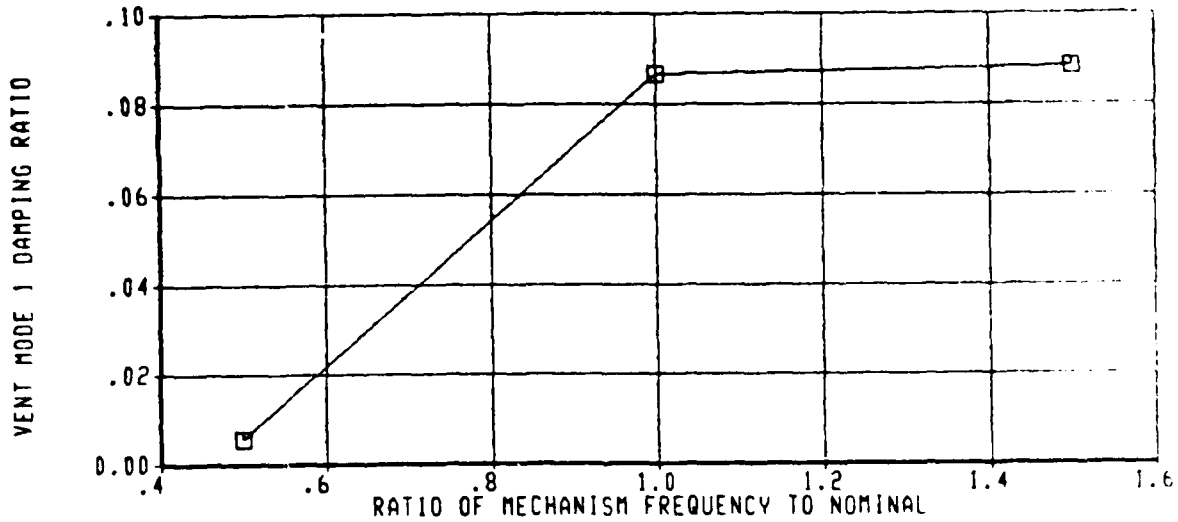
CALC	02AUG84	REVISED	DATE	ACET STABILITY ANALYSIS EFFECT OF VENT MECHANISM FREQUENCY ON PITCH MODE CHARACTERISTICS THE BOEING COMPANY	Figure 7 PAGE
CHECK					
APPD.					
APPD.					

EASY DYNAMIC ANALYSIS  
LUMPED ACET/F-101 MODEL  
STABILITY ANALYSIS



CALC	02AUG84	REVISED	DATE	ACET STABILITY ANALYSIS EFFECT OF VENT MECHANISM FREQUENCY ON HEAVE MODE CHARACTERISTICS  THE BOEING COMPANY	Figure 8
CHECK					PAGE
APPO.					
APPO.					

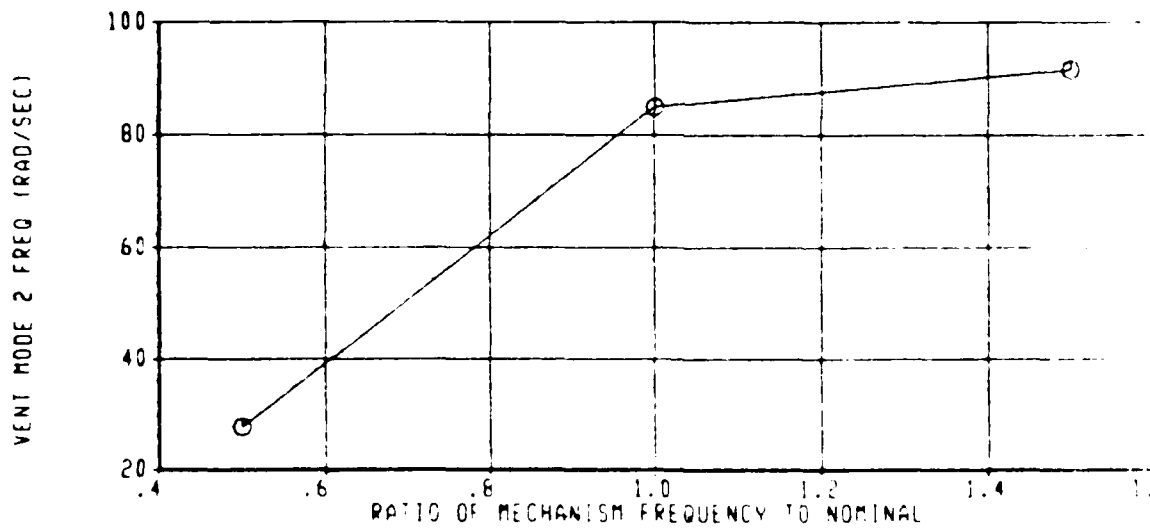
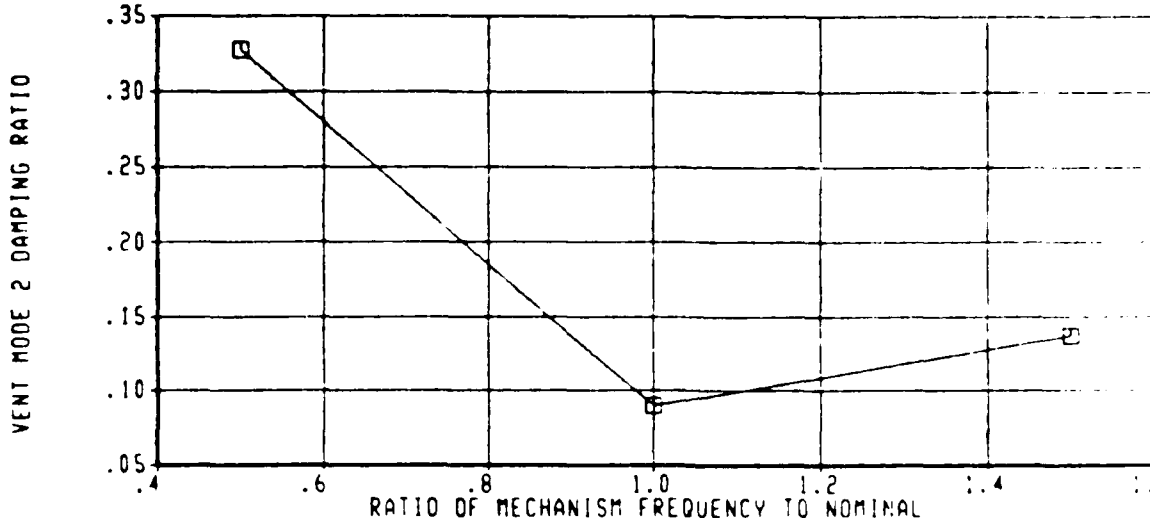
EASY DYNAMIC ANALYSIS  
LUMPED ACET/F-101 MODEL  
STABILITY ANALYSIS



CALC	02AUG84	REVISED	DATE	ACET STABILITY ANALYSIS EFFECT OF VENT MECHANISM FREQUENCY ON FIRST VENT MODE CHARACTERISTICS THE BOEING COMPANY
CHECK				
APPD.				
APPD.				

Figure 1  
PAGE

EASY DYNAMIC ANALYSIS  
LUMPED ACET/F-101 MODEL  
STABILITY ANALYSIS

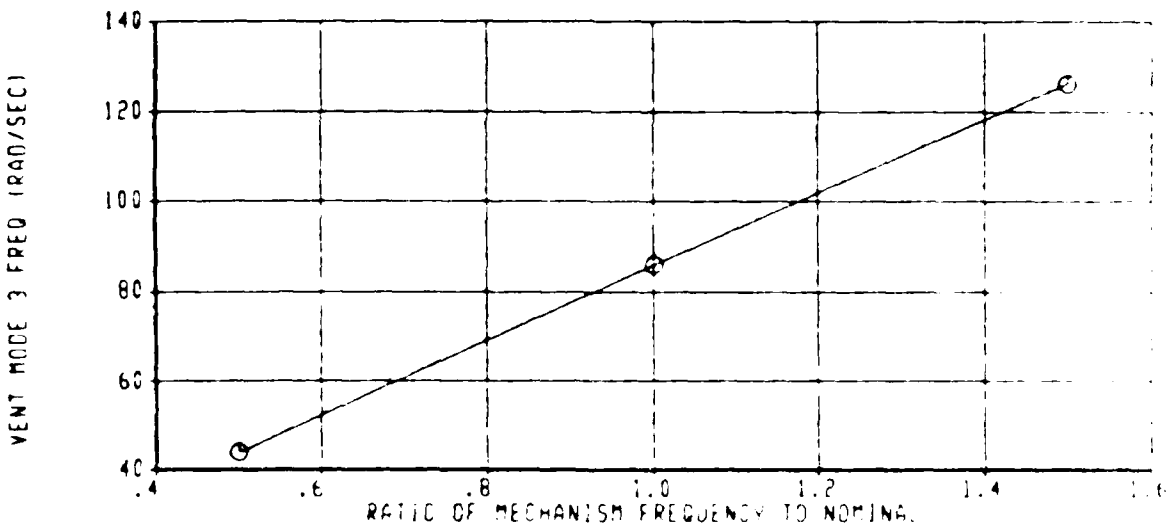
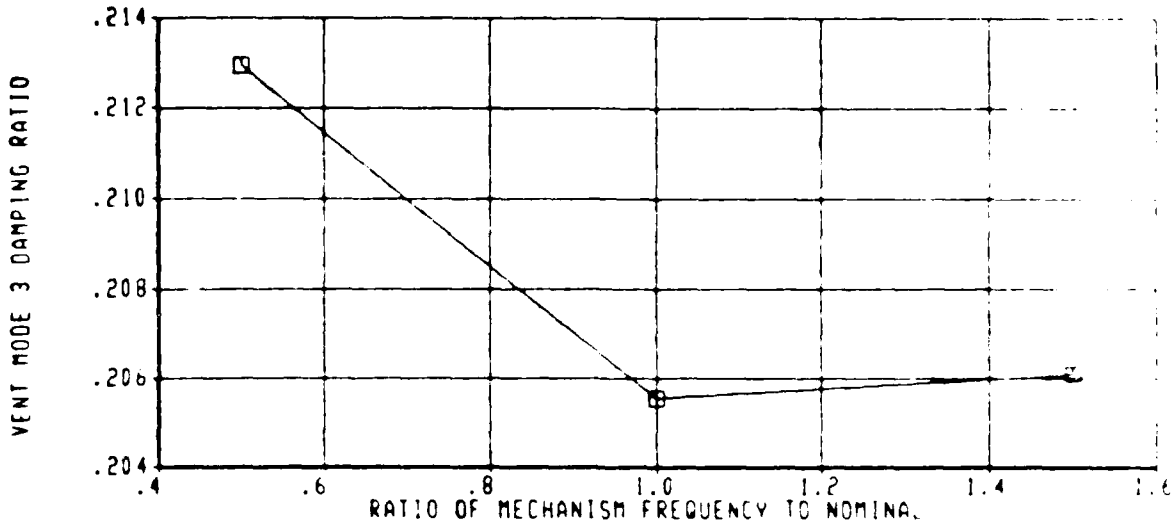


CALC	02AUG84	REVISED	DATE
CHECK			
APPD.			
APPD.			

ACET STABILITY ANALYSIS  
EFFECT OF VENT MECHANISM FREQUENCY  
ON SECOND VENT MODE CHARACTERISTICS  
THE BOEING COMPANY

FIGURE 1

EASY DYNAMIC ANALYSIS  
LUMPED ACET/F-101 MODEL  
STABILITY ANALYSIS

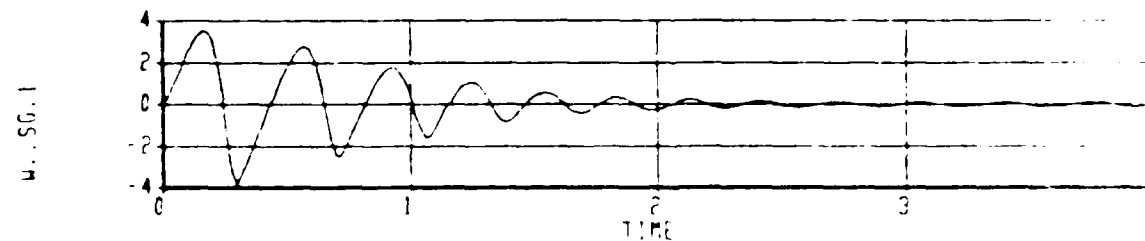
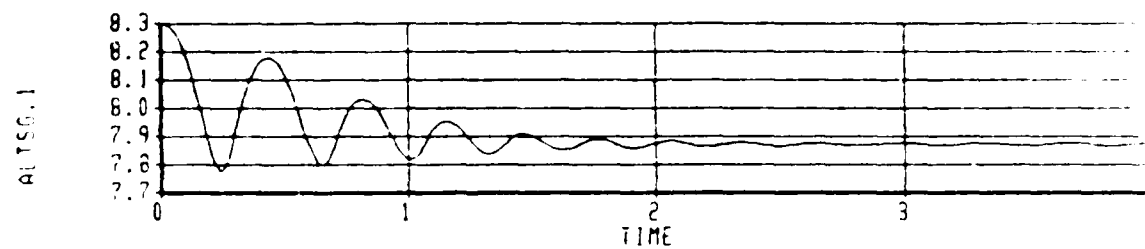
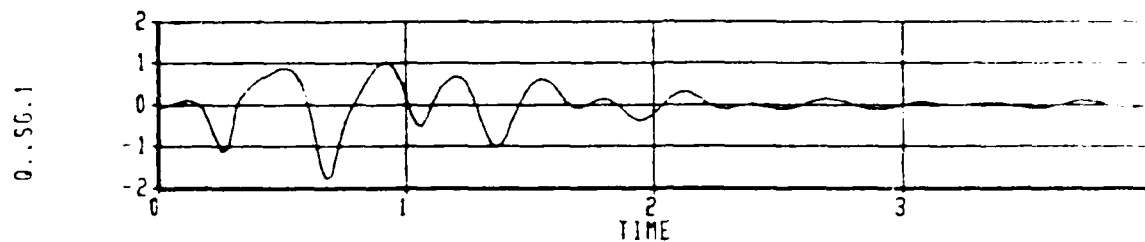
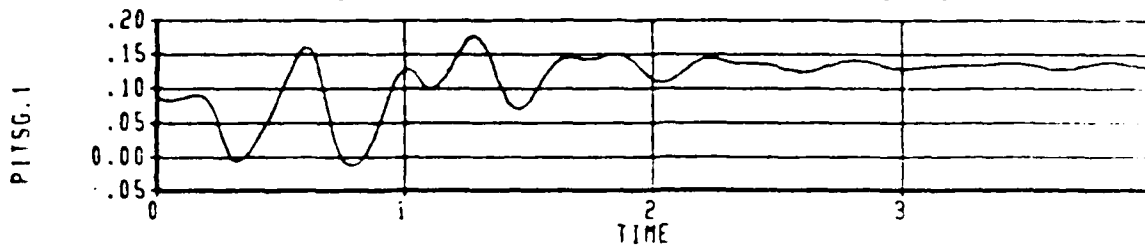


CALC	02AUG64	REVISED	DATE
CHECK			
APPD.			
APPD.			

ACET STABILITY ANALYSIS  
EFFECT OF VENT MECHANISM FREQUENCY  
ON THIRD VENT MODE CHARACTERISTICS  
THE BOEING COMPANY

Figure 2  
PAGE

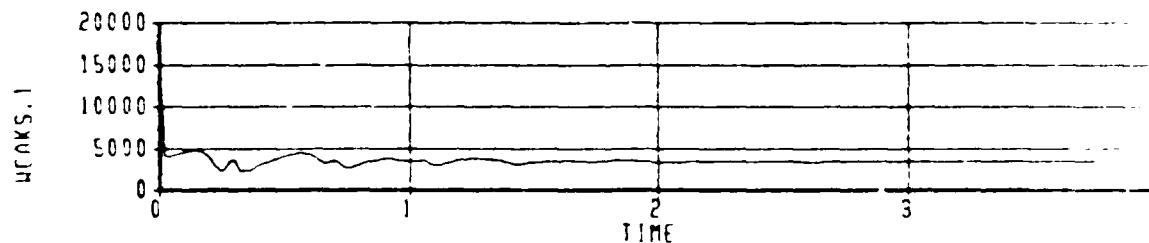
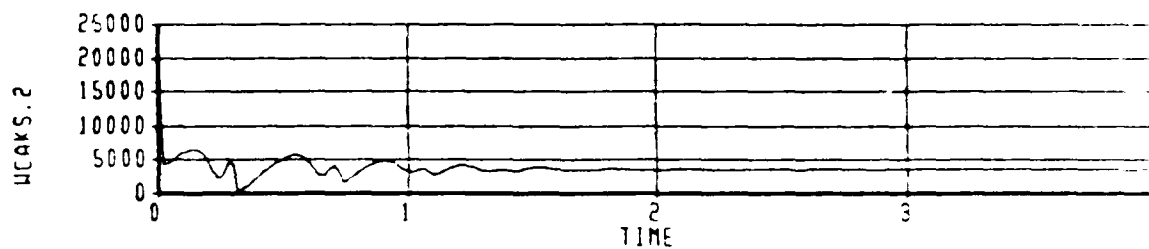
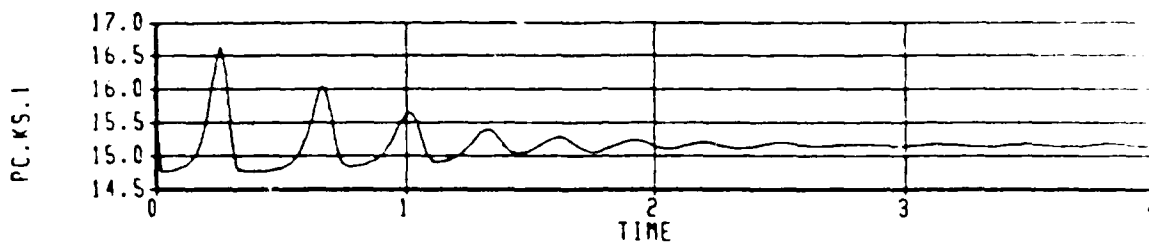
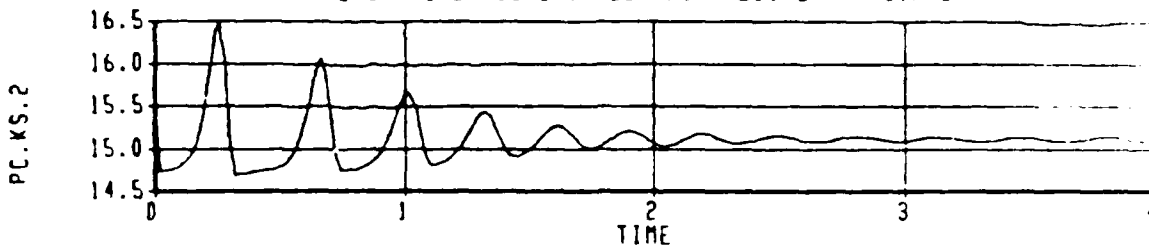
ACET 35000 LB. WITHOUT VENTS  
 RUN DATE= 84/07/27. RUN TIME= 18.41.03.  
 EASY TIME HISTORY PLOT WITH 201 DATA POINTS



PITSG.1 Vehicle pitch attitude deg  
 P. SG.1 Vehicle pitch rate deg/sec  
 ALTSG.1 Vehicle altitude ft  
 W. SG.1 Vehicle Z body axis velocity ft/sec

CA C	DIAGRAM	REVISED	DATE	ACET STABILITY ANALYSIS 5 IN. DROP AT 35000 POUNDS WITHOUT STABILIZING VENTS	THE BOEING COMPANY
ONE					
APPO					
APPO					

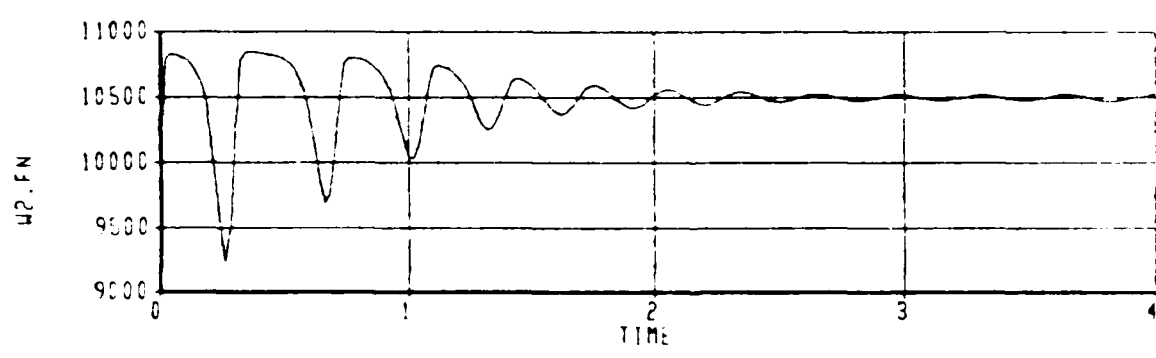
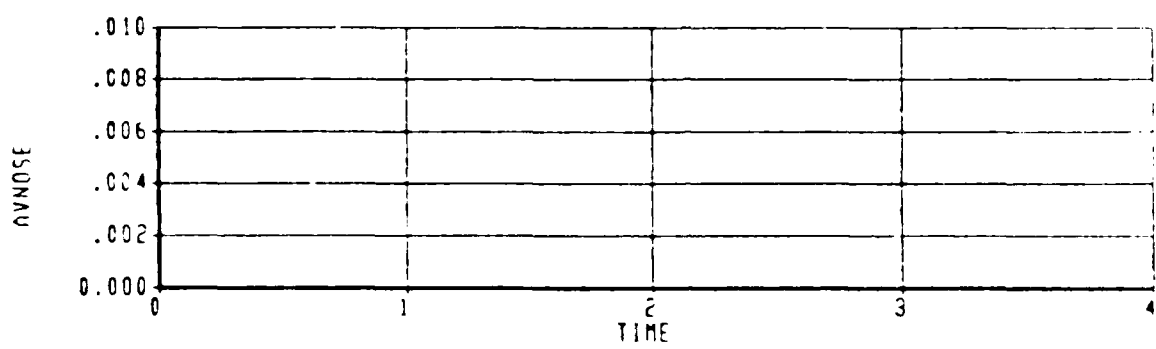
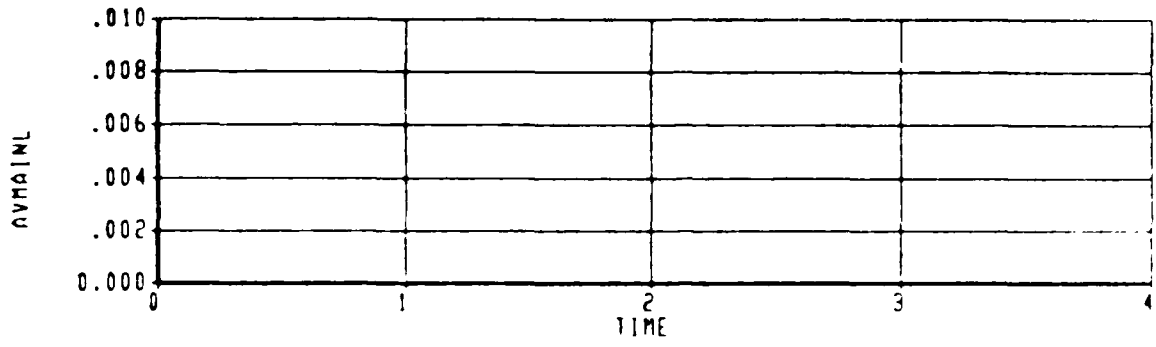
ACET 35000 LB. WITHOUT VENTS  
 RUN DATE= 84/07/27. RUN TIME= 18.41.03.  
 EASY TIME HISTORY PLOT WITH 201 DATA POINTS



PC.KS.2 Left main skirt cushion pressure psia  
 PC.KS.1 Nose skirt cushion pressure psia  
 WCAKS.2 Left main skirt air flow to atmosphere lb/min  
 WCAKS.1 Nose skirt air flow to atmosphere lb/min

CALC	01:AUG84	REVISED	DATE	ACET STABILITY ANALYSIS 5 IN. DROP AT 35000 POUNDS WITHOUT STABILIZING VENTS	Figure 12b
CHECK					
APPD.					
APPD.				THE BOEING COMPANY	PAGE

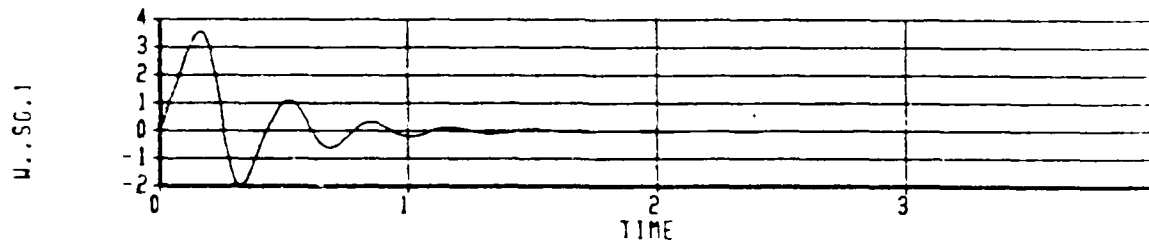
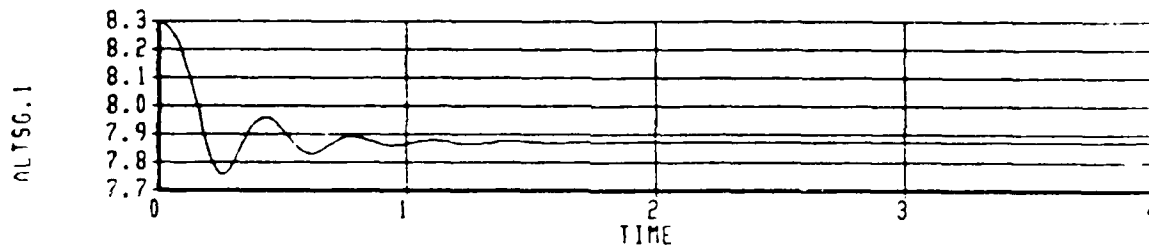
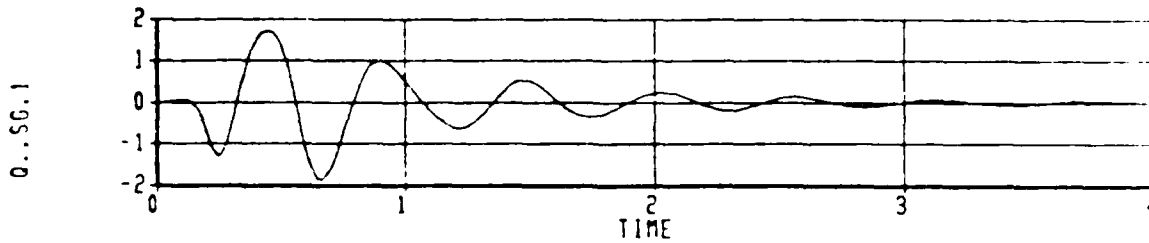
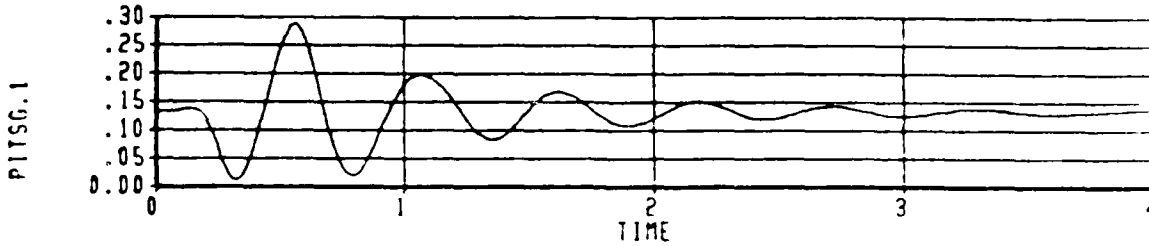
ACET 35000 LB. WITHOUT VENTS  
 RUN DATE= 84/07/27. RUN TIME= 18.41.03.  
 EASY TIME HISTORY PLOT WITH 201 DATA POINTS



AVMAINL      Stabilizing vent area - left main skirt sq in  
 AVNOSE      Stabilizing vent area - nose skirt (total) sq in  
 W2.FN        Fan flow lb/min

CALC	01AUG84	REVISED	DATE	ACET STABILITY ANALYSIS 5 IN. DROP AT 35000 POUNDS WITHOUT STABILIZING VENTS	Figure 120
CHECK					
APPD.					
APPD.					
				THE BOEING COMPANY	PAGE

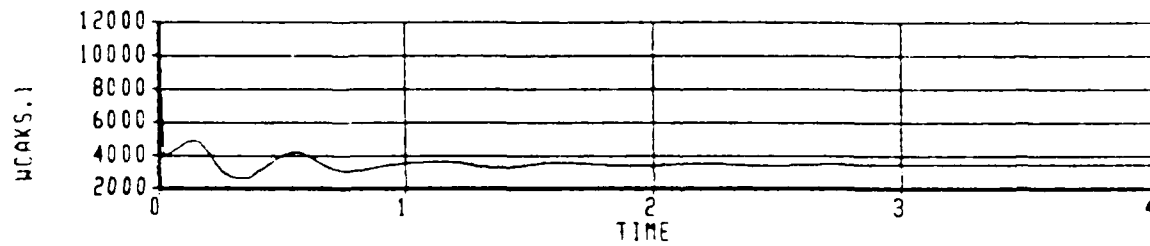
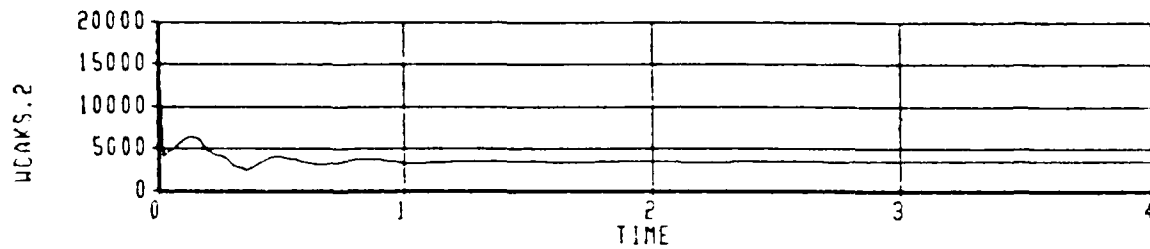
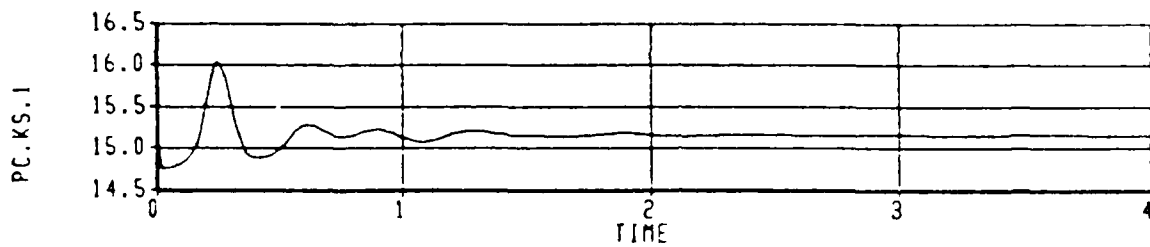
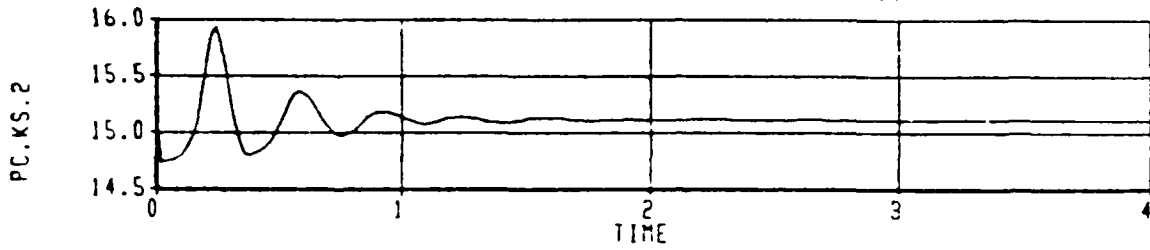
ACET 35000 LB. WITH VENTS  
 RUN DATE= 84/07/27. RUN TIME= 18.45.16.  
 EASY TIME HISTORY PLOT WITH 201 DATA POINTS



PITSG.1 Vehicle pitch attitude deg  
 P..SG.1 Vehicle pitch rate deg/sec  
 ALTSO.1 Vehicle altitude ft  
 W..SG.1 Vehicle Z body axis velocity ft/sec

CALC	01AUG84	REVISED	DATE	ACET STABILITY ANALYSIS 5 IN. DROP AT 35000 POUNDS WITH STABILIZING VENTS	Figure 13a
CHECK					
APPO.					
APPO.					
				THE BOEING COMPANY	PAGE

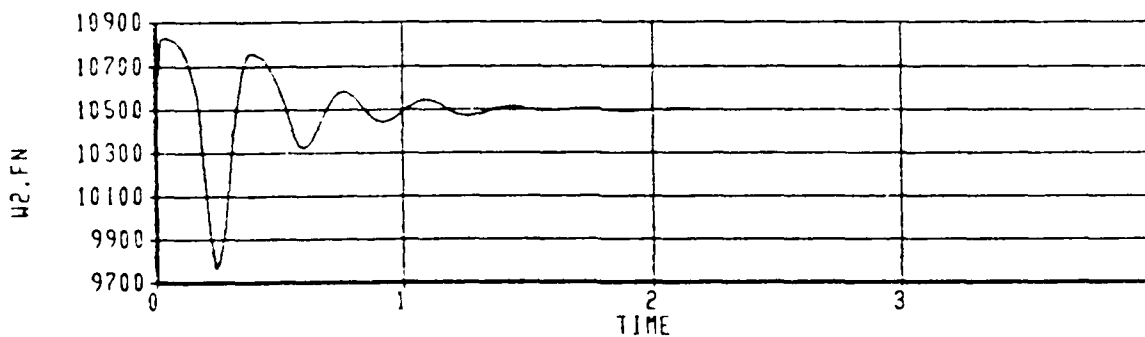
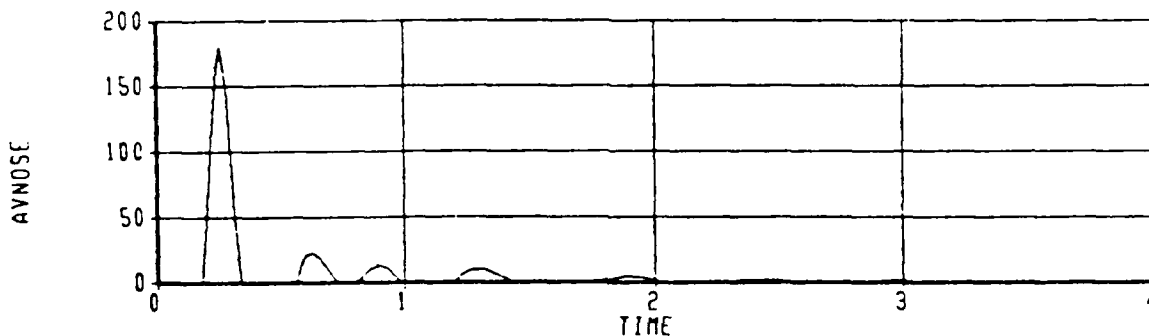
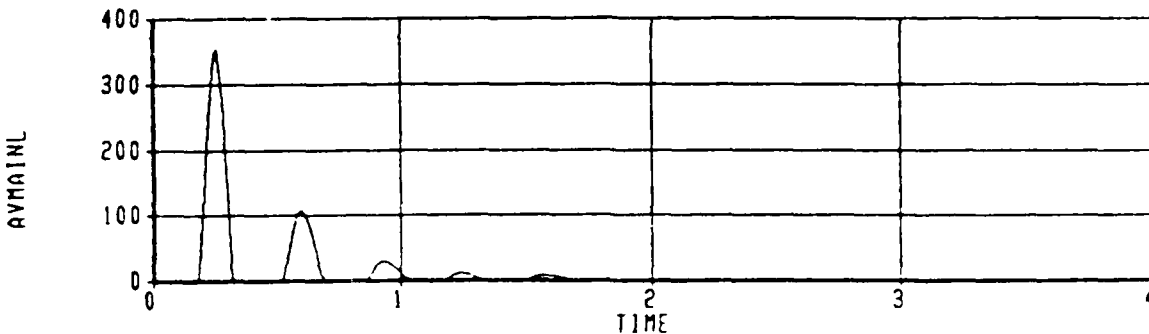
ACET 35000 LB. WITH VENTS  
 RUN DATE= 84/07/27. RUN TIME= 18.45.16.  
 EASY TIME HISTORY PLOT WITH 201 DATA POINTS



PC.KS.2 Left main skirt cushion pressure psia  
 PC.KS.1 Nose skirt cushion pressure psia  
 WCAKS.2 Left main skirt air flow to atmosphere lb/min  
 WCAKS.1 Nose skirt air flow to atmosphere lb/min

CALC	01AUG84	REVISED	DATE	ACET STABILITY ANALYSIS 5 IN. DROP AT 35000 POUNDS WITH STABILIZING VENTS	Figure 13b
CHECK					
APPD.					
APPD.					
				THE BOEING COMPANY	PAGE

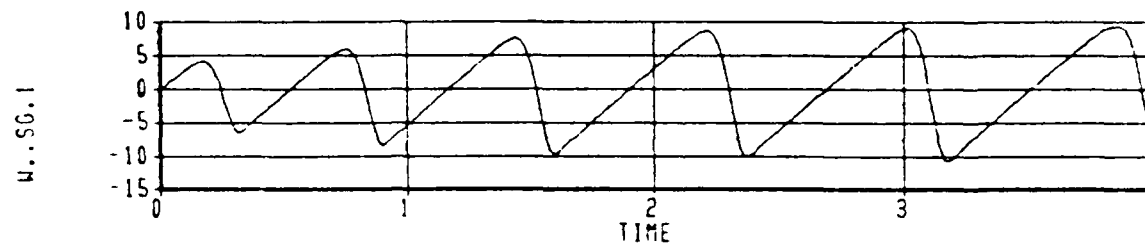
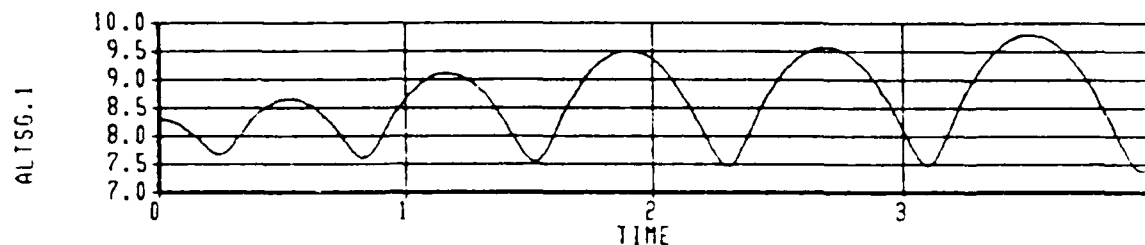
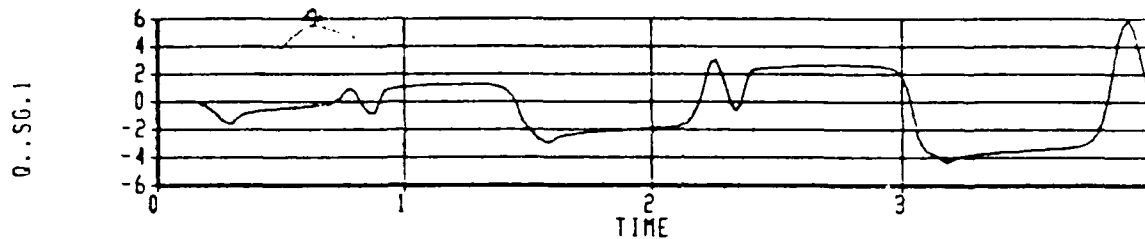
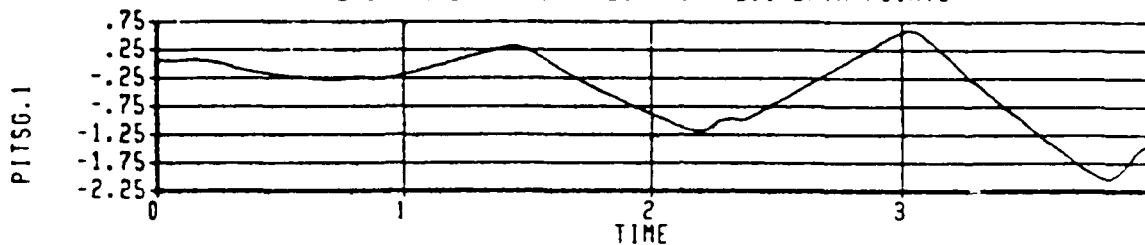
ACET 35000 LB. WITH VENTS  
 RUN DATE= 84/07/27. RUN TIME= 18.45.16.  
 EASY TIME HISTORY PLOT WITH 201 DATA POINTS



AVMAINL Stabilizing vent area - left main skirt sq in  
 AVNOSE Stabilizing vent area - nose skirt (total) sq in  
 W2.FN Fan flow lb/min

CALC	01AUG84	REVISED	DATE	ACET STABILITY ANALYSIS 5 IN. DROP AT 35000 POUNDS WITH STABILIZING VENTS	Figure 13c
CHECK					
APPO.					
APPO.					
				THE BOEING COMPANY	PAGE

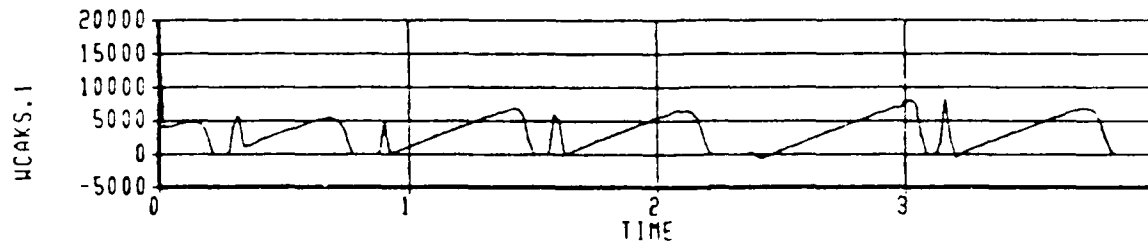
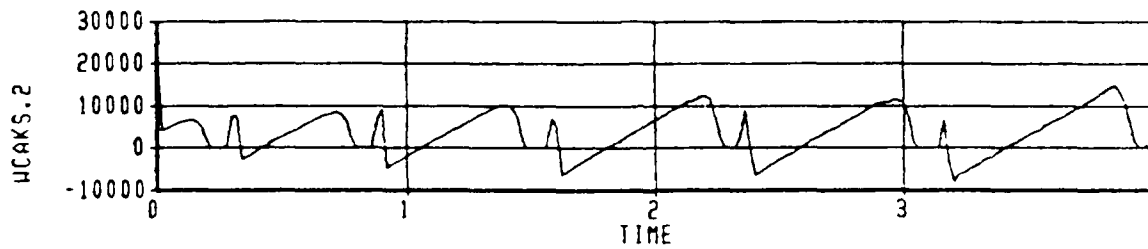
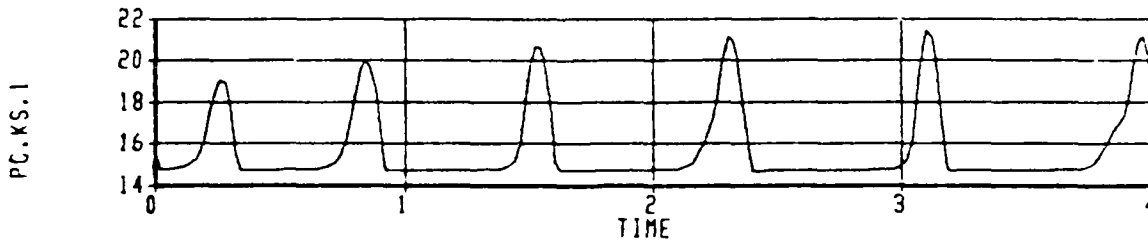
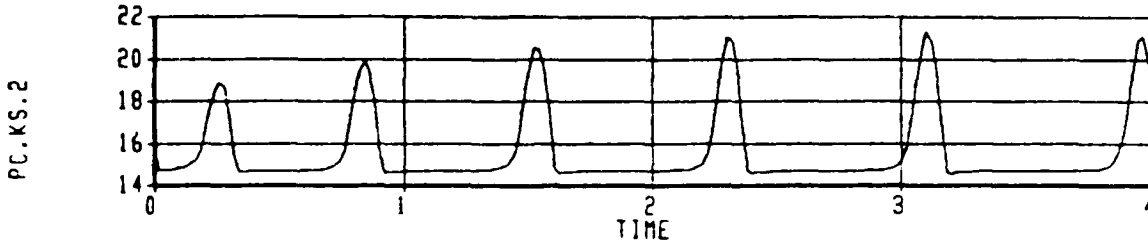
ACET 70000 LB. WITHOUT VENTS  
 RUN DATE= 84/07/27. RUN TIME= 18.48.41.  
 EASY TIME HISTORY PLOT WITH 201 DATA POINTS



PITSG.1 Vehicle pitch attitude deg.  
 Q..SG.1 Vehicle pitch rate deg/sec  
 ALTSG.1 Vehicle altitude ft  
 W..SG.1 Vehicle Z body axis velocity ft/sec

CALC		01AUG84	REVISED	DATE	ACET STABILITY ANALYSIS 5 IN. DROP AT 70000 POUNDS WITHOUT STABILIZING VENTS	Figure 14a
CHECK						
APPD.						
APPD.						
					THE BOEING COMPANY	PAGE

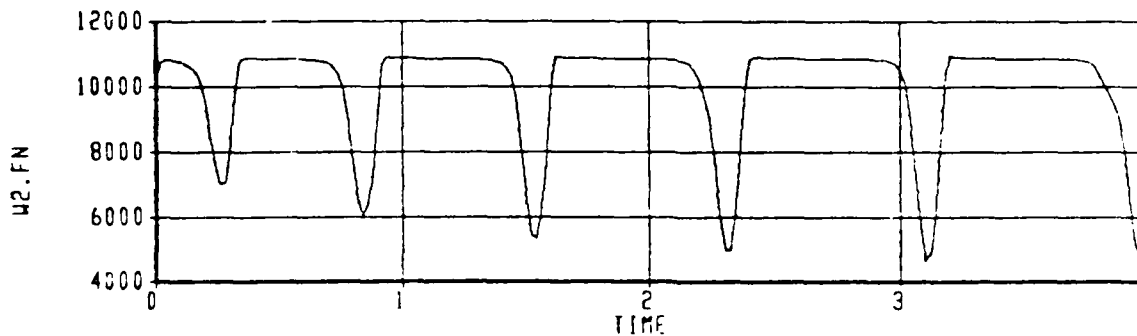
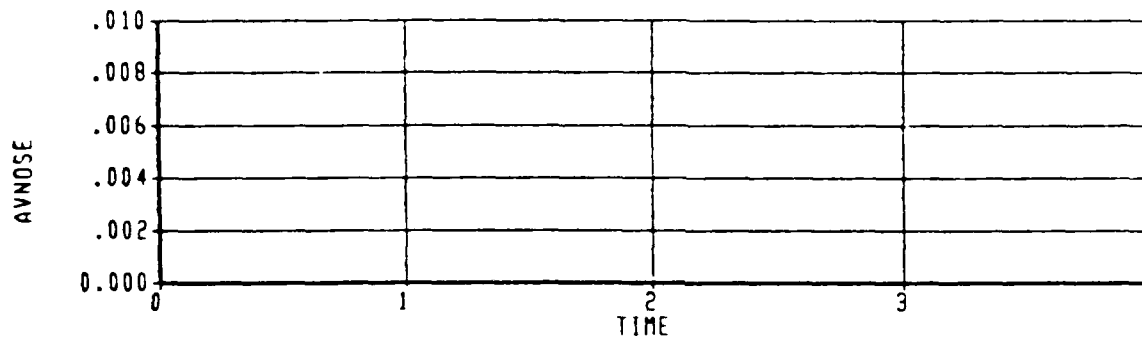
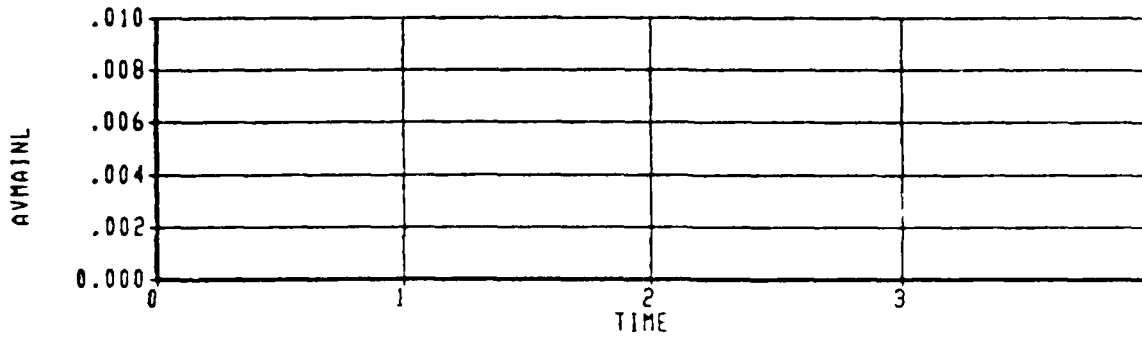
ACET 70000 LB. WITHOUT VENTS  
 RUN DATE= 84/07/27. RUN TIME= 18.48.41.  
 EASY TIME HISTORY PLOT WITH 201 DATA POINTS



PC.KS.2 Left main skirt cushion pressure psia  
 PC.KS.1 Nose skirt cushion pressure psia  
 WCAKS.2 Left main skirt air flow to atmosphere lb/min  
 WCAKS.1 Nose skirt air flow to atmosphere lb/min

CALC	01AUG84	REVISED	DATE	ACET STABILITY ANALYSIS 5 IN. DROP AT 70000 POUNDS WITHOUT STABILIZING VENTS	Figure 14b
CHECK					
APPD.					
APPD.					
				THE BOEING COMPANY	PAGE

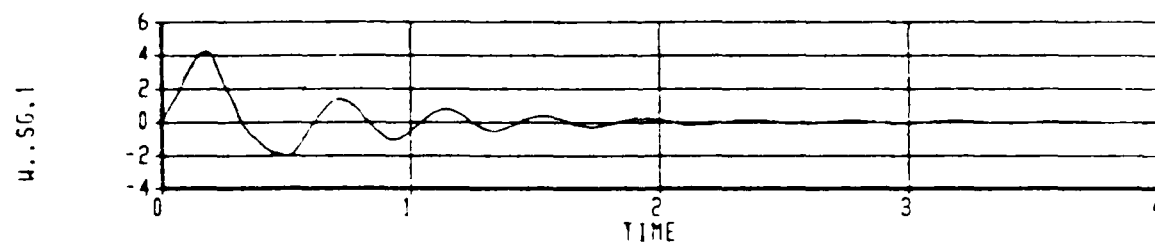
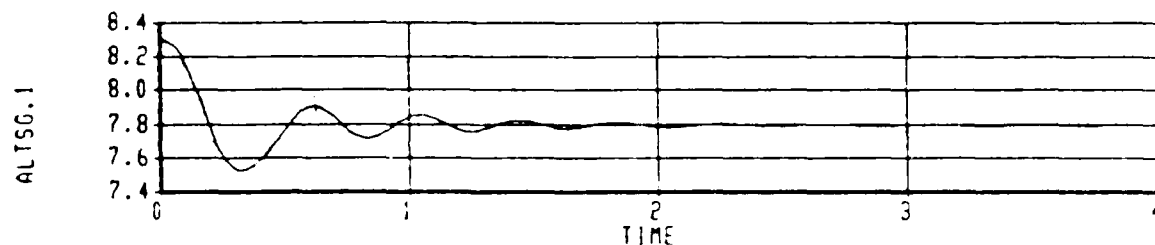
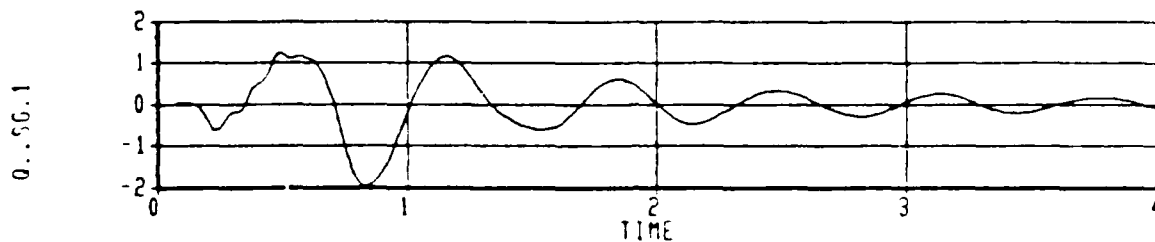
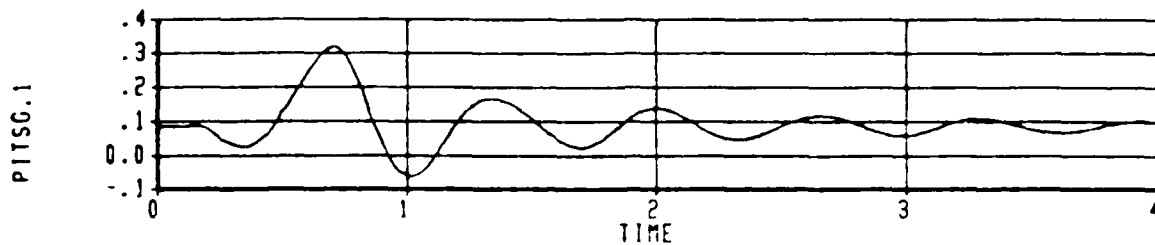
ACET 70000 LB. WITHOUT VENTS  
 RUN DATE= 84/07/27; RUN TIME= 18.48.41.  
 EASY TIME HISTORY PLOT WITH 201 DATA POINTS



AVMAINL Stabilizing vent area - left main skirt sq. in.  
 AVNOSE Stabilizing vent area - nose skirt (total) sq. in.  
 W2.FN Fan flow lb/min

CALC	01AUG84	REVISED	DATE	ACET STABILITY ANALYSIS 5 IN. DROP AT 70000 POUNDS WITHOUT STABILIZING VENTS	
CHECK					Figure 14c
APPD.					PAGE
APPD.					
				THE BOEING COMPANY	

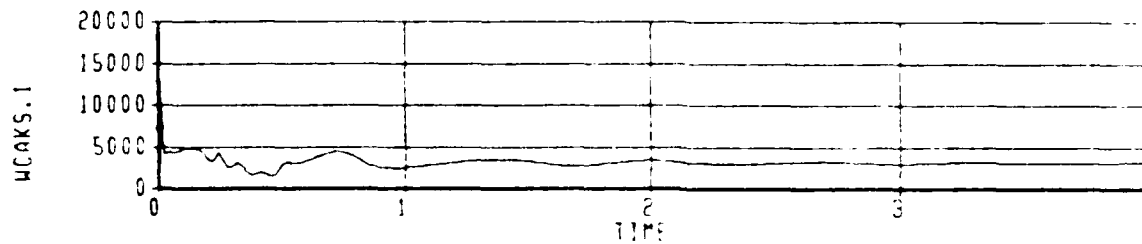
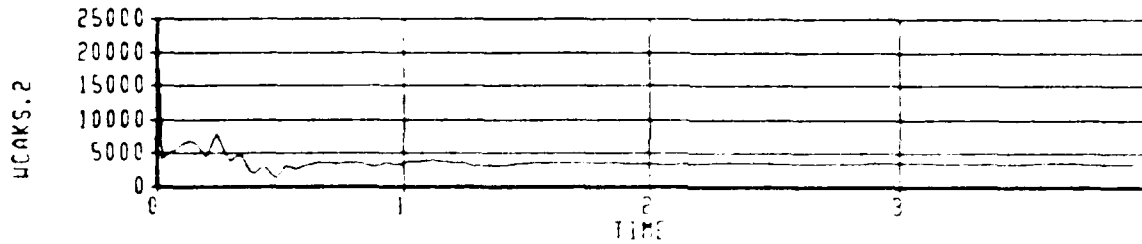
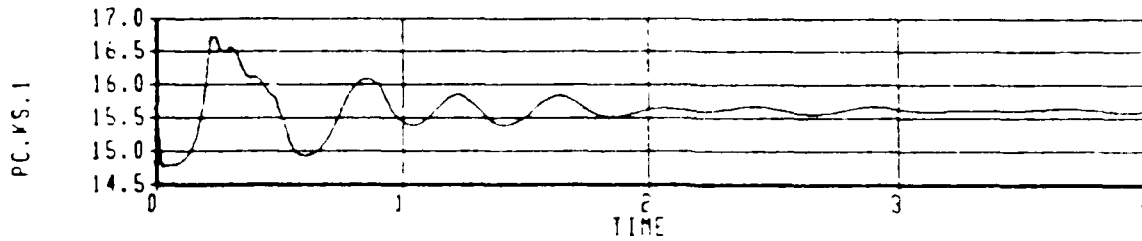
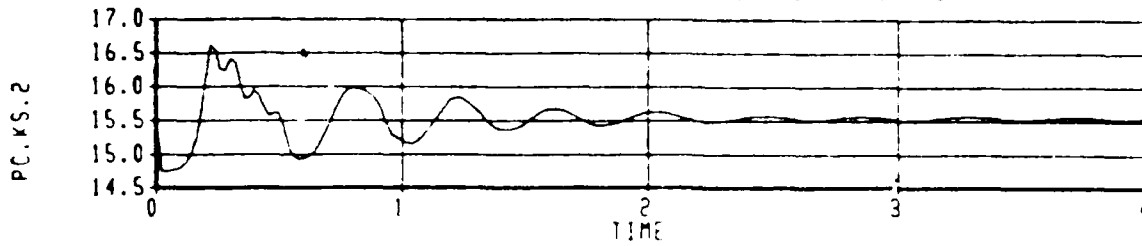
ACET 70000 LB. WITH VENTS  
 RUN DATE = 84/07/27. RUN TIME = 18.46.54.  
 EASY TIME HISTORY PLOT WITH 201 DATA POINTS



PITSG.1 Vehicle pitch attitude deg  
 Q..SG.1 Vehicle pitch rate deg/sec  
 ALTSG.1 Vehicle altitude ft  
 W..SG.1 Vehicle Z body axis velocity ft/sec

CALC	01AUG84	REVISED	DATE	ACET STABILITY ANALYSIS 5 IN. DROP AT 70000 POUNDS WITH STABILIZING VENTS	Figure 15a
CHECK					
APPD.					
APPD.					
				THE BOEING COMPANY	PAGE

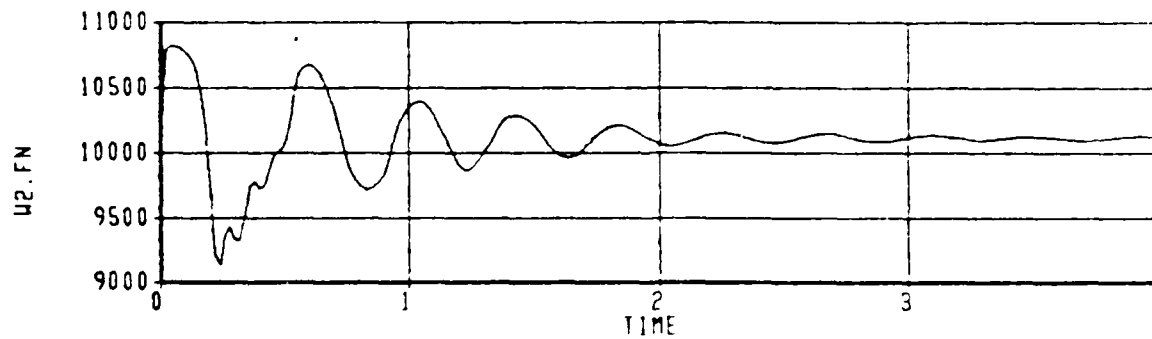
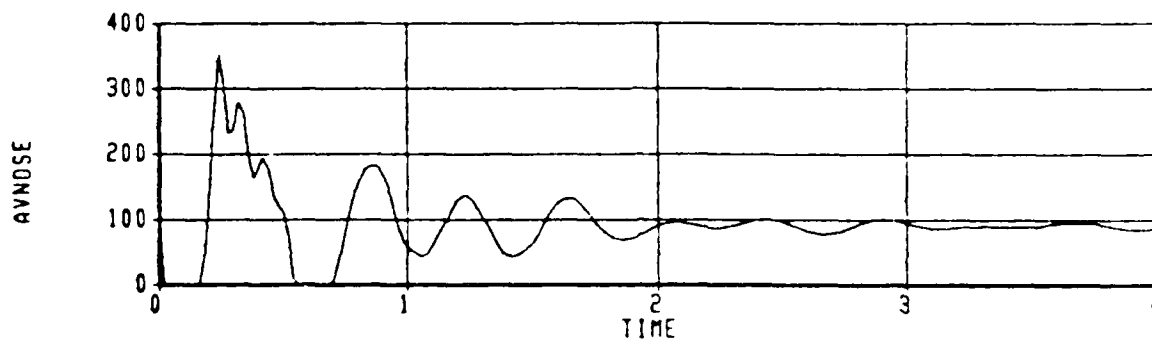
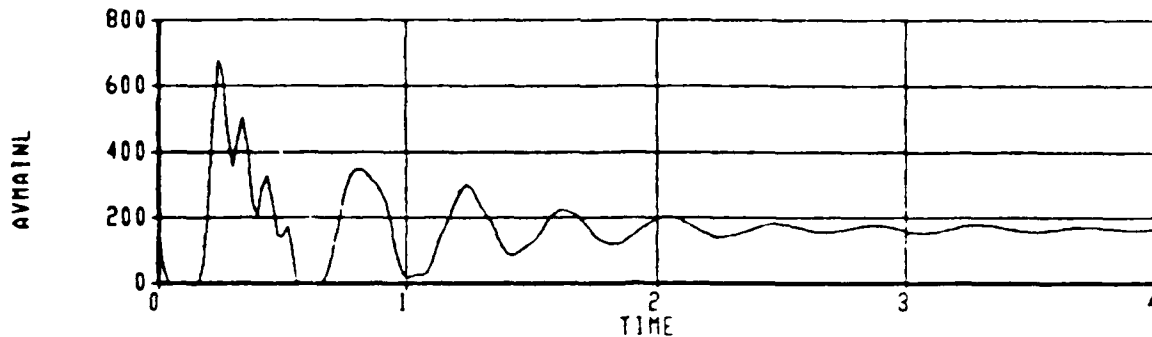
ACET 70000 LB. WITH VENTS  
 RUN DATE= 84/07/27. RUN TIME= 18.46.54  
 EASY TIME HISTORY PLOT WITH 201 DATA POINTS



PC.KS.2 Left main skirt cushion pressure psia  
 PC.KS.1 Nose skirt cushion pressure psia  
 WCAKS.2 Left main skirt air flow to atmosphere lb/min  
 WCAKS.1 Nose skirt air flow to atmosphere lb/min

CALC		01AUG84	REVISED	DATE	ACET STABILITY ANALYSIS 5 IN. DROP AT 70000 POUNDS WITH STABILIZING VENTS THE BOEING COMPANY	Figure 15b PAGE
CHECK						
APPD.						
APPD.						

ACET 70000 LB. WITH VENTS  
 RUN DATE= 84/07/27. RUN TIME= 18.46.54.  
 EASY TIME HISTORY PLOT WITH 201 DATA POINTS



AVMAINL . Stabilizing vent area - left main skirt sq in  
 AVNOSE Stabilizing vent area - nose skirt (total) sq in  
 U2.FN Fan flow lb/min

CALC		01AUG84	REVISED	DATE	ACET STABILITY ANALYSIS 5 IN. DROP AT 70000 POUNDS WITH STABILIZING VENTS	Figure 15c	
CHECK						PAGE	
APPD.							
APPD.						THE BOEING COMPANY	

## REFERENCES

1. Earl, T. D.; DePuy, I. W.; Tothill, G. "ACET Interim Technical Report", BAC Report 7624-928001, AFWAL-TR-83. January 1983.
2. Amyot, J. R.; Fowler, H. S., "An Experiment on Active Control of Air Cushion Heave Dynamics". Canadian Aeronautics and Space Journal, Vol. 30, No. 3, September 1984.

END

FILMED

MARCH, 19 88

DTIC